STRUCTURE-FUNCTION STUDIES OF LATE STAGES OF E. COLI MMR: INTERACTION OF DNA HELICASE II WITH SINGLE-STRANDED DNA BINDING PROTEIN (SSB) AND MUTL

Junghoon In

A dissertation submitted to the faculty of the University of North Carolina at Chapel Hill in partial fulfillment of the requirements for the degree of Doctor of Philosophy in the Curriculum in Applied and Material Sciences

Chapel Hill
2008

Approved by:

Dr. Dorothy Erie

Dr. Linda Spremulli

Dr. Thomas Kunkel

Dr. Richard Superfine

Dr. Steve Matson

ABSTRACT

Junghoon In

Structure-Function studies of late stages of *E. coli* MMR:
Interaction of DNA helicase II with Single-stranded DNA binding protein (SSB) and MutL
(Under the direction of Dr. Dorothy Erie)

DNA mismatch repair (MMR) is the post-replicative mechanism by which errors made during DNA replication and recombination are corrected. *E. coli* UvrD (DNA helicase II) is involved in mismatch repair, where it unwinds dsDNA to correct DNA errors following DNA incision by the combined activation of MutS-MutL-MutH. This dissertation focuses on the interaction of UvrD with SSB on DNA substrates, with each other, and with other protein (ie: MutL) in the MMR pathway.

Using Atomic Force Microscopy, I was able to demonstrate that UvrD interacts with SSB and stimulates UvrD-catalyzed unwinding of double-nicked circular DNA. This result suggests that the interaction of SSB with UvrD facilitates unwinding of DNA substrates. Deletion of acidic 10 acidic residues from the C-terminus of SSB results in a mutant, SSBΔC10, that neither interacts with UvrD nor stimulates the function of UvrD, indicating that the C-terminus of SSB mediates its interaction with UvrD. WtSSB recruits UvrD onto a nick of the DNA substrate to initiate unwinding of DNA, as demonstrated by wtSSB reducing UvrD binding to blunt-ended and 3' overhang DNA. I observed that wtSSB

facilitates UvrD-catalyzed unwinding of nicked DNA in a 3'→5' direction. These findings suggest that the stimulatory effect of SSB on UvrD helicase activity is not solely due to SSB's binding function to ssDNA, but due to the specific interaction of SSB with UvrD.

I have shown that UvrD also interacts with MutL. The interaction of UvrD and MutL facilitates unwinding of DNA in the presence of ATP onto duplex DNA including 3-nt 3' overhang, suggesting that oligomerization of MutL and UvrD on DNA may facilitate DNA unwinding.

Taken together, these findings suggest that UvrD mediates the late stage of MMR machinery by the interaction with SSB and MutL. It is these interactions of UvrD with SSB and MutL that facilitate the processivity of the unwinding of DNA by UvrD to maintain genomic stability.

To my little one in my tummy for bringing in such a new joy to us and for “behaving” throughout mommy’s agonizing journey of thesis writing.

ACKNOWLEDGEMENTS

I am most especially grateful to my wonderful husband, mother, and all my family members for their encouragement, support and extraordinary dedication.

I cannot thank enough Dorothy who was very generous in giving me invaluable feedback and input. They are the countless reviews that Dorothy gave me that made me think and my work stay on track. My sincere appreciation also goes to all members of my dissertation committee for their mentorship, support and commitment to my dissertation.

I want to thank each of our group members, Erika, Vanessa, Cherie, Na, and Dan, for always being supportive. Especially I am indebted to Erika and Vanessa for their gift of time in reading and providing me with comments on my countless thesis draft versions. A very special thanks goes to a former Erie lab member, Liz, whose cheerful words of encouragement and countless reviews and comments made possible the final version of my thesis work into existence.

TABLE OF CONTENTS

LIST OF FIGURES

LIST OF TABLES

List of Abbreviations

3-D	Three-dimensional
A	Alanine
ADP	adenosine diphosphate
AFM	atomic force microscopy
AID	activation induced cytidine deaminase
Ala	Alanine
AMPPPNP	5'-adenylyl-β-γ-imidodiphosphate
ATP	adenosine triphosphate
bp	Base pair
C-	carboxy
χ	chi subunit of DNA polymerase III
ddH2O	doubly deionized water
DNA	Deoxyribonucleic acid
dsDNA	double stranded DNA
DTT	dithiothreitol
E. coli	*Escherichia coli*
EDTA	Ethylamine diamine tetraacetic acid
EMSA	Electromobioity gel shift assay
ExoI	Exonuclease I
FRET	Fluorescence resonance energy transfer
g	gram
Glu	Glutamate

H	Histidine
HEPES	(4-(2-hydroxyethyl)-1-piperazineethanesulfonic acid
His	Histidine
HNPCC	hereditary non-polyposis colorectal cancer
hsp90	Family of 90 kDa heat shock proteins found in the cytoplasm & endoplasmic reticulum
IDL	insertion-deletion loop
KC1	Potassium chloride
λ	wavelength
L	Liter
Li	Lithium
μm	micron
μM	micromolar
M	molar
Mg	Magnesium
MgCl	Magnesium Chloride
min	minute
mL	milliliter
Mlh	MutL homolog
mM	millimolar
mmol	millimole
MMR	DNA mismatch repair
MutLα	Mlh1-Pms2 (yPms1)

MW	Molecular weight
N	Structured N-terminal domain of either MutL or MutS
N-	amino
Na	Sodium
NaCL	Sodium chloride
NaOH	Sodium hydroxide
nM	nanomolar
nm	nanometer
nm^3	Cubic nanometers
nt	nucleotide
OD_{595}	Optical density at λ=595
OH-	base
P	Proline
PcrA	Plasmid copy number reduction, DNA helicase, SF1
PCNA	proliferating cell nuclear antigen
PMSF	Phenylmethylsufonylfluoride
Polymin P	Poly(ethylenimine)
Rep	DNA helicase, SF1
RNA	ribonucleic acid
RPA	Replication protein A
rpm	Revolutions per minute
S. cerevisiae	Saccharomyces cerevisiae
SBS	Single-stranded binding protein

SDS	Sodium dodecyl sulfate
ssDNA	single stranded DNA
T	Threonine
T	Thymine
Taq	Thermus auaticus
TBE	Tris-borate-EDTA buffer
T4 gene 32 protein	gene 32 protein of bacteriophage T4
Tris	2-amino-2-hydroxymethyl-1,3-propanediol
U	uracil
UvrD	DNA helicase II
W	Adenine or Thymine
Wt	wild-type
X	Any amino acid
Y	Pyrimidine (C or T)

Chapter 1

Introduction

DNA mismatch repair (MMR)

DNA mismatch repair (MMR) is one of several DNA repair systems conserved from bacteria to humans (Au 1992; Buermeyer 1999; Jiricny 2003). MMR is the primary mechanism by which DNA-synthesis errors are corrected post-replicatively. MMR recognizes and repairs insertion/deletion loops (IDLs) and non-Watson Crick base pairs, e.g., G:T, which can arise during DNA replication and recombination (Buermeyer 1999; Kolodner 1999; Genschel 2000; Hsieh 2001). Non-Watson-crick base pairs, or mismatches, within the DNA helix can result from nucleotide misincorporation during DNA synthesis. The error of base-pairing and editing is corrected by mismatch repair, further elevating fidelity of DNA replication 50 to 1,000-fold (Kolodner 1996; Modrich 1996; Jiricny 1998; Buermeyer 1999; Kolodner 1999; Schofield 2003). Inactivation of the human mismatch repair system is associated with > 85% of occurrences of hereditary non-polyposis colon cancer (HNPCC) and has been implicated in the development of a subset of sporadic tumors that occur in a variety of tissues (Eshleman 1995; Peltomaki 2001; Peltomaki 2003; de la Chapelle 2004; Rowley 2005).

MMR pathway in Escherichia coli (E. coli)

Escherichia coli (*E. coli)* provides the best understood mismatch repair system and serves as a model system for the more complicated, but homologous, eukaryotic systems (Modrich 1996; Harfe 2000). In *E. coli*, the DNA mismatch repair system takes advantage of the transient post–replicative hemi-methylation of the adenosine in GATC sites to discriminate between parent and daughter DNA strands (Modrich 1996). The mismatch repair pathway is bi-directional (Figure 1.1). MutS, MutL and MutH are responsible for the initiation of MMR in *E.coli* (Su 1986; Su 1988; Grilley 1989; Modrich 1996). MMR is initiated by the recognition of DNA mismatches or insertion deletion loops (IDL) by MutS (Su 1986; Su 1988). Subsequently, MutL binds to the MutS-DNA complex in a ATP-dependent manner (Grilley 1989). This MutS-MutL-mismatch complex activates MutH, which incises the newly-synthesized strand at a hemimethlylated GATC site (Modrich 1987; Welsh 1987; Au 1992). This incision confers strand specificity of MMR, directing repair exclusively to the newly synthesized strand containing the error. DNA helicase II (UvrD) unwinds the DNA toward the mismatch and the appropriate exonucleases. The excision depends on the position of the mismatch relative to the GATC site, a 5' to 3' exonuclease (RecJ or Exo VIII) or a 3' to 5' (Exo I, Exo X or Exo VIII) (Cooper 1993; Grilley 1993; Yamaguchi 1998; Mechanic 2000). The DNA polymerase III holoenzyme resynthesizes the DNA correctly, and DNA ligase seals the nick (Lahue 1989).

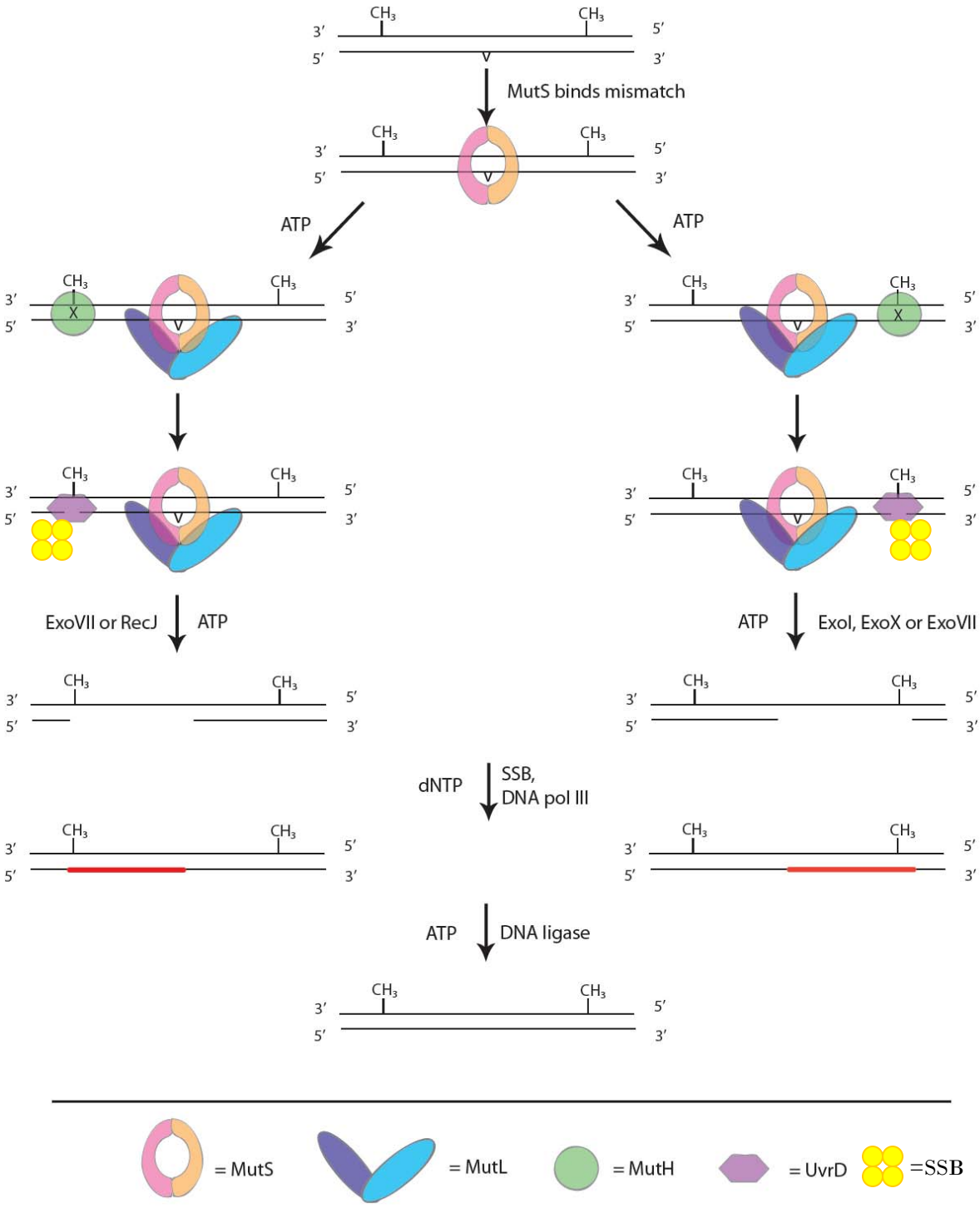
CH3
3′
5′
MutS binds mismatch
ATP
ATP
X
ExoVII or RecJ
ATP
ATP
ExoI, ExoX or ExoVII
dNTP
SSB,
DNA pol III
ATP
DNA ligase
= MutS
= MutL
= MutH
= UvrD
=SSB

Figure 1.1

Figure 1.1 Schematic of Bi-directional MMR in *E. coli*

The MMR process is bi-directional. The pathway includes steps of mismatch recognition, initiation, strand discrimination, excision, re-synthesis and ligation. (See text)

Initiation of repair by MutS and MutL

The crystal structures of MutS-DNA complexes have been determined for *Thermus aquaticus* (*Taq*) MutS binding to a number of different mismatched DNA bases and IDLs (Obmolova 2000; Natrajan 2003) (Figure 1.2), and for *E.coli* MutS bound to a G: T mismatch and ADP (Lamers 2000). The MutS homodimer contains a carboxyl-terminal ATPase domain, as well as a mismatch base recognition domain (Haber 1991; Wu 1994). A sharp 60° kink in the DNA at the mismatch site is observed with MutS only 2 residues of MutS interacting with the mismatched base. A phenylalanine, conserved in the MutS family (Phe 36 in *E.coli*, Phe 39 in *Taq*), stacks with one of the mismatched bases: this base also forms a hydrogen bond to a conserved glutamic acid (Glu 38 in *E.coli*, Glu 41 in *Taq*).

There are three models that describe the initiation events in DNA MMR. One model, the translocation model, proposes that the DNA-bound MutS moves along the helix and that this movement is coupled to adenosine triphosphate binding and hydrolysis (Blackwell 1998). In the molecular switch model, mismatch recognition by the MutS·ADP complex promotes exchange of ADP for ATP and MutS slides away from the mismatch (Gradia 1999). The third model, the trans-activation model, suggests that upon recognizing and binding to a mismatch or insertion/deletion loop, MutS remains in the vicinity of the mismatch. The MutS-MutL-mismatch ternary complex is postulated to interact with MutH at the strand discrimination signal site by DNA bending and protein-protein interactions (Junop 2001; Schofield 2001). In this model, the MutS-MutL complex may provide the signal for termination of the excision step involving the DNA helicase II and exonucleases (Schofield 2001).

A **B**

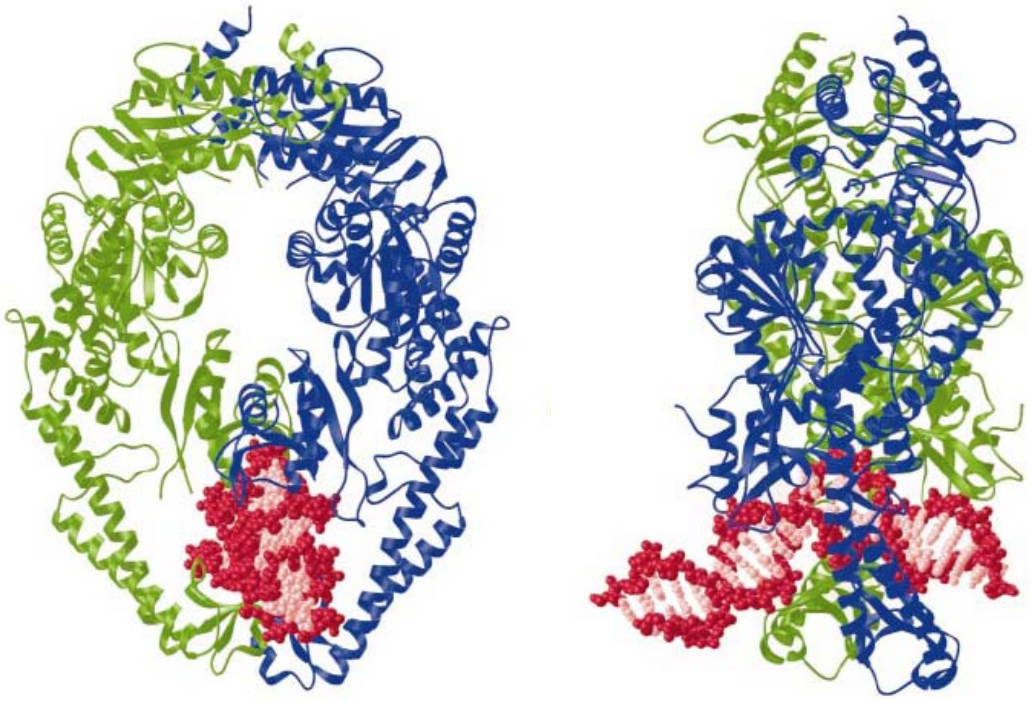

Figure 1.2 Crystal structure of Taq MutS (Obmolova 2000)

(A) *Taq* MutS bound to DNA. Two subunits are represented by ribbon (blue and green) and DNA is shown in red and pink. The backbone of DNA is pink. (B) Side view of the *Taq* MutS-DNA complex.

MutL plays an essential role in coupling of mismatch recognition by MutS to the activation of MutH and DNA helicase II. In *E. coli*, MutL mediates initiation steps and downstream repair events in MMR. Previous crystallographic and biochemical studies have shown that MutL contains an N-terminal ATPase region (residues 1-349) and a C-terminal dimerization region (residues 432-615) (Ban 1998; Ban 1999) (Figure 1.2). The N-terminal ATPase domain is conserved in all members of the MutL family (Ban 1998), but the C-terminal region, which is responsible for dimerization, is diverse among MutL homologs (Pang 1997; Drotschmann 1998) The C-terminal domain of MutL crystallizes as a V-shaped dimer, while the N-terminal domain forms a saddle-shape dimmer in the presence of AMPPNP. The N-terminal ATPase fragment is monomeric in the absence of nucleotide. In the presence of the nonhydrolyzable ATP analog AMPPNP, the ATPase fragment is dimeric and is fully folded (Ban 1998; Ban 1999). MutL and MutL homologs are conserved from prokaryotes to eukaryotes (Modrich 1996). In eukaryotes, MutL homologs are called MLH and PMS. Like MutL, MutL homologs catalyze a weak ATPase activity, which is necessary in DNA repair (Ban 1998; Ban 1999; Spampinato 2000).

Conformational changes that occur upon ATP binding and hydrolysis have been proposed to allow MutL to coordinate various protein-protein interactions during the mismatch repair process (Ban 1999). In the absence of MutS and a mismatch, MutL can activate MutH endonuclease to a relatively low level in an ATP binding-dependent, yet ATP hydrolysis-independent, manner (Ban 1998). Yeast two hybrid assays suggest that MutL physically interacts with UvrD (Hall 1998). The C-terminal 219 amino acids (residues 398-615) of MutL are adequate to interact with UvrD, indicating that this region may contain the potential interaction sites for UvrD (Hall 1998). The interaction of MutL and UvrD

facilitates the loading of UvrD onto DNA (Mechanic 2000). Helicase activity assays have shown that MutL stimulates UvrD helicase unwinding (Dao 1998; Yamaguchi 1998), and DNA binding assays have revealed that MutL increases UvrD binding to partial duplex DNA (Mechanic 2000).

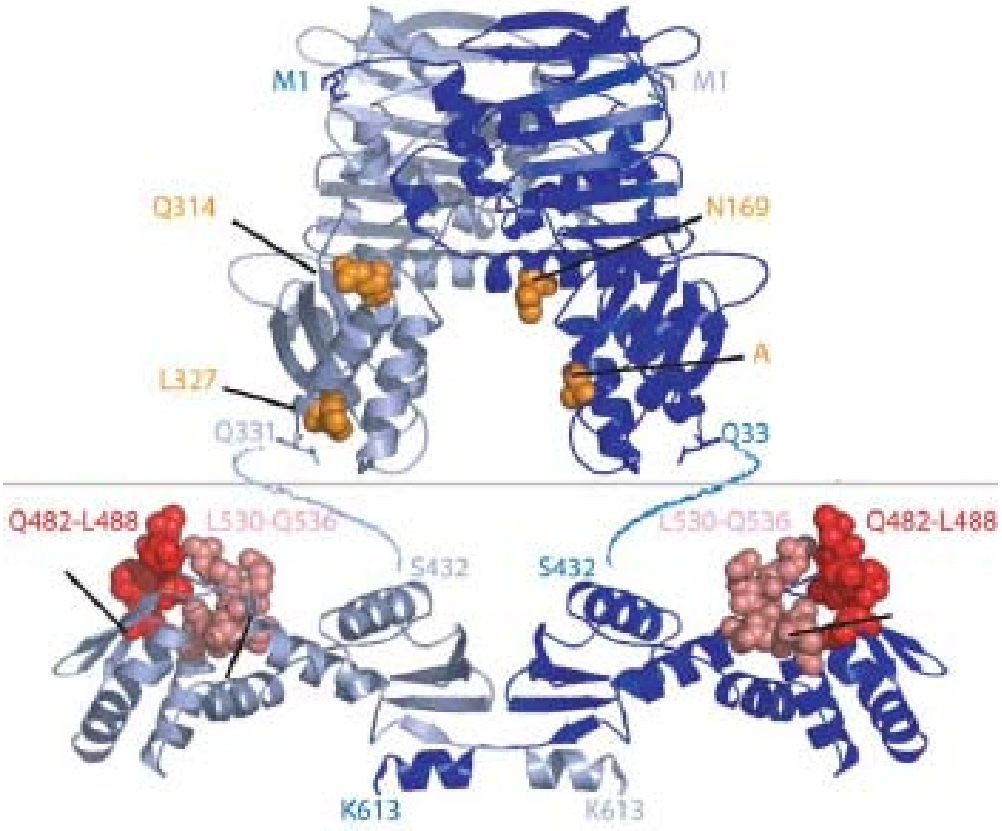

Figure 1.3 Crystal structure of MutL

The ribbon diagram of the homodimeric N-terminal domain and C-terminal domain aligned. Subunits are colored in light blue and dark blue. Residues of N-terminal domain shown to be bound to MutH are indicated by orange spheres. The highly conserved surface of C-terminal domain is shown in light and dark red **(Kosinskia 2005)**.

Helicases

The helicase superfamily

Helicases have been identified and characterized from different organisms, including bacteria, yeast and humans. Based on sequence alignments, helicases can be classified into six families: three superfamilies (I, II, III), DnaB-like family, Rho-like family and a branch in the AAA+ family (Gorbalenya 1993; Lyer 2004) (Table 1.1). SF1 and SF2 members share seven conserved sequence motifs (Hodgman 1988; Gorbalenya 1993). PcrA helicase from *Bacillus stearothermophilus*, which is in the SF1 family and shares 42 % sequence similarity with UvrD, is a 3' → 5' helicase (Bird 1998; Petit 1998; Soultanas 1999) (Table1.1). PcrA is involved in DNA repair and rolling circle plasmid replication (Petit 1998; Soultanas 1999). *E. coli* Rep helicase shares 37 % sequence homology with UvrD and is also in the SF1 family (Lohman 1996). Rep helicase participates in the replication of *E. coli* bacteriophages M13 and ΦX174 (Takahashi 1979). The Rep protein is monomer in the absence of DNA (Lohman 1989), but *in vitro,* Rep monomers are inactive as helicases (Cheng 2001). While the monomers of Rep protein can translocate on ssDNA in the 3' → 5' direction, the dimeric form appears to be required to unwind dsDNA *in vitro* (Wong 1992; Cheng 2001; Ha 2002; Brendza 2005). Wong and Lohman (1992) have proposed that Rep helicase unwinds and translocates along DNA by an "active, rolling" mechanism, in which Rep requires at least two DNA binding sites, so that both subunits of the Rep dimer can bind either ss- or dsDNA.

Superfamily I	Superfamily II	Superfamily III	DnaB-like helicase	Rho-like family
UvrD (*E. coli*, DNA repair)	**RecQ** (*E. coli*, DNA repair)	**LTag** (Simian Virus 40, replication)	**dnaB** (*E. coli*, replication)	**Rho** (*E. coli*, transcription termination)
Rep (*E. coli*, DNA replication)	**eIF4A** (Baker's Yeast, RNA translation)	**E1** (human papillomavirus, replication)	**gp41** (bacteriophage T4, DNA replication)	
PcrA (*Staphylococcus aureus*, recombination)	**WRN** (human, DNA repair)	**Rep** (Adeno-Associated Virus, replication, viral integration, virion packaging)	**T7gp4** (bacteriophage T7, DNA replication)	
Dda (*bacteriophage* T4, replication initiation)	**NS3** (Hepatitis C virus, replication)			
	TRCF (Mfd) (*E.coli*, transcription-repair coupling)			

Table 1.1: Members of helicase families

DNA helicase II (UvrD gene)

UvrD catalyzes unwinding of duplex DNA, which is necessary to form ssDNA intermediates during DNA replication, recombination and repair (Lohman 1996). UvrD is a motor protein that translocates along single-stranded (ss)- and unwinds double-stranded (ds) DNA using the energy derived from ATP hydrolysis (Matson 1990; von Hippel 2003). *E. coli* UvrD (DNA helicase II) is involved in mismatch repair, where it unwinds dsDNA to correct DNA errors, following DNA incision by the combined activation of MutS-MutL-MutH (Modrich 1994).

E. coli UvrD helicase, which is in the SF1 family of helicases, is essential for both MMR and nucleotide excision repair (NER) (Sancar 1994; Modrich 1996). UvrD is a 82 kDa protein and binds both ss- and dsDNA (Abdel-Monem 1977). UvrD unwinds duplex DNA with a 3'→ 5' direction with respect to the DNA strands on which UvrD is bound (Matson 1986). There is a controversy regarding the functional states of UvrD. Yeast two hybrid and biochemical assays identified a mutant, UvrDΔ40C, that is defective in oligomerization, but whose ATPase and unwinding activities are indistinguishable from wtUvrD (Mechanic 1999).

In addition, crystallographic studies suggest that one helicase molecule is bound at a ss-dsDNA junction (Lee 2006). Although mutational and structural studies suggest that the monomeric state is functional (Mechanic 1999; Lee 2006), systematic DNA unwinding kinetic studies suggested that the dimeric form is required for helicase activity, at least on some substrates (Ali 1999; Maluf 2003). Pre-steady state quenched-flow studies suggest that an oligomeric form of UvrD is required for helicase activity (Ali 1999). It has also been

demonstrated that UvrD is predominantly dimeric when binding to ssDNA (Runyon 1993) and that UvrD becomes oligomerized at the junction of ss-dsDNA region (Matson 1987).

UvrD structure

The first helicase structure solved was that of *Bacillus stearothermophilus* PcrA protein (Subramanya 1996). PcrA complexed with DNA and SO_4^{2-} or DNA and AMPPNP showed that the enzyme crystallizes as a monomer that consists of two domains (domains 1and 2) (Figure 1.4). Each domain contains two subdomains (A and B). Subdomain 1A carries the Walker A and B motifs, and subdomain 2A is similar in structure to 1A. Both subdomains contain a large insertion within the polypeptide sequences (Velankar 1999). Given that the 2B domain of PcrA undergoes conformational changes upon binding to ss-dsDNA junction, it is likely that 2B domain is essential for binding and unwinding of duplex DNA (Soultanas 2000).

Lee and Yang (2006) reported crystal structures of *E. coli* UvrD showing distinct steps during ATP hydrolysis: (1) UvrD and DNA (Figure 1.5A), (2) UvrD with a nonhydrolyzable ATP analog (AMPPNP) (Figure 1.5B), and (3) UvrD with an ATP hydrolysis intermediate (ADP-MgF_3). In these crystal structures, each ds-ss DNA junction is bound by one UvrD monomer. UvrD contains four structural domains, like PcrA, which include 1A, 2A, 1B and 2B:1A (1-89, 215-280 aa), 2A (281-377, 551-647 aa), 1B (90-214 aa) and 2B (378-550 aa). Domain 1A and 2A are responsible for ATP binding and hydrolysis (Figure 1.4B) and Domain 1B and 2B interact with DNA (Lee 2006). The 3' ssDNA tail is bound across domains 1A and 2A, and duplex DNA interactes with 1B and 2B (Figure 1.5). In the absence of nucleotides, domain 2B is held in a closed conformation against domain 1B.

In the presence of AMPPNP molecule or ADP-MgF_3 complex, domain 2B is reoriented and forms an open conformation. The binding of ATP induces a closed conformation between domain 2A and the rest of the protein, which leads to separation of the first base pair at the ss-dsDNA junction. ATP hydrolysis leads to domain 2B opening and translocation of 1bp, suggesting that the unwinding of UvrD steps 1 bp per ATP hydrolysis (Lee 2006).

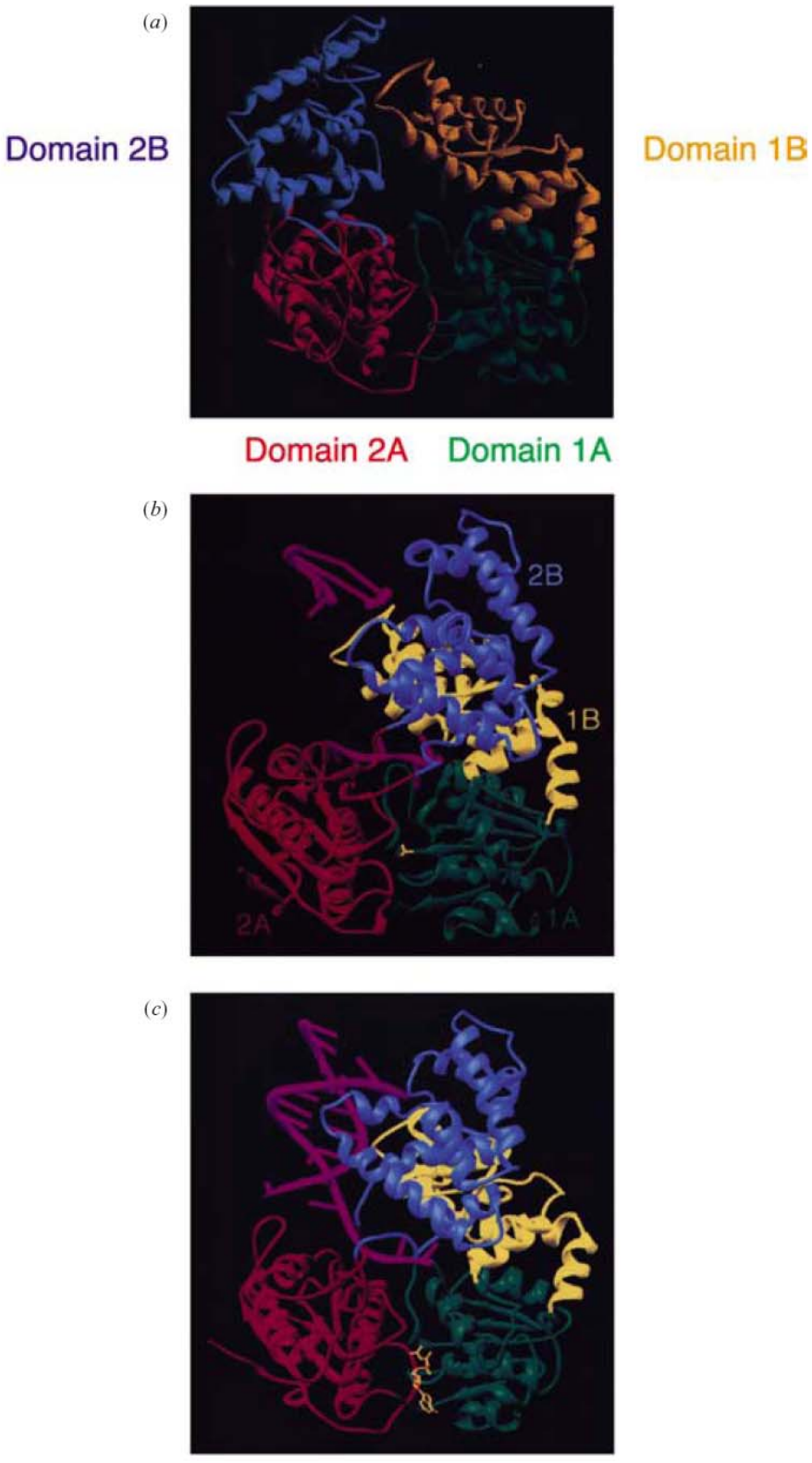

Figure 1.4

Figure 1.4 Structure of the PcrA helicase

(A) apo PcrA (B) PcrA-DNA (C) PcrA-DNA-AMPPNP: Domain 1A (green), 2A (red), 2B (blue), 1B (orange in (a) or yellow). The bound DNA is magenta. The AMPPNP and the sulfate are gold in (B) (C). **(Subramanya 1996; Velankar 1999)**

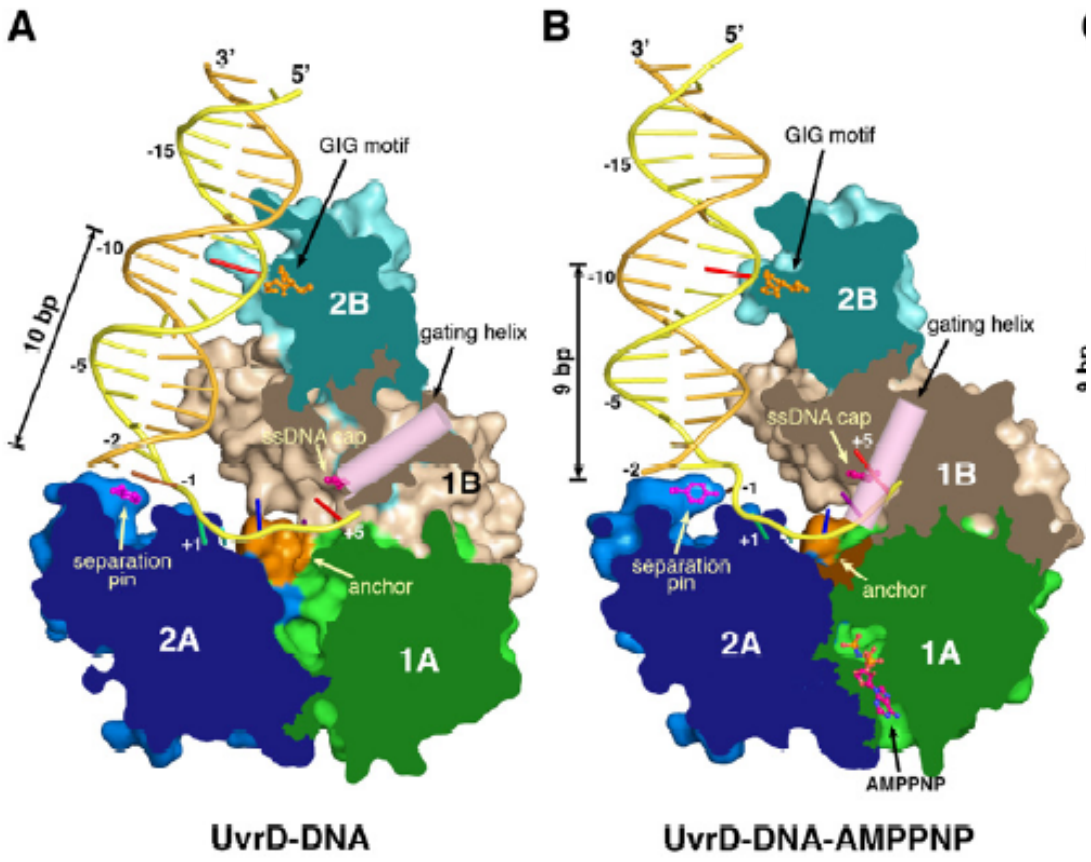
A
3'
5'
-15
GIG motif
-10
10 bp
2B
gating helix
-5
-2
ssDNA cap
-1
1B
+1
+5
separation pin
anchor
2A
1A
UvrD-DNA
B
3'
5'
GIG motif
-15
-10
9 bp
2B
gating helix
-5
ssDNA cap
+5
-2
1B
-1
+1
separation pin
anchor
2A
1A
AMPPNP
UvrD-DNA-AMPPNP

Figure 1.5

Figure 1.5 Crystal structures of UvrD-DNA complexes (Lee 2006)

(A) Binary complex of UvrD-DNA, (B) UvrD-DNA-AMPPNP. UvrD contains four structural domains 1A, 1B, 2A and 2B. Domain 1A and 2A are responsible for ATP binding and hydrolysis. Domain 1B and 2B interact with the DNA duplex.

Single-stranded binding protein (SSB)

SSB plays a critical role in replication, is involved recombination and repair, and interacts with other proteins involved in DNA metabolism (Meyer 1990; Lohman 1994). SSB protein binds preferentially and cooperatively to ssDNA depending on the salt concentration. In the absence of DNA, the protein exists as a homotetramer (Chase 1986; Lohman 1994) and there is no evidence for distinct higher-order forms (Meyer 1990). Each subunit of SSB possesses an oligonucleotide/oligosaccharide binding (OB) fold, which has potential ssDNA binding sites (Roy 2007).

SSB binding modes

SSB binds to DNA in several different binding modes with different 'site sizes', defined as the average number of nucleotides occluded by the bound protein. In the two main modes of DNA binding by SSB, there are "35 base" and "65 base" modes. In the $(SSB)_{35}$ binding mode, in which the average site size per tetramer is 35 nucleotides, only two SSB subunits interact in a highly cooperative fashion with ssDNA, and long protein tracts form along the DNA. Since more SSB proteins can bind to DNA in the $(SSB)_{35}$ as compared to the $(SSB)_{65}$ mode, high protein concentrations favor the $(SSB)_{35}$ mode, which is stable at [NaCl] $\leq$ 10 mM (Ferrari 1994).

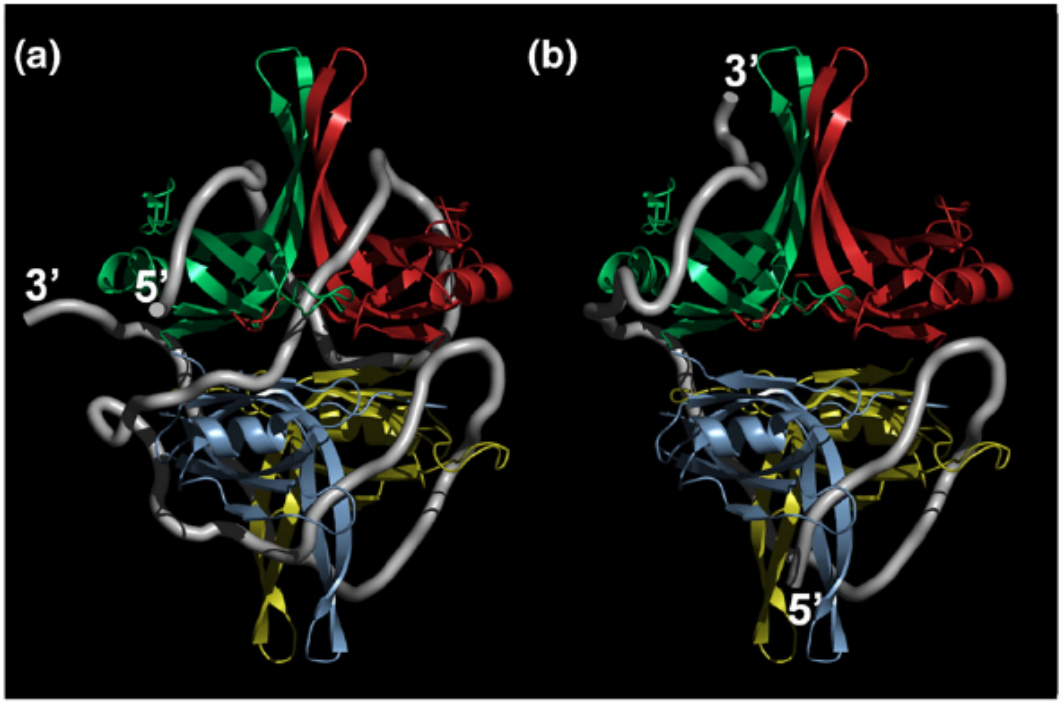

Figure 1.6 SSB binding mode in the presence of DNA (Roy 2007)

Model of the binding mode derived from the crystal structure of a chymotrypsin truncated SSB tetramer (missing 42 C-terminal residues) (Raghunathan 2000) (A) $(SSB)_{65}$ mode. ssDNA interacts with all four subunits of SSB (B) In the $(SSB)_{35}$ mode, only two subunits of the SSB tetramer interact with ss DNA. Each SSB subunit is color coded. DNA is shown in grey color in (a), (b).

The $(SSB)_{65}$ binding mode, in which ssDNA interacts with all four SSB subunits, is stable at high salt, [NaCl] ≥ 0.2 M. This binding mode displays "limited" type cooperativity, in which the SSB cluster size is limited to clusters of two SSB tetramers (Lohman 1994; Raghunathan 2000). There is another minor binding mode of SSB, which is the $(SSB)_{56}$ mode and is grouped with $(SSB)_{65}$ mode by molecular similarity. In the $(SSB)_{56}$ binding mode observed at intermediate [NaCl], all four subunits interact with DNA, but the details of the interaction remain unknown (Kuil 1990) (Figure 1.6). The concentration of monovalent and divalent cations, protein concentrations, pH, and temperature influence the stability of these modes. Recently, single molecule fluorescence resonance energy transfer (smFRET) experiments (Ha 2001; Ha 2001) determined the direct dynamics of structural changes between the two binding modes, "35" and "65" (Roy 2007) (Figure 1.6). These smFRET experiments revealed the two major binding modes, $(SSB)_{35}$ and $(SSB)_{65}$, as well as a new binding configuration, $(SSB)_{35b}$, which can be formed from the $(SSB)_{35}$ mode without protein dissociation (Roy 2007).

Interaction with other proteins

It has been known that a major function of SSB is to protect ssDNA from nuclease degradation *in vitro* (Delagoutte 2003); however, SSB also interacts with several other proteins and modulates their activity. SSB containing a single amino acid substitution (a proline to serine) in the C-terminus still binds ssDNA with similar affinity as wild-type protein, but it does not interact with the χ subunit of DNA polymerase III (Kelman 1998). Recently, Cadman and McGlynn (2000) have revealed that SSB physically interacts with the helicase PriA, which is responsible for restarting DNA replication. This interaction with

SSB stimulates PriA unwinding of branched DNA substrates (Cadman 2004). PriA helicase activity and binding assays using a number of different DNA substrates have shown that SSB significantly stimulates PriA helicase at branched DNA substrates including the lagging strand duplex and the single-stranded leading strand, but not other substrates (Cadman 2004). SSB also interacts with RecQ helicase, which is critical in replication fork maintenance, DNA damage checkpoint signaling, and recombination regulation (Bachrati 2003; Bennett 2004; Ozgenc 2005; Shereda 2007). Helicase and electrophoretic mobility shift assays have revealed that SSB stimulates RecQ unwinding of 70-nt 3' overhang DNA (Shereda 2007). The observation of interactions between SSB and these helicases lead to the question of whether or not SSB interacts with SSB.

C-terminus of SSB mediates interactions with proteins

The last 5 amino acids of *E. coli* SSB are negatively charged, making the C-terminus highly acidic. This region is suggested to be involved in interactions with other accessory proteins in DNA replication, recombination and repair (Lohman 1994; Curth 1996; Kelman 1998; Genschel 2000; Handa 2001). The SSB C-terminal domain is required for interactions with proteins, including ExoI (Genschel 2000), the χ subunit of DNA polymerase III (Kelman 1998; Witte 2003), PriA DNA helicase (Cadman 2004) and RecQ helicase (Shereda 2007).

Atomic Force Microscopy (AFM)

Since its invention in 1986, Atomic Force Microscopy (AFM) has been developed as a powerful tool for studying nonconductive, soft, and live biological samples (Bustamante

1995; Fotiadisa 2002). The use of AFM has extended to studies of DNA, RNA, proteins, lipids, carbohydrates, biomolecular complexes, and cells (Ratcliff 2001; Yang 2003).

In AFM, a cantilever is oscillated as it scans the surface of a sample (X- and Y-directions). The deflection of the cantilever, which is caused by forces of interaction between the sample and the tip, is monitored by a laser beam that is reflected into a photodiode. A feedback loop between the piezo and photodiode keeps the amplitude of the cantilever constant through vertical motion of the piezo (Z). A topographic image of the sample is generated by plotting the vertical movement of the piezo (Z-direction) over X, Y positions (Hansma 1993; Bustamante 1995) (Figure. 1.7).

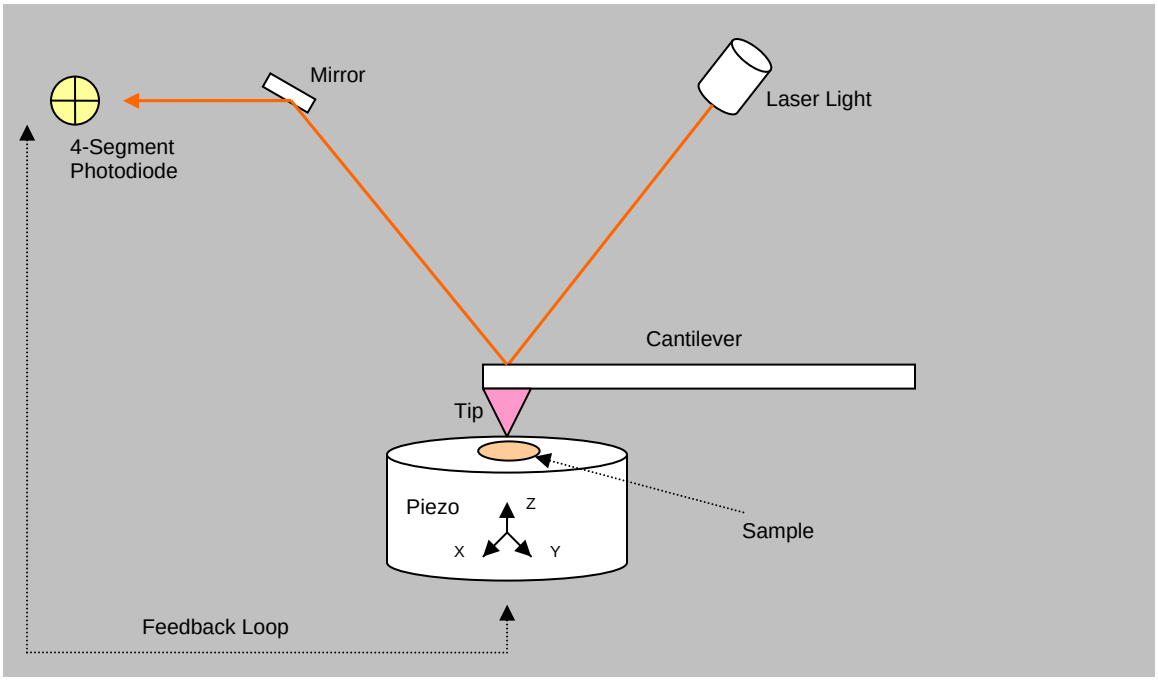

Figure 1.7 Schematic of AFM

The sample is placed on a piezo, which is scanned in the X and Y directions by a tip attached to a cantilever. The laser monitors the tip over the sample and measures the vertical deflection of the cantilever. The feedback loop keeps the cantilever deflection constant. The z movement of the scanner is plotted over x, y positions.

AFM was developed as a powerful tool for studing protein-protein and protein-DNA complexes, mainly with its relative simplicity and reliability in sample preparation and imaging processes, contributing to the majority of the AFM studies of biological assemblies.

It has been demonstrated that there is a linear relationship between AFM scan volume and molecular weight of proteins which allows the stoichiometries and the oligomerization states of proteins and a multi-protein complex to be determined. In addition, it is possible to estimate protein-protein and protein-DNA binding constants (Ratcliff 2001; Yang 2005), as well as visualize conformational changes including bending and wrapping of a protein and protein-DNA complexes (Bustamante 1996; Rivetti 1999; Rivetti 2003; Yang 2003), suggesting that specific recognition sites of proteins on DNA, i.e. the binding specificity of protein to a site in DNA, can be observed. As the mismatch repair machinery corrects mismatches in base-pairing, AFM imaging is a useful technique for structure-function relationships of proteins involved in MMR (Wang 2003; Yang 2005).

References

Abbel-Monem, M., Channal, M. C. and Hoffmann-Berling, H. (1977). "DNA unwinding enzyme II of Escherichia coli. 2. Characterization of the DNA unwinding activity." Eur. J. Biochem. **79**: 39-45.

Abdel-Monem, M., Channal, M. C. and Hoffmann-Berling, H. (1977). "DNA unwinding enzyme II of Escherichia coli. 1. Purification and characterization of the ATPase activity." Eur. J. Biochem. **79**: 33-38.

Ali, J. A. M., N. K. and Lohman, T. M. (1999). "An oligomeric form of *E. coli* UvrD is required for optimal helicase activity " J. Mol. Biol. **293**: 815-834.

Ali, M. M., Roe, S. M., Vaughan, C. K., Meyer, P., Panaretou, B., Piper, P. W., Prodromou, C., and Pearl, L. H. (2006). "Crystal structure of an Hsp90-nucleotide-p23/Sba1 closed chaperone complex." Nature **440**: 1013-1017.

Allen, D. J., Markhow, A., Grilley, M., Taylor, J., Thresher. R., Modrich, P. and Griffith, J. D. (1997). "MutS mediates heteroduplex loop formation by a translocation mechanism." EMBO J. **16**: 4467-4476.

Amaratunga, M. a. L., T. M. (1993). "*E.coli* Rep Helicase Unwinds DNA by an Active Mechanism." Biochmistry **32**: 6815-20.

Au, K. G., Welsh, K. et al. (1992). "Initiation of methyl-directed mismatch repair." J. Biol. Chem. **267**(17): 12142-8.

Bachrati, C. Z., and Hickson, I. D. (2003). " RecQ helicases: suppressors of tumorigenesis and premature aging" Biochem. J. **374**: 577-606.

Ban, C., Junop, M. and Yang, W. (1999). "Transformation of MutL by ATP binding and hydrolysis: a switch in DNA mismatch repair." Cell **97**: 85-97.

Ban, C. a. Y., W. (1998). "Crystal structure and ATPase activity of MutL: implications for DNA repair and mutagenesis." Cell **95**: 541-552.

Bennett, R. J., and Keck, J. L. (2004). " Structure and function of RecQ DNA helicases" Crit. Rev. Biochem. Mol. Biol. **39**: 79-97.

Bird, L. E., Subramanya, H. S. and Wigley, D. B. (1998). "Helicases, a unifying structural theme?" Curr. Opin. Struct. Biol. **8**: 14-18.

Bjornson, K. P., Amaratunga, M., Moore, K. J. M. and Lohman, T. M. (1994). "Single-turnover Kinetics of Helicase-catalyzed DNA Unwinding Monitored Continuously by Fluorescence Energy Transfer." Biochmistry **33**: 14306-16.

Blackwell, L. J., Martik, D., Bjornson, K. P., Bjornson, E. S. and Modrich, P. (1998). "Nucleotide-promoted release of hMutSα from heteroduplex DNA is consistent with an ATP-dependent translocation mechanism." J. Biol.Chem. **273**: 32055-32062.

Brendza, K. M. e. a. (2005). "Auto-inhibition of *E. coli* Rep monomer helicase activity by its 2B sub-domain." Proc. Natl. Acad. Sci. **102**: 10081.

Buermeyer, A. B., Deschenes, S. M., Baker, S. M., Liskay, R. M. (1999). "Mammalian DNA Mismatch Repair." Annu. Rev. Genet. **33**: 533-564.

Bustamante, C. a. K., D. (1995). "Scanning Force Microscopy in Biology." Physics Today **48**: 32-38.

Bustamante, C. a. R., C. (1996). "Visualizing protein-nucleic acid interactions on a large scale with the scanning force microscope." Annu. Rev. Biophys. Biomol. Struct **25**: 395-429.

Cadman, C. J., and Mcglynn, P. (2004). "PriA helicase and SSB interact physically and functionally." Nucleic Acids Res. **32**: 6378-6397.

Caron, P. R., Kushner, S. and Grossman, L. (1985). "Involvement of helicase Ii (uvrD gene product) and DNA polymerase I in excision mediated by the UvrABC protein complex." Proc. Natl. Acad. Sci. U. S. A. **82**: 4925-4929.

Caruthers, J. M., and McKay, D. B. (2002). "Helicase structure and mechanism." Curr. Opin. Struct. Biol. **12**: 123-133.

Chao, K., Lohman, T. M. (1991). "DNA-induced dimerization of the *Escherichia coli* Rep helicase." J. Mol. Biol. **221**: 1165-81.

Chase, J. W., L'Italien, J. J., Murphy, J. B., Spicer, E. K. and Williams, K. R. (1984). "Characterization of the Escherichia coli SSB-113 mutant single-stranded DNA-binding protein. Cloning of the gene, DNA and protein sequence analysis, high pressure liquid chromatography peptide mapping, and DNA-binding studies" J. Biol. Chem. **259**: 805-814.

Chase, J. W. W., K. R. (1986). "Single-stranded DNA binding proteins required for DNA replication." Annu. Rev. Biochem. **55**: 103-136.

Cheng, W., Hsieh, J., Brendza, K. M. and Lohman, T. M. (2001). "*E.coli* Rep oligomers are required to initiate DNA unwinding *in vitro*." J. Mol. Biol. **310**: 327-350.

Chu, F., Maynard, J. C., Chiosis, G., Nicchitta, C. V., and Burlingame, A. L. (2006). "Identification of novel quaternary domain interactions in the Hsp90 chaperone, GRP94." Protein Sci. **15**: 1260-1269.

Cooper, D. L., Lahue, R. S. , and Modrich, P. (1993). "Methyl-directed mismatch repair is bidirectional." J. Biol. Chem. **268** 11823-11829

Corbett, K. D., and Berger, J. M. (2003). "Structure of the topoisomerase VI-B subunit: implications for type II topoisomerase mechanism and evolution." EMBO J. **22**: 151-163.

Curth, U., Genschel,J., Urbanke,C. and Greipel,J. (1996). "In vitro and in vivo function of the C-terminus of Escherichia coli single-strandedDNA binding protein. ." Nucleic Acids Res. **24**: 2706–2711.

Dabrowski, S., Olszewski, M., Piatek, R., Brillowska-Dabrowska, A., Konopa, G. and Kur, J. (2002). "Identification and characterization of single-stranded DNA binding proteins fro *Thermus thermophilus* and *Thermus aquaticus*-new arrangement of binding domains." Microbiology **148**: 3307-3315.

Dao, V. a. M., P. (1998). "Mismatch-, MutS-, MutL-, and Helicase II-dependent unwinding from the single-strand break of an incised heteroduplex." J. Biol. Chem. **273**: 9202-9207.

de la Chapelle, A. (2004). "Genetic predisposition to colorectal cancer." Nat. Rev. Cancer **4**: 769-780.

Delagoutte, E. a. v. H., Peter H. (2003). "Helicase mechanisms and the coupling of helicases within macromolecular machines. Part II." Q. Rev. Biophys. **36**: 1-69.

Dollins, D. E., Immormino, R. M., and Gewirth, D. T. (2005). "Structure of unliganded GRP94, the endoplasmic reticulum Hsp90. Basis for nucleotide-induced conformational change." J. Biol. Chem. **280**: 30438-30447.

Drotschmann, K., Aronshtam, A., Fritz, H. J. and Marins, M. G. (1998). "*The Escherichia coli* MutL protein stimulates binding of Vsr and MutS to heteroduplex DNA." Nucleic Acids Res. **26**: 948-953.

Dutta, R., and Inouye, M. (2000). "GHKL, an emergent ATPase/kinase superfamily. ." Trends Biochem. Sci. **25**: 24-28.

Eggington, J. M., Haruta, N., Wood, E. A. and Cox, M. M. (2004). "The single-stranded DNA binding protein of Deincoccus radiodurans." BMC Microbiol **4**: 2.

Eshleman, J. R., Markowitz, S. D. (1995). "Microsatellite instability in inherited and sporadic neoplasms." Curr. Opin. Oncol. **7**: 83-89.

Fay, P. J., Johanson, K. O., MaHenry, C. S. and Bambara, R. A. (1982). "Size classes of products synthesized processively by two subassemblies of *Escherichia coli* DNA polymerase III holoenzyme." J. Biol. Chem. **257**: 5692-99.

Fedorov, R., Witte, G., Urbanke, C., Manstein, D. J. and Curth, U. (2006). "3D structure of *Thermus aquaticus* single-stranded DNA-binding protein gives insight into the functioning of SSB proteins." Nucleic Acids Res. **34**: 6708-6717.

Ferrari, M. E. B., W. and Lohman, T. M. (1994). "Co-operative binding of *Escherichia coli* SSB tetramers to single-stranded DNA in the (SSB)35 binding mode." J. Mol. Biol. **236**: 106-123.

Fotiadisa, D., Scheuringa, S., Müllera, S. A., Engela, A. and Müller, D. J. (2002). "Imaging and manipulation of biological structures with the AFM " Micron **33**: 385-397.

Genschel, J., Curth,U. and Urbanke,C. (2000). "Interaction of E. coli single-stranded DNA binding protein (SSB) with exonuclease I. The carboxy-terminus of SSB is the recognition site for the nuclease." Biol. Chem. **381**: 183–192.

Gorbalenya, A. E. a. K., E. V. (1993). "Helicases: amino acid sequence comparisons and structure-function relationships." Curr. Opin. Struct. Biol. **3**: 419-429.

Gradia, S., Subramanian, D., Wilson, T., Acharya, S., Makhov, A., Griffith, J. and Fishel, R. (1999). "hMSH2-hMSH6 forms a hydrolysis-independent sliding clamp on mismatched DNA." Mol. Cell. Biol **3**: 255-261.

Grilley, M., Griffith, J., and Modrich, P. (1993). "Bidirectional excision in methyl-directed mismatch repair." J. Biol. Chem. **268**: 11830-11837

Grilley, M., Welsh, K. M., Su, S.-S., and Modrich, P. (1989). "Isolation and Characterization of the Escherichia coli mutL Gene Product." J. Biol. Chem. **264**: 1000-1004

Guarne, A., Junop, M. S., and Yang, W. (2001). "Structure and function of the N-terminal 40 Da fragment of human PMS2: a monomeric GHL ATPase." EMBO J. **20**: 5521-5531.

Gulbis, J. M., Kazmirski, S. L., Finkelstein, J., Kelman, Z., O'Donnell, M., and Kuriyan, J. (2004). "Crystal structure of the chi:psi subassembly of the *Escherichia coli* DNA polymerase clamp-loader complex." Eur. J. Biochem. **271**: 439-449.

Ha, T. (2001). "Single-mlecule fluorescence resonance energy transfer." Methods **25**: 78-86.

Ha, T. (2001). "Single-molecule fluorescence methods for the study of nucleic acids." Curr. Opin. Struct. Biol. **11**: 287-292.

Ha, T. e. a. (2002). "Initiation and reinitiation of DNA unwinding by the *Escherichia coli* Rep helicase." Nature **419**: 638-641.

Haber, L. T. a. W., G. C. (1991). "Altering the conserved nucleotide binding motif in the Salmonella typhimurium MutS mismatch repair protein affects both its ATPase and mismatch binding activities." EMBO J. **10**: 2707-2715.

Hall, M. C., Jordan, J. R. and Matson, S. W. (1998). "Evidence for a physical interaction between the *Escherichia coli* methyl-directed mismatch repair proteins MutL and UvrD." EMBO J. **17**: 1535-1541.

Hall, M. C., Matson, S. W. (1999). "The Escherichia coli MutL protein physically interacts with MutH and stimulates the MutH-associated endonuclease activity." J. Biol. Chem. **274**: 1306-1312.

Handa, P., Acharya,N. and Varshney,U. (2001). "Chimeras between single-stranded DNA-binding proteins from Escherichia coli and Mycobacterium tuberculosis reveal that their C-terminal domains interact with uracil DNA glycosylases." J. Biol. Chem. **276**: 16992–16997.

Hansma, H. G., Sinsheimer, R. L., Groppe, J., Bruice, T. C., Elings, V., Gurley, G., Bezanilla, M., Mastrangelo, I. A., Hough, P. V. and Hansma, P. K. (1993). "Recent advances in atomic force microscopy of DNA." Scanning **15**: 296-299.

Harfe, B. D. a. J.-R., S. (2000). "Mismatch repair porteins and mitotic genome stability." Mutat. Res. **451**(1-2): 151-167.

Harmon, F. G. a. K., S. C. (2001). "Biochemical characterization of the DNA helicase activity of the *Escherichia coli* RecQ helicase." J. Biol. Chem. **276**(1): 232-243.

Hodgman, T. C. (1988). "A new superfamily of replicative proteins." Nature **333**: 22-23.

Hsieh, P. (2001). "Molecular mechanisms of DNA mismatch repair." Mutat. Res. **486**(2): 71-87.

Hu, X., Machius, M., and Yang, W. (2003). "Monovalent cation dependence and preference of GHKL ATPases and kinases." FEBS lett. **544**: 268-273.

Hurley, J. M., Chervitz, S. A., Jarvis, T. C., Singer, B. S. and Gold, L. (1993). " Assembly of the bacteriophage T4 replication machine requires the acidic carboxy terminus of gene 32 protein." J. Mol. Biol. **229**: 398-418.

Husain, I., van Houten, B., Thomas, D. C., Abdel-monem, M. and Sangar, A. (1985). "Effect of DNA polymerase I and DNA helicase II on the turnover rate of UvrABC excision nuclease." Proc. Natl. Acad. Sci. U. S. A. **82**: 6774-6778.

Immormino, R. M., Dollins, D. E., Shaffer, P. L., Soldano, K. L., Walker, M. A. and Gewirth, D. T. (2004). "Ligand-induced conformational shift in the N-terminal domain of GRP94, an Hsp90 chaperone." J. Biol. Chem. **279**: 46162-46171.

Jiang, H., Giedroc, D. and Kodadek, T. (1993). " The role of protein-protein interactions in the assembly of the presynaptic filament for T4 homologous recombination" J. Biol. Chem. **268**: 7904-7911.

Jiricny, J. (1998). "Replication errors: cha(lle)nging the genome." EMBO J. **17**(6427-6436).

Jiricny, J. a. G. M. (2003). "DNA repair defects in colon cancer." Curr. Opin. Genet Dev. **13**(1): 61-69.

Jones, J. M. a. N., H. (1999). "Duplex opening by primosome protein PriA for replisome assembly on a recombination intermediate." J. Mol. Biol. **289**: 503-516.

Jones, J. M. a. N., H. (2001). "*Escherichia coli* PriA Helicase:fork binding orients the helicase to unwind the lagging strand side of arrested replication forks." J. Mol. Biol. **312**: 935-947.

Junop, M. S., Obmolova, G., Rausch, K., Hsieh, P. and Yang, W. (2001). "Composite active site of an ABC ATPase MutS uses ATP to verify mismatch recognition and authorize DNA repair." Mol. Cell **7**(1): 1-12.

Kelman, Z., Yuzhakov,A., Andjelkovic,J. and O'Donnell,M. (1998). "Devoted to the lagging strand-the c subunit of DNA polymerase III holoenzyme contacts SSB to promote processive elongation and sliding clamp assembly." EMBO J. **17**: 2436–2449.

Kolodner, R. (1996). "Biochemistry and genetics of eukaryotic mismatch repair." Genes Dev. **10**: 1433-1442.

Kolodner, R. D., Marsischky, G.T. (1999). "Eukaryotic DNA mismatch repair." Curr. Opin. Genet Dev. **9**(1): 89-96.

Kosinskia, J., Steindorfa, I., Bujnickib, J. M., Giron-Monzona, L., andFriedhoff, P. (2005). "Analysis of the Quaternary Structure of the MutL C-terminal Domain." J. Mol. Biol. **351**(4): 895-909.

Kuhn, B. M., Abdel-Monem, M., and Hoffmann-Berling, H (1978). "DNA helicases." Cold Spring Harbor Symp. Quant. Biol. **43**: 63-67.

Kuhn, B. M., Abdel-Monem, M., Krell, H., and Hoffmann-Berling, H (1979). "Evidence for two mechanisms for DNA unwinding catalyzed by DNA helicases " J. Biol. Chem. **254**: 11343-11350.

Kuhn, H., Protozanova, E., and Demidov, V. (2002). "Monitoring of single nicks in duplex DNA by gel electrophoretic mobility-shift assay." Electrohporesis **23**: 2384-2387.

Kuil, M. E., Holmlund, K., Vlaanderen, C. A., and van Grondelle, R. (1990). " Study of the binding of single-stranded DNA-binding protein to DNA and poly(rA) using electric field induced birefringence and circular dichroism spectroscopy" Biochmistry **29**: 8184-8189.

Kumura, K., Sekiguchi, M., Steinum, A. L. and Seeberg, E. (1985). "Stimulation of the UvrABC enzyme-catalyzed reactions by the UvrD protein (DNA helicase II)." Nucleic Acids Res. **13**: 1483-1492.

Lahue, R. S., Au, K. G., and Modrich, P. (1989). "DNA mismatch correction in a defined system." Science **245**: 160-164.

Lamers, M. H., Perrakis, A., Enzlin, J. H., Winterwerp, H. H. K., de Wind, N. and Sixma, T. K. (2000). "The crystal structure of DNA mismatch repair protein MutS binding to a G•T mismatch." nature **407**: 711-717.

LeBowitz, J. H. a. M., R. (1986). "The *Escherichia coli* dnaB replication protein is a DNA helicase." J. Biol. Chem. **261**: 4738-4748.

Lee, J. Y., and Yang, W. (2006). "UvrD helicase unwinds DNA one base pair at a time by a two-part power stroke." Cell **127**: 1349-1360.

Lohman, T. M. (1992). "*E.coli* DNA Helicases: Mechanisms of DNA Unwinding." Mol. Microbial. **6**: 5-14.

Lohman, T. M. (1993). "Helicase-catalyzed DNA Unwinding." J. Biol. Chem. **268**: 2269-72.

Lohman, T. M., Chao, K., Green, J. M. Sage, S. and Runyon, G. T. (1989). "Large-scale purification and characterization of the *Escherichia coli* rep gene product." J. Biol. Chem. **264**: 10139-10147.

Lohman, T. M. a. B., K. P. (1996). "Mechanisms of helicase-catalyzed DNA unwinding." Annu. Rev. Biochem. **65**: 169.

Lohman, T. M. F., M. E. (1994). "*Escherichia coli* single-stranded DNA-binding protein: Multiple DNA-binding modes and cooperativites." Annu. Rev. Biochem. **63**: 527-570.

Lyer, L. M., Leipe, D. D., Koonin, E V. and Aravind, L. (2004). "Evolutionary history and higher order classification of AAA+ATPases." J. Struct. Biol. **146**: 11-31.

Maluf, N. K., Fischer, C. J. and Lohman, T. M. (2003). "A dimer of Escherichia coli UvrD is the active form of the helicase in vitro." J. Mol. Biol. **325**: 913–935.

Maluf, N. K., Lohman, T.M. (2003). "Self-association equilibria of *Escherichia coli* UvrD helicase studied by analytical ultracentrifugation." J. Mol. Biol. **325**: 889-912.

Matson, S. W. (1986). "Escherichia coli helicase II (urvD gene product) translocates unidirectionally in a 3' to 5' direction." J. Biol. Chem. **261**: 10169-10175.

Matson, S. W., Bean, D. W. and George, J. W. (1994). "DNA helicases: Enzymes with essential roles in all aspects of DNA metabolism." BioEssays **16**(1): 13-22.

Matson, S. W. a. G., J. W. (1987). "DNA helicase II of *Escherichia coli*. Characterization of the single-stranded DNA-dependent NTPase and helicase activities." J. Biol. Chem. **262**: 2066-2076.

Matson, S. W. a. K.-R., K. A. (1990). "DNA helicases." Annu. Rev. Biochem. **59**: 289–329.

Mechanic, L. E., Frankel, B. A. and Matson, S. W. (2000). "*Excherichia coli* MutL loads DNA helicase II onto DNA." J. Biol. Chem. **275**: 38337-38346.

Mechanic, L. E., Hall, M. C. and Matson, S. W. (1999). "Escherichia coli DNA helicase II is active as a monomer." J. Biol. Chem. **274**: 12488–12498.

Meyer, R. R. L., P.S. (1990). "The single-stranded DNA-binding protein of *Escherichia coli*." Microbiol. Rev. **54**: 342-380.

Modrich, P. (1987). "DNA Mismatch Correction." Annu. Rev. Biochem. **56**: 435-466

Modrich, P. (1994). "Mismatch repair, genetic stability, and cancer." Science **266**: 1959-1960.

Modrich, P. a. L., R. (1996). "Mismatch repair in replication fidelity, genetic recombination, and cancer biology." Annu. Rev. Biochem. **65**: 101-133.

Molineux, I. J. a. G., M. L. (1974). " Properties of the Escherichia coli DNA Binding (Unwinding) Protein: Interaction with DNA Polymerase and DNA" Proc. Natl. Acad. Sci. U. S. A. **71**: 3858-62.

Moore, K. J. M. a. L., T. M. (1994). "Kinetic Mechanism of Adenine Nucleotide Binding to the *E. coli* Rep Monomer. II. Application of a Kinetic Competition Approach." Biochmistry **33**: 14565-78.

Moore, K. J. M. a. L., T. M. (1994). "Kinetic Mechanism of Adenine Nucleotide Binding to and Hydrolysis by the *E. coli* Rep Monomer. I. Use of Fluorescent Nucleotide Analogues." Biochmistry **33**: 14550-64.

Natrajan, G., M. H. Lamers, et al (2003). "Structures of Escherichia coli DNA mismatch repair enzyme MutS in complex with different mismatches: a common recognition mode for diverse substrates." Nucleic Acids Res. **31**: 4814-4821.

Obmolova, G., Ban, C., Hsieh, P. and Yang, W. (2000). "Crystal structure of mismatch repair protein MutS and its complex with a substrate DNA." Nature **407**: 703-710.

Oeda, K., Horiuchi, T. and Sekiguchi, M. (1982). "The UvrD gene of E. coli encodes a DNA-dependent ATPase." Nature **298**: 98-100.

Orren D. K., S., C. P., Hearst, J. E. and Sancar, A. (1992). "Post-incision steps of nucleotide excision repair in *Escherichia coli*. Disassembly of the UvrBC-DNA complex by helicase II and DNA polymerase I." J. Biol. Chem. **267**: 780-788.

Ozgenc, A., and Loeb, L. A. (2005). " Current advances in unraveling the function of the Werner syndrome protein" Mutat. Res. **577**: 237-251.

Pang, Q., Prolla, T. A. and Liskay, M. (1997). "Functional domains of the Saccharomyces cerevisiae Mlh1pand Pms1p DNA mismatch repair protein and their relevance to human hereditary nonpolyposis colorectal cancer-associated mutations." Mol. Cell. Biol **17**: 4465-4473.

Peltomaki, P. (2001). " DNA mismatch repair and cancer" Mutat. Res. **488**(77-85): 77.

Peltomaki, P. (2003). " Role of DNA Mismatch Repair Defects in the Pathogenesis of Human Cancer" J. Clin. Oncol. **21**: 1174-1179.

Petit, M. A., Dervyn, E., Rose, M., Entian, K. D., McGovern, S., Ehrich, S. D. and Bruand, C (1998). "PcrA is an essential DNA helicase of Bacillus subtilis fulfilling functions in repair and rolling-circle replication." Mol. Microbiol. **29**: 261-273.

Prolla, T. A., Pang, Q., Alani, E., Kolodner, R. D. and Liskay, R. M. (1994). "Interactions between the MSH2, MLH1 and PMS1 proteins during the initiation of DNA mismatch repair." Science **265**: 1091-1093.

Raghunathan, S., Kozlov, A. G., Lohman, T. M. and Waksman, G. (2000). "Structure of the DNA binding domain of *E. coli* SSB bound to ssDNA." Nature Struct. Biol. **7**: 648-652.

Ratcliff, G. C., and Erie, D. A. (2001). "A novel single-molecule study to determine protein-protein association constants." J.Am. Chem. Soc. **123**: 5632-5635.

Rivetti, C., Codeluppi, S., Dieci, G. and Bustamante, C. (2003). "Visualizing RNA extrusion and DNA wrapping in transcription elongation complexes of bacterial and eukaryotic RNA polymerases." J. Mol. Biol. **326**(5): 1413-1426.

Rivetti, C., Guthold, M. and Bustamante, C. (1996). "Scanning force microscopy of DNA deposited onto mica: equilibration versus kinetic trapping studied by statistical polymer chain analysis." J. Mol. Biol. **264**(5): 919-932.

Rivetti, C., Guthold, M. and Bustamante, C. (1999). "Wrapping of DNA around the *E. coli* RNA polymerase open promoter complex." EMBO J. **18**(16): 4464-4475.

Robertson, A., Pattishall, S. R., and Matson, S. W. (2006). "The DNA binding activity of MutL is required for Methyl-directed mismatch repair in *Escherichia coli*." J. Biol. Chem. **281**(13): 8399-8408.

Rowley, P. T. (2005). " Inherited susceptibility to colorectal cancer" Annu. Rev. Med. **56**: 539-554.

Roy, R., Kozlow, A. G., Lohman, T. M., and Ha, T. J. (2007). "Dynamic structural rearrangements between DNA binding modes of *E. coli* SSB protein." J. Mol. Biol. **269**: 1244-1257.

Runyon, G. T., Wong, I. and Lohman, T. M. (1993). "Overexpression, purification, DNA binding , and dimerization of the *Escherichia coli* uvrD gene product (helicase II)." Biochmistry **32**: 602-612.

Sacho, E. J., Kadyrov, F., Modrich, P., Kuncel, T. A. and Erie, D. A. (2008). "Direct visualization of asymmetric adenine nucleotide-induced conformational changes in MutL(αλπηα)." Mol. Cell **29**: 112-121.

Sancar, A. (1994). "Mechanisms of DNA excision repair. ." Science **266**: 1954-1956.

Sandler, S. J. a. M., K. J. (2000). "Role of PriA in replication fork reactivation in Escherichia coli." J. Bacteriol. **182**: 9-13.

Schofield, M. J., Hsidh, P. (2003). "DNA mismatch repair: Molecular mechanisms and biological fuction." Annu. Rev. Microbiol. **57**: 579-608.

Schofield, M. J., Nayak, S., Scott, T. H., Du, C. and Hsieh, P. (2001). "Interaction of *Escherchia coli* MutS and MutL at a DNA mismatch." J. Biol. Chem. **276**: 28291-28299.

Shereda, R. D., Bernstein, D. A. and Keck, J. L. (2007). "A central role for SSB in E.coli RecQ DNA helicase function." J. Biol. Chem. **282**: 19247-19258.

Shiau, A. K., Harris, S. F., Southworth, D. R., and Agard, D. A. (2006). "Structural analysis of *E. coli* hsp90 reveals dramatic nucleotide-dependent conformational rearrangements." Cell **127**: 329-340.

Sigal, N., Delius, H., Kornberg, T., Gefter, M. L. and Alberts, B. M. (1972). " A DNA-Unwinding Protein Isolated from Escherichia coli: Its Interaction with DNA and with DNA Polymerases" Proc. Natl. Acad. Sci. U. S. A. **69**: 3537-41.

Soultanas, P., Dillingham, M. S., Papadopoulos, F., Philips, S. E. V., Thomas, C. D. and Wigley, D. B. (1999). "Plasmid replication initiator protein RepD increases the processivity of PcrA DNA helicase." Nucleic Acids Res. **27**: 1421-1428.

Soultanas, P., Dillingham, M. S., Wiley, P., Webb, M. R. and Wigley, D. B. (2000). "Uncoupling DNA translocation and helicase activity in PcrA: direct evidence for an active mechanism." EMBO J. **19**: 3799-3810.

Spampinato, C. a. M., P. (2000). "The MutL ATPase Is Required for Mismatch Repair." J. Biol. Chem. **275**: 9863-9869.

Su, S.-S., Lahue, R. S., Au, K. G., and Modrich, P. (1988). "Mispair Specificity of Methyl-directed DNA Mismatch Correction in Vitro." J. Biol. Chem. **263**(14): 6829-6835.

Su, S.-S. a. M., P. (1986). "Escherichia coli mutS-encoded protein binds to mismatched DNA base pairs." Proc. Natl. Acad. Sci. U. S. A. **83**(14): 5057-5061.

Subramanya, H. S., Bird, L. E., Brannigan, J. A., and Wigley, D. B. (1996). "Crystal structure of a DE xx box DNA helicase." Nature **384**: 379-383.

Takahashi, S., Hours, C., Chu, A., and Denhardt, D. T. (1979). "The rep mutation. VI. Purification and properties of the Escherichia coli rep protein, DNA helicase III." Can. J. Biochem. **57**: 855-866.

Umezu, K. a. N., H. (1993). "RecQ DNA helicase of *Escherichia coli* characterization of the helix-unwinding activity with emphasis on the effect of single-stranded DNA-binding protein." J. Mol. Biol. **230**: 1145-1150.

Velankar, S. S., Soltanas, P., Dillingham, M. S., Subramanya, H. S. and Wigley, D. B. (1999). "Crystal structures of complexes of PcrA DNA helicase with a DNA substrate indicate an inchworm mechanism." Cell **97**: 75-84.

von Hippel, P. H. a. D., E. (2003). "Macromolecular complexes that unwind nucleic acids." Bioessays **25**: 1168-1177.

Wang, H., Yang, Y., Schofield, M. J., Du, C., Fridman, Y., Lee, S. D., Larson, E. D., Drummond, J. T., Alani, e., Hsieh, P., and Erie, D. A., (2003). "DNA bending and unbending by MutS govern mismatch recognition and specificity." PNAS **100**(25): 14822-14827.

Welsh, K. M., Lu, A. L., Clark, S., and Modrich, P. (1987). "Isolation and characterization of the Escherichia coli mutH gene product " J. Biol. Chem. **262**: 15624-15629

Williams, K. R., Spicer, E. K., LoPresti, M. B., Guggenheimer, R. A. and Chase, J. W. (1983). J. Biol. Chem. **258**: 3346-3355.

Witte, G., Urbanke, C. & Curth, U. (2003). "DNA polymerase III chi subunit ties single-stranded DNA binding protein to the bacterial replication machinery." Nucleic Acids Res. **31**: 4434-4440.

Witte, G., Urbanke, C. and Curth, U. (2005). "Single-stranded DNA binding protein of Deinococcus radiodurans: a biophysical characterization." Nucleic Acids Res. **33**: 1662-1670.

Wold, M. S. (1997). "Replication protein A: a heterotrimeric, single-stranded DNA-binding protein required for eukaryotic DNA metabolism." Annu. Rev. Biochem. **66**: 61-92.

Wong, I., Amaratunga, M. and Lohman, T. M. (1993). "Heterodimer formation between *Escherichia coli* Rep and UvrD proteins." J. Biol. Chem. **268**: 20386-20391.

Wong, I., and Lohman TM. (1992). "Allosteric Effects of Nucleotide Cofactors on *E. coli* Rep Helicase-DNA Binding." Science **256**: 350-55.

Wong, I., Chao, K. L., Bujalowski, W. and Lohman, T. M. (1992). "DNA-induced Dimerization of the *E. coli* Rep Helicase: Allosteric Effects of Single Stranded and Duplex DNA." J. Biol. Chem. **267**: 7596-610.

Wu, T. H., and Marinus, M. G. (1994). "Dominant negative mutator mutations in the MutS gene of Escherichia coli." J. Bacteriol. **176**: 5393-5400.

Yamaguchi, M., Dao, V. and Modrich, P. (1998). "MutS and MutL activate DNA helicase II in a mismatch-dependent manner." J. Biol. Chem. **273**: 9197-9201.

Yang, Y., Sass, L. E., Du, C., Hsieh, P., Erie, D. (2005). "Determination of protein-DNA binding constants and specificities from statistical analyses of single molecules: MutS-DNA interactions." Nucleic Acids Res. **33**: 4322-4334.

Yang, Y., Wang, H., and Erie, D. A. (2003). "Quantitative characterization of biomolecular assemblies and interactions using atomic force microscopy." Methods **29**: 175-187.

Yuzhakov, A., Kelman, Z. and O' Donnell, M. (1999). "Trading places on DNA- a three-point switch underlies primer handoff from primase to the replicative DNA polymerase." Cell **96**: 153-163.

Chapter 2

Structure-Function studies of the interaction of *E. coli* UvrD and SSB

Introduction

Helicases participate in various cellular processes requiring the manipulation of DNA, including replication, transcription, repair and recombination (Caruthers 2002; Delagoutte 2003). Helicases, which work to separate nucleic acid strands using the energy derived from hydrolysis of ATP, are found in both prokaryotes and eukaryotes (Matson 1994; Lohman 1996). The unwinding of DNA by helicase yields single-stranded (ss) sequences for correcting DNA errors by other proteins, such as DNA polymerases. Thus, helicases play an essential role in genomic maintenance and stability in biological systems.

E.coli Rep helicase, which exists predominantly as a homodimeric protein (Chao 1991; Lohman 1992; Wong 1992; Wong 1992; Amaratunga 1993; Lohman 1993; Bjornson 1994; Moore 1994; Moore 1994), is well characterized in prokaryotes. The dimeric form of Rep helicase appears to be the active form that unwinds duplex DNA and translocates on ssDNA in the 3' to 5' direction using ATP hydrolysis (Cheng 2001; Ha 2002; Brendza 2005).

E. coli DNA helicase II (UvrD gene) is a protein that translocates along DNA and unwinds DNA in ATP dependent and is involved in MMR and nucleotide excision repair (NER) (Sancar 1994; Modrich 1996). UvrD helicase, which shares 37 % sequence identity with Rep (Lee 2006), is an enzyme capable of unwinding duplex DNA in a 3' to 5' direction (Abbel-Monem 1977; Abdel-Monem 1977; Matson 1986). Although many studies have

characterized the oligomeric state of UvrD, some discrepancy exists as to the oligomerization state of the active form. Mechanic *et al*. (Mechanic 1999) identified a mutant of UvrD that is in monomer, even at high concentration of UvrD, and this monomeric form exhibits helicase activity indistinguishable from wtUvrD. Crystal structures of UvrD also suggeste that the monomeric UvrD is the active form (Lee 2006). However, cross-linking studies have shown that UvrD dimers are stabilized by binding to ssDNA (Runyon 1993), and DNA unwinding kinetic studies suggest that UvrD dimers or higher oligomers are the active forms (Ali 1999; Maluf 2003).

Previous studies have suggested that UvrD interacts with other MMR proteins involved in MMR (Hall 1998; Yamaguchi 1998). In the absence of other proteins, UvrD helicase unwinds DNA with a specific 3' to 5' directionality (Matson 1986), however, in MMR, UvrD can unwind DNA in either direction. A interaction between UvrD and MutL has been shown, in which MutL strongly stimulates UvrD helicase activity (Hall 1998; Yamaguchi 1998) Their interaction leads us to the questionary whether UvrD interacts with other proteins that could assist in the loading of UvrD and/or could increase its processivity.

While studies have been done regarding the role of SSB in DNA replication, recombination and repair (Meyer 1990; Lohman 1994), how SSB functions during the mismatch repair process remains unknown. Some studies have shown that interaction of SSB with various helicases plays a critical role in replication. It has been demonstrated that SSB and PriA interact physically, and that SSB stimulates unwinding of DNA duplex by PriA (Cadman 2004). It also has been shown that SSB interaction with RecQ stimulates the activity of RecQ helicase (Shereda 2007). Whether this interaction of SSB and helicases applies to all helicases, however, remains unknown. Based on interactions observed between

SSB and other helicases, we set out to investigate any potential interactions between SSB and UvrD using AFM and other biochemical techniques.

In this study, we demonstrate that UvrD interacts with SSB using AFM. This interaction stimulates UvrD helicase unwinding of DNA. In contrast, SSBΔC10, which does not contain the final 10 residues of C-terminus, neither interacts with UvrD nor stimulates the function of UvrD.

Results

Physical interaction of UvrD and wtSSB

From AFM images, it is possible to determine the stoichiometries and conformational properties of protein-protein and protein-DNA complexes, as well as protein-protein and protein-DNA binding constants (Yang 2005). AFM has been used to investigate structure-function relationships of the proteins involved in DNA mismatch repair (Rivetti 1996; Wang 2003; Yang 2003). There is a linear relationship between AFM volume and the molecular weight of proteins defined by the equation V = (1.2 MW) – 14.7, where V is the volume measured by AFM and MW is the molecular mass. Using this equation, the stoichiometry of proteins can be determined (Ratcliff 2001; Yang 2003). To quantify the volume of the molecules, we counted all molecules in the images and analyzed molecular volume.

To examine whether or not UvrD and SSB interact with one another, we used AFM to visualize UvrD and SSB alone and together, and measured their volumes. Table 2.1 shows the expected volumes based on the molecular weight of the proteins as well as the observed volumes. In the image of UvrD alone, both monomers and dimers can be seen (Figure 2.1A). The histogram of the AFM volumes of UvrD (Figure 2.1C) shows that the majority of

proteins exists around 78 nm^3, which is consistent with a predicted volume for the monomer (Table 2.1). UvrD also exists as a dimer, with a volume around 160 nm^3 (Figrue 2.1C). These results are consistent with previous AFM results (Ratcliff 2001) as well as previous results showing that UvrD exists as monomer and dimer in solution (Runyon 1993; Ali 1999; Mechanic 1999; Maluf 2003). In the image of SSB alone (20 nM in tetramer), tetramers can be seen (Figure 2.1D), consistent with previous studies in which SSB forms a homotetramer (Lohman 1994). The oligomerization of SSB appears to be predominantly tetramer (~58 nm^3) (Figure 2.1F); however, there appear to be some smaller or larger species.

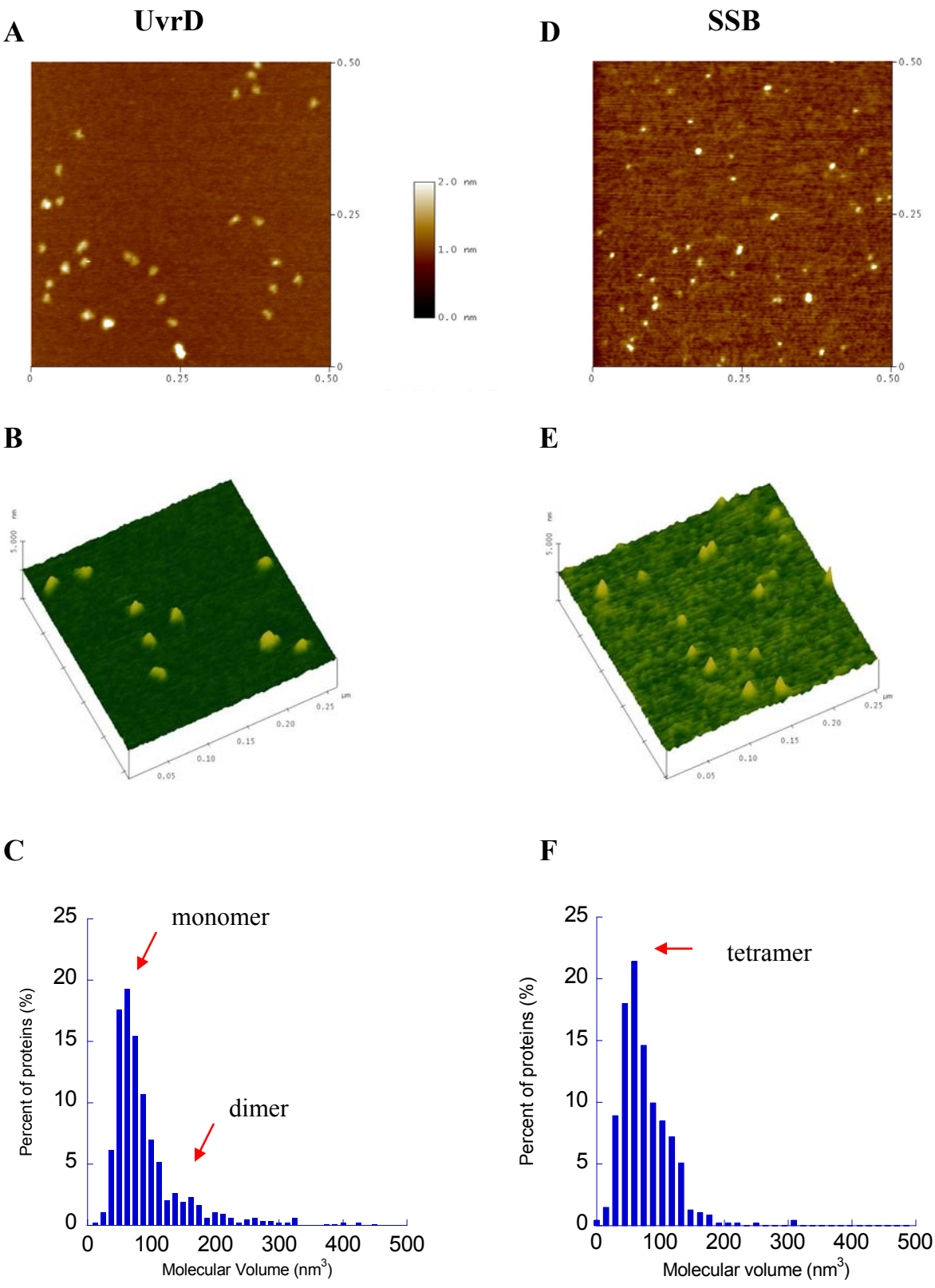
A
UvrD
D
SSB
2.0 nm
1.0 nm
0.0 nm
B
E
C
F
monomer
dimer
Percent of proteins (%)
Molecular Volume (nm3)
tetramer
Molecular volume (nm3)

Figure 2.1

Figure 2.1 Representative of AFM images.

(A) 500 nm x 500 nm images of *E. coli* UvrD deposited in the absence of nucleotide. 20 nM UvrD were deposited onto the mica surface. (B) The image of surface plot of (A) under a same condition. (C) Volume histogram for UvrD (20 nM, n=834). The peaks show the volume for monomer (~78 nm^3) and dimer (~160 nm^3). (D) Representative image of wtSSB. 20 nM in tetramer were deposited. We refer the concentration of SSB as tetramer in all reactions (E) Surface plot of (C). (F) Histogram of wtSSB (20 nM in tetramer, n=505). The oligomerization of SSB is tetramer (~58 nm^3).

complex	molecular mass (kDa)	predicted AFM volume (nm^3)
monomer UvrD	82	83.7
dimer UvrD	162	182
monomer SSB	18	6.9
tetramer SSB	72	71.7
monomer UvrD- tetramer SSB	152	170
dimer UvrD – tetramer SSB	236	268.5

Table 2.1 Predicted AFM volumes for UvrD and SSB

Predicted volumes were calculated by the equation V = (1.2 MW)-14.7, where V is the volume measured by AFM and MW is the molecular mass.

To investigate if UvrD and SSB interact with one another, UvrD and SSB were incubated together, deposited and imaged, these images were compared to those of UvrD or SSB deposited alone. If UvrD interacts with wtSSB, the volume of proteins observed will be larger due to the physical association of the two proteins. The image of UvrD and SSB shows larger volume of complexes compared to those of UvrD or SSB alone (compare Figure 2.1 A and D with 2.2A). Incubation of SSB with UvrD results in a shift of the protein sizes to larger volumes (Figure 2.2C). To compare depositions of UvrD and SSB together with those from deposition of either UvrD or SSB alone, the individual volume histograms for UvrD (Figure 2.1A) and SSB (Figure 2.1D) were summed and divided by 2, and the resultant volumes were plotted for reference in the histogram (Figure 2.2D). The volume distribution would be expected to be similar if there were no interaction between UvrD and SSB. The volume of UvrD and SSB together results in an increase in the population of protein with higher volumes (Figure 2.2D). There is a new peak in the histogram (Figure 2.2D) with a volume of ~180 nm^3, which is consistent with a tetramer of SSB interacting with a monomer of UvrD. This volume would also to be consistent with a dimmer of UvrD but since there is no significant population of this volume in the absence of SSB, it is likely that this peak infact represent a tetramer of SSB and monomer of UvrD. There is also a significant increase in the population of higher volume species that would be consistent with a tetramer of SSB interacting with a dimer of UvrD (Table 2.1). Roughly 30% of the UvrD and SSB proteins appear to be in complexes with one another. This extent of oligomerizatin is consistent with a SSB-UvrD binding constant around 20 nM to 50 nM. These results show that UvrD and SSB interact physically in the absence of nucleotides.

UvrD + SSB

A

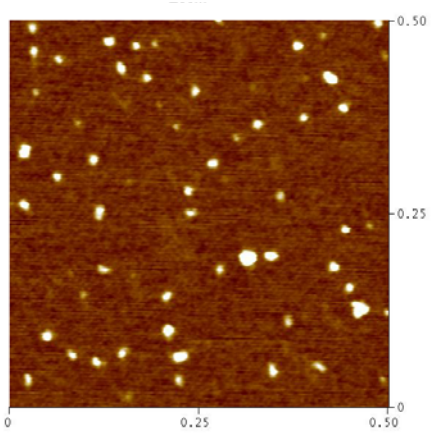

B

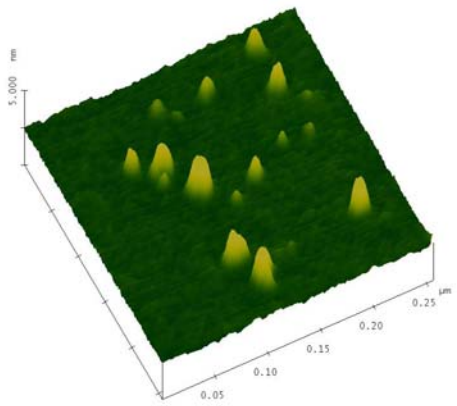

C

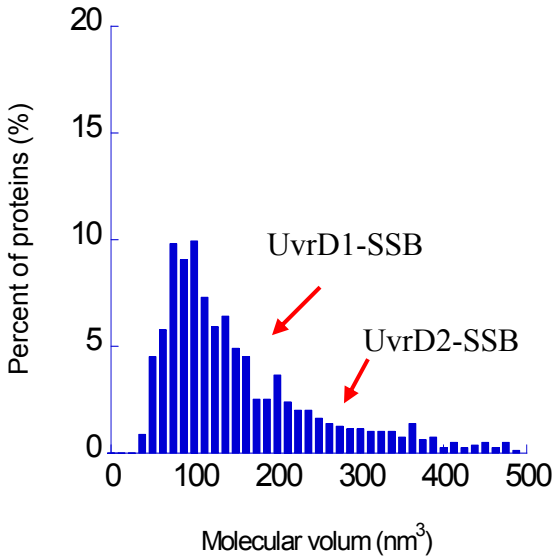

D

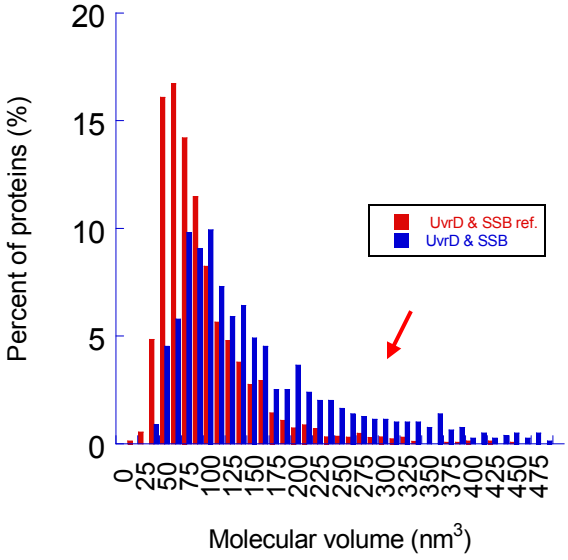

Figure 2.2

Figure 2.2 Histogram of volume

(A) AFM image of UvrD and wtSSB. 16 nM UvrD and 15 nM SSB were deposited under a same condition. (B) Surface plot of (A). All concentration of SSB is in tetramer. (C) Histogram of volume for UvrD (16 nM) and wtSSB (15 nM) in the absence of nucleotide. UvrD and wtSSB (n=795) were analyzed. The peaks around 180 and 265 nm^3 represent the binding of UvrD to wtSSB. The binding of UvrD-SSB are shown (D) Comparison of reference volume and UvrD-SSB volume. Reference histogram of volume for UvrD and wtSSB: summed (A) and (B) data points and divided by 2. The red bars represent the reference volume (A and B) and the blue bars represent (C). The bars are shifted by the interaction of UvrD with wtSSB.

Wild-type SSB stimulates UvrD helicase activity

Our observation that UvrD physically interacts with SSB suggests that SSB may play an important role in the function of helicase activity. To test this idea, the effects of *E. coli* SSB on UvrD helicase activity on double nicked-circular DNA were analyzed. Although nicked duplex DNA is the natural substrate for UvrD, the helicase activity of UvrD on nicked DNA has not studied in detail previously. Thus, we designed this nicked DNA substrate for UvrD helicase reaction. The DNA substrate employed in these studies is a circular double-nicked DNA with a 37-nt fragment labeled on the 5'-end with ^{32}P.

Figures 2.3A and 2.3B show that UvrD (40 nM) by itself promotes unwinding of nicked DNA duplex to a limited extent over time. There is ~10% free fragment at time=0. However, the presence of SSB (200 nM in tetramer), significantly increases the extent of unwinding of these double-nicked DNA substrates (Figure 2.3A and 2.3B). SSB increased unwinding of the substrate by UvrD to ~ 85%, while the unwound DNA products by UvrD alone reached ~ 35% (Figure 2.3B). The initial rate is similar for all reactions, but the extent of unwinding is different (Figure 2.3B).

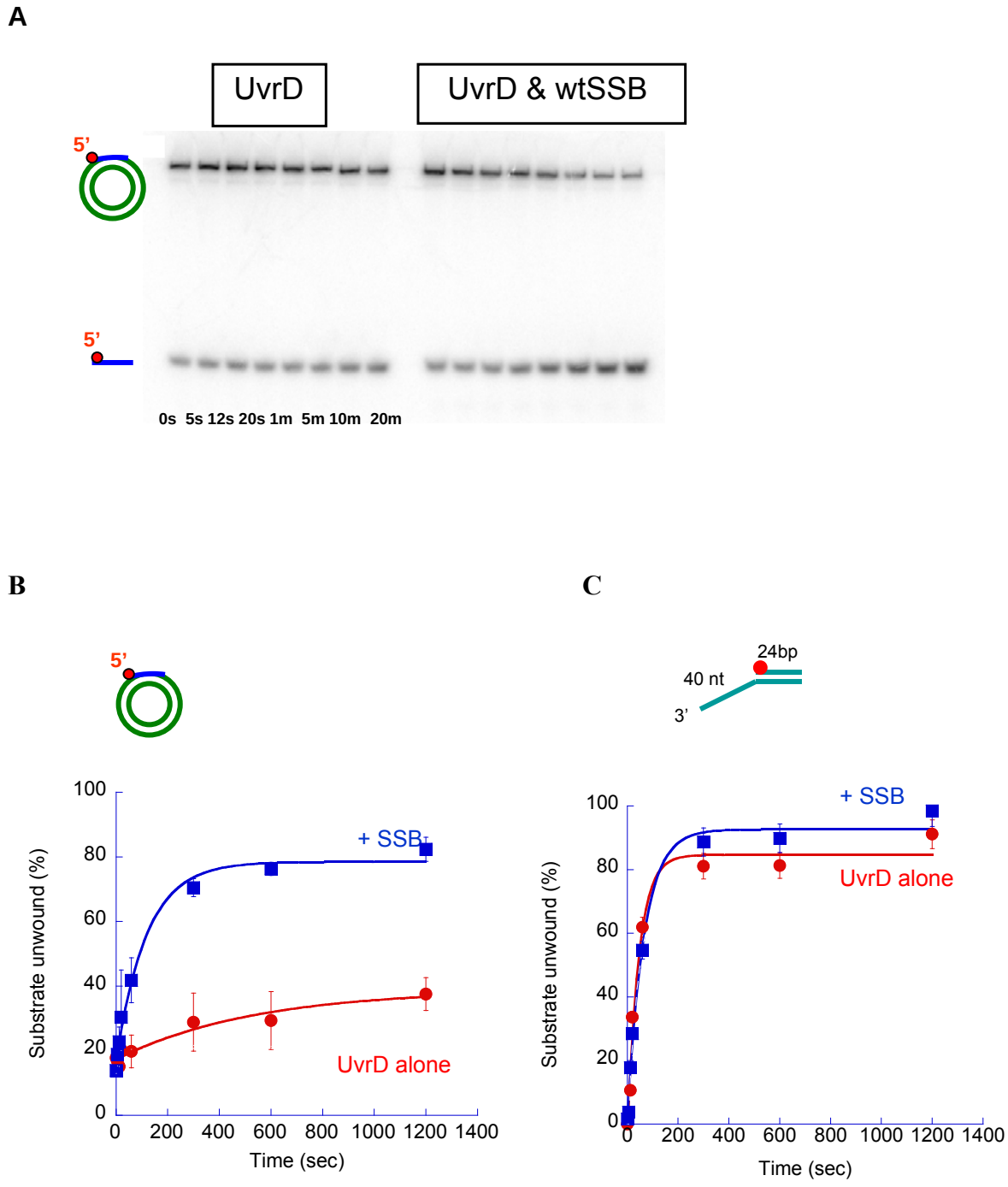
A
UvrD
UvrD & wtSSB
5'
5'
0s 5s 12s 20s 1m 5m 10m 20m
B
5'
100
80
60
40
20
0
Substrate unwound (%)
+ SSB
UvrD alone
0 200 400 600 800 1000 1200 1400
Time (sec)
C
24bp
40 nt
3'
100
80
60
40
20
0
Substrate unwound (%)
+ SSB
UvrD alone
0 200 400 600 800 1000 1200 1400
Time (sec)

Figure 2.3

Figure 2.3 Helicase activity assays of UvrD and UvrD-wtSSB at different substrates. (A) 40 nM UvrD and/or 100 nM wtSSB (in tetramer) was incubated with 4nM of nicked DNA (^{32}P 5'-end labeled) in the reaction buffer (20 mM Tris, 80 mM NaCl, 0.1 mg/ml BSA, 2.6 mM $MgCl_2$, 1 mM DTT). Reactions were initiated by adding 2 mM ATP to the final 10 µl reaction mixture and terminated by the adding 5µl of stop solution (glycerol, EDTA, Bromophenol blue, SDS) at times shown. Upper bands show DNA substrates and the products of unwinding are shown on the bottom. The reaction products were analyzed by electrophoresis on an 8 % non-denaturing polyacrylamide gel. (B) Quantification of unwinding on a double nicked DNA as a function of time. In the presence (blue squares), and absence (red circles) of SSB. Based on concentration-dependent studies (Figure 2.4), we chose an SSB concentration where SSB exhibited the maximal effect or helicase activity. (C) Rates of unwinding of 3' ssDNA extension under the same condition. Symbols are as described in (B)

To examine whether or not the observed SSB stimulation of UvrD unwinding activity depended on the type of DNA substrate, we also used different substrates: a 24 bp blunt DNA and an overhang DNA, with a 24-basepair duplex and a 40-nt 3' overhang. Neither UvrD (40 nM) alone nor with SSB catalyzed the unwinding of blunt DNA, which is consistent with previous studies (Ali 1999). With the 3' overhang DNA, SSB may slightly stimulate UvrD unwinding of overhang DNA substrates (Figure 2.3C). The unwound products by UvrD alone reached to around 80 %, whereas in the presence of SSB, unwinding of substrates by UvrD was increased to 90 %. Since UvrD by itself already catalyzes unwinding of overhang DNA substrates to a high extent, wtSSB may have only a small effect on unwinding of DNA substrates by UvrD. Therefore, the substrate on which biggest effect of SSB on UvrD helicase activity was observed is the nicked DNA. Taken together with the AFM data, these results suggest that the interaction of SSB with UvrD facilitates unwinding of DNA.

Apparent Binding of UvrD-SSB to DNA

To determine the $K_{½}$ for UvrD unwinding of nicked DNA and the $K_{½}$ of SSB for the stimulation of helicase activity, we characterized protein concentration-dependence of helicase unwinding. For these studies, we measured the extent of unwinding at a single time point (10 minutes) as a function of either [UvrD] or [SSB], Figure 2.4A shows that SSB strongly stimulates unwinding of nicked DNA strands by UvrD (40 nM). We measured $K_{½}$ of SSB for the activation of UvrD helicase activity and that value is 4.5 nM (Figure 2.4A), indicating that SSB exhibits a significant effect on helicase activity even at very low concentration.

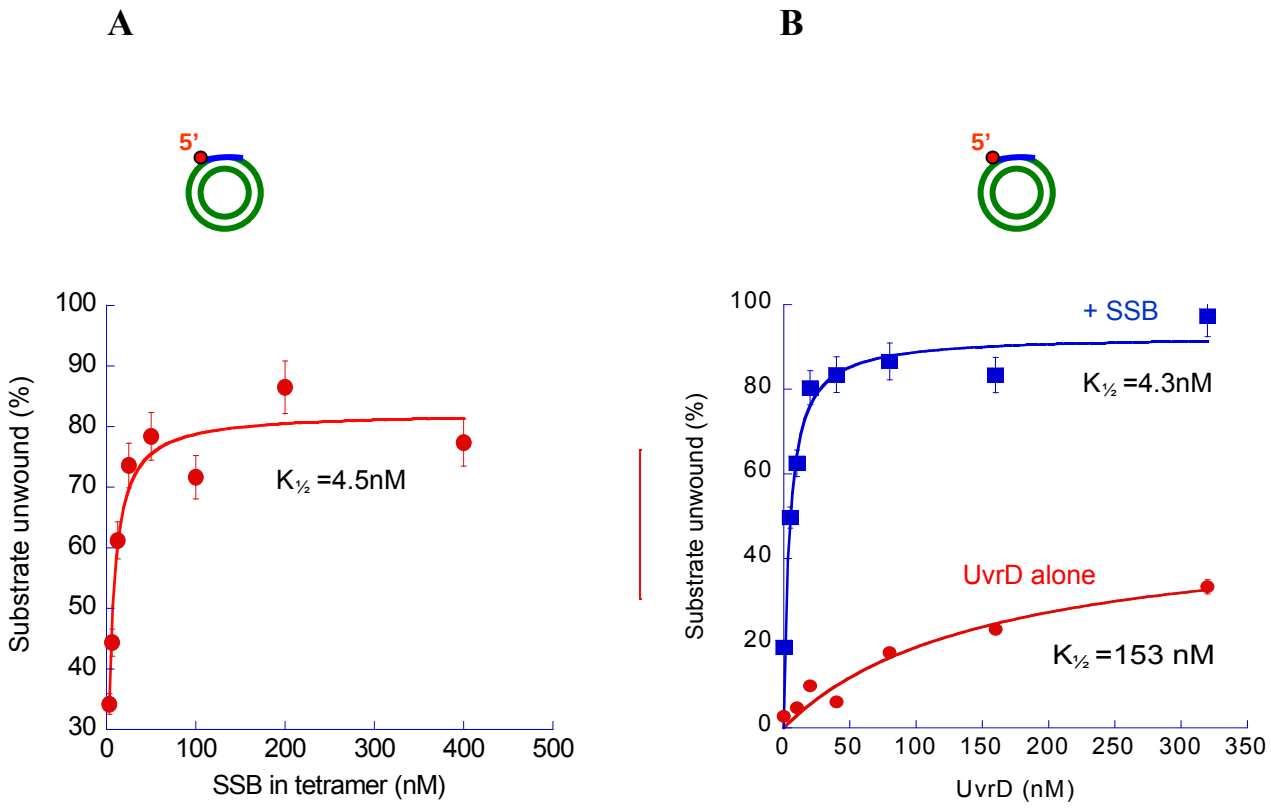
A
B
5'
5'
100
90
80
70
60
50
40
30
Substrate unwound (%)
0
100
200
300
400
500
SSB in tetramer (nM)
K½ =4.5nM
100
80
60
40
20
0
Substrate unwound (%)
+ SSB
K½ =4.3nM
UvrD alone
K½ =153 nM
0
50
100
150
200
250
300
350
UvrD (nM)

Figure 2.4

Figure 2.4 Binding of UvrD and UvrD-wtSSB to DNA substrates.

(A) Unwinding data of UvrD (40 nM) on a double nicked DNA in the presence of increasing concentration of wtSSB. (B) The degree of unwinding with increasing concentration of UvrD protein on a double nicked DNA. In the absence of SSB (red circles), in the presence of wtSSB (200 nM) (blue squares).

These data are consistent with AFM data (Figure 2.2C), which suggest that there is a relatively tight interaction between UvrD and SSB.

To analyze if the stimulation of unwinding of the substrates is due to the interaction of SSB with UvrD, $K_{½}$ of UvrD in the presence of SSB were measured at double-nicked DNA. In this reaction, we chose the highest SSB concentration based on SSB saturation in Figure 2.4A. In the absence of SSB, the $K_{½}$ of UvrD is 153 nM (Figure 2.4B); whereas, in the presence of SSB, $K_{½}$ is 4.3 nM, a 30-fold increase in apparent affinity. These values suggest that wtSSB may increase the binding activity of UvrD to double nicked DNA substrates (Figure 2.4). Interestingly, the $K_{½}$ for UvrD in the presence of SSB is the same as that for SSB on helicase activity. This increase in $K_{½}$ of UvrD in the presence of SSB suggest that SSB may recruit UvrD onto DNA. The data presented above suggest that the stimulation of unwinding of DNA substrates results from direct interaction UvrD with wtSSB.

C-terminus of SSB is required for its interaction with UvrD and the stimulation of UvrD unwinding of DNA

Although our results strongly suggest that interaction of SSB and UvrD stimulates unwinding of DNA, SSB's interaction with ssDNA may be playing a significant role. The final 10 residues of the C-terminus of SSB have previously been shown to mediate its interaction with other proteins, including ExoI (Genschel 2000), the χ subunit of DNA polymerase III (Kelman 1998; Witte 2003), PriA DNA helicase (Cadman 2004) and RecQ helicase (Shereda 2007). Accordingly, we obtained an SSB mutant in which the last 10 residues are deleted (gift from Peter McGlynn) (SSBΔC10) and examined its interaction with helicase and its effect on helicase activity.

We imaged SSBΔC10 alone and in the presence of UvrD (Figure 2.5A and B). The histogram of volume of SSBΔC10 (Figure 2.5C) is similar to that of wtSSB. In contrast, the volume histogram of ΔC10 deposited in the presence of UvrD does not show any significant increase of species with higher volumes volumes (compare Figure 2.2D and 2.5D). Binding of UvrD to SSBΔC10 is not detected, while the complex of wtSSB and UvrD is populated in higher volumes due to the interaction. According to our volume analysis, the majority of volumes are around 80 nm^3, which represents monomer of UvrD or tetramer of SSB, and there is the helicase dimer peak around 170 nm^3 (Figure2.5D). Consistent with AFM images, no peaks were found in higher volumes which indicate the volume of complexes of UvrD and wtSSB in the histogram (Figure 2.2 C). These results show that the SSB C-terminus is required for binding with UvrD, as it is for RecQ (Shereda 2007).

The observation that SSBΔC10 does not interact with UvrD (Figure2.5D), but still binds ssDNA (Cadman 2004) (see Chapter 3), allows us to directly examine the role of the UvrD-SSB interaction in stimulating unwinding. To examine this role, we used SSBΔC10 with either double-nicked circular DNA substrate, or the 3'-40 nt overhang DNA substrate. In the presence of SSBΔC10, no significant unwinding of double-nicked DNA is observed (Figure 2.6A). Experiments showed that SSBΔC10 failed to stimulate UvrD activity on overhang DNA as well (Figure 2.6B). In fact, SSBΔC10 seems to slightly inhibit unwinding of both double-nicked and overhang DNA (Figure 2.6A and B).

UvrD + SSBΔC10

A

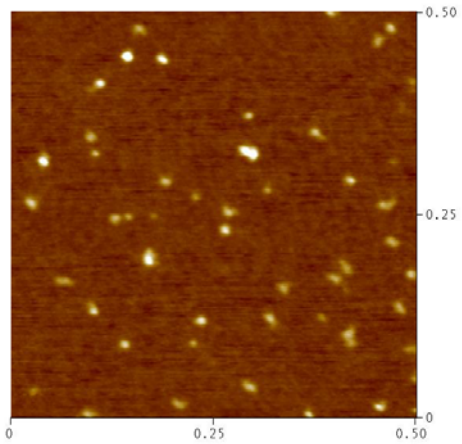

B

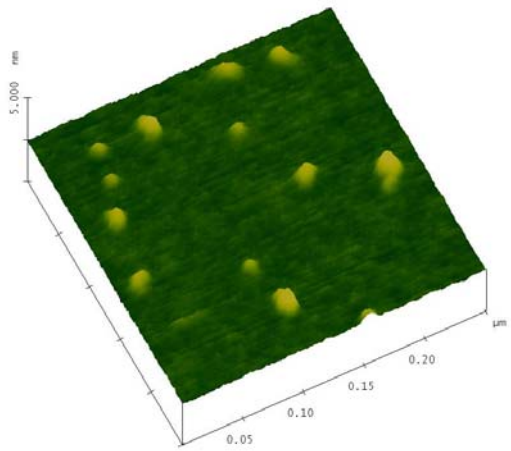

C SSBΔC10

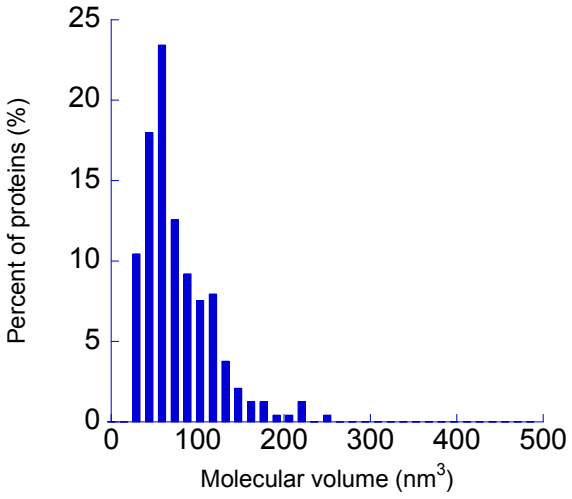

D UvrD+SSBΔC10

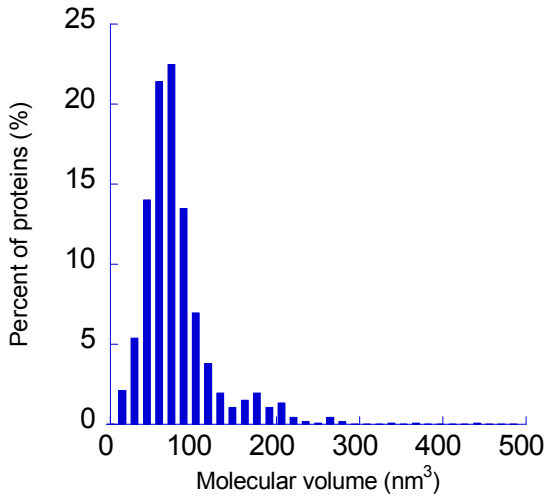

Figure 2.5

Figure 2.5 Representative of AFM images and volume of UvrD and SSBΔC10

(A) AFM image of UvrD (16 nM) and SSBΔC10 (15 nM). Protein data were analyzed under a same condition as Figure 2.1. (B) Surface plot of (A). (C) Histogram of volume of SSBΔC10 (n=410). The solid line shows tetramer states of SSBΔC10. (D) Sum plot of UvrD and SSBΔC10 (n=1135). The solid bars represent that the predominant protein volume is around 80 nm^3.

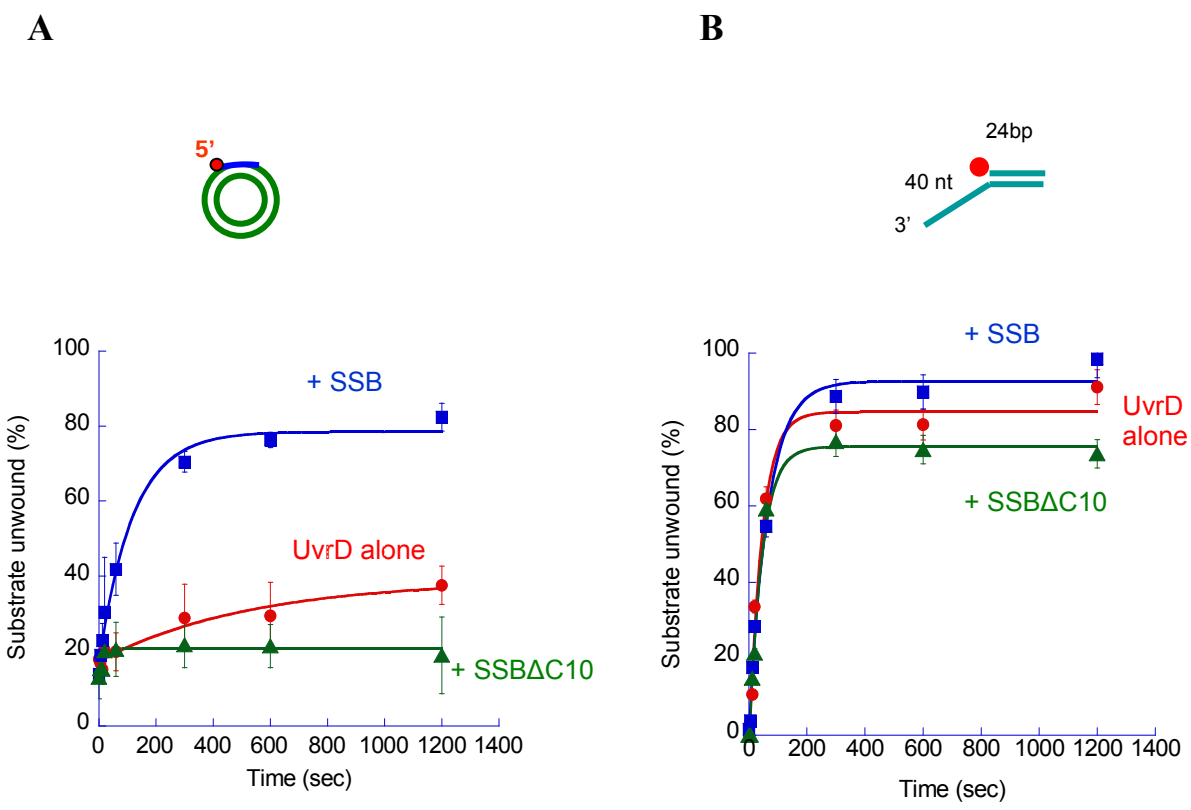
A
B
5'
24bp
40 nt
3'
+ SSB
UvrD alone
+ SSBΔC10
Substrate unwound (%)
Time (sec)
0
20
40
60
80
100
0
200
400
600
800
1000
1200
1400

Figure 2.6

Figure 2.6 Helicase activity assays of UvrD and SSBΔC10

(A) Rates of unwinding on double nicked DNA in the presence of SSBΔC10 (200 nM) (green triangles). (B) Unwinding data for 3' ssDNA extension possessing a 40-nt. Symbols are described in (A).

These results indicate that the stimulation of UvrD on both double-nicked and overhang DNA requires the SSB C-terminus and that stimulation is not due to SSB binding to ssDNA, but due to interactions between UvrD and wtSSB.

Discussion

We were able to observe the binding of *E.coli* SSB to UvrD using AFM. The oligomerization of UvrD-SSB was viewed in the absence of nucleotides and may provide further understanding of the downstream events in the MMR pathway. Biochemical techniques, such as the helicase activity assay, helped to elucidate the properties of this interaction. This interaction stimulated UvrD-catalyzed unwinding activity on nicked DNA.

SSB stimulates UvrD unwinding activity of nicked DNA by physical interaction

Our experiments show that UvrD interacts physically with SSB in the absence of nucleotides. Because UvrD unwinds mismatched DNA strands starting from a nick past the mismatch (Dao 1998), the type of DNA substrate we chose is quite relevant given the nature of UvrD's role. Nicked circular DNA, which is a physiological relevant substrate in living cells, was used in helicase reaction. WtSSB strongly stimulates unwinding of double-nicked DNA by UvrD, while the unwinding by UvrD alone is relatively low (Figure 2.3A). SSB appears to increase the binding affinity of UvrD for the nicked substrates with the $K_{½}$ of UvrD becoming 30 fold tighter in the presence of SSB ($K_{½}$ of UvrD= 153 nM, $K_{½}$ of UvrD-SSB= 4.3 nM) (Figure 2.4). Taken together, these results suggest that SSB increases the binding affinity of UvrD and recruits UvrD onto the DNA.

Although the stimulatory effects of SSB on the unwinding of duplex DNA possessing a 3' ssDNA tail by UvrD is not strong, the amount of products of unwinding by UvrD in the presence of SSB is still higher than those in the absence of SSB (Figure 2.3) and SSBΔC10 appears to slightly inhibit unwinding. Cadman and McGlynn (2004) have studied the functional role of SSB on PriA helicase activity with various DNA substrates. SSB significantly stimulates PriA helicase at branched DNA substrates including the lagging strand duplex and the single-stranded leading strand. In contrast to branched substrates, SSB failed to stimulate PriA unwinding of duplex DNA bearing 3' ssDNA extension, suggesting that SSB may enhance PriA helicase unwinding only on the certain DNA structures (Cadman 2004).

Similarly, in this study, we find that SSB has a large effect on the unwinding of double-nicked DNA but little to no effect on the unwinding of overhang or blunt end DNA. Notably, nicked DNA is the physiological substrate for UvrD. Perhaps this apparent specificity for nicked substrates induced by SSB is involved in directing UvrD to its substrates, in *vivo*.

Function of SSB-C terminus on UvrD helicase activity

We demonstrate that the acidic C-terminus of SSB, which is required for the interaction with other proteins that are necessary in replication and recombination (Curth 1996; Kelman 1998; Genschel 2000; Handa 2001), is also essential for the interaction between SSB and UvrD helicase. SSBΔC10, which is capable of binding ssDNA (Chapter 3), neither interacts with UvrD nor stimulates the function of UvrD (Figure 2.6). These results indicate that the SSB C-terminus mediates its interaction with UvrD and that the stimulation

of UvrD activity is not simply due to binding of SSB to DNA, but infact is a result of the interaction of SSB and UvrD.

It has been suggested that SSBΔC10 might have higher affinity for ssDNA than wild-type SSB (Curth 1996). If this is the case, the results observed with 3' overhang DNA suggest that SSBΔC10 may compete with UvrD for binding to ssDNA and thereby inhibit UvrD helicase unwinding of the substrates.

Conservation of UvrD-SSB binding

The interaction of helicases and SSB has been discovered and characterized within the last decade. *E. coli* PriA helicase, which is a DNA replication restart initiator, is required to load DnaB at repaired forks or D-loops (Sandler 2000). DnaB, which catalyses unwinding of the parental DNA strands (LeBowitz 1986), should be able to load onto ssDNA, which PriA helicase can generate during unwinding of any lagging strand DNA (Jones 1999). Cadman and McGlynn (2004) studied direct physical interaction between PriA and SSB via the C-terminus, and showed that this interaction stimulates PriA helicase activity on branched DNA structures (Cadman 2004). They suggested that the role of the interaction of PriA-SSB C terminus might enhance the loading of DnaB onto ssDNA and further lead to the processivity of unwinding (Cadman 2004). It also has been shown that RecQ helicase interacts with wtSSB, as evidenced by a precipitation (Shereda 2007). Prior to this evidence of interaction between RecQ and wtSSB, studies showing that SSB stimulates RecQ helicase unwinding of DNA had been performed, although the physical interaction of these proteins had not been defined (Umezu 1993; Harmon 2001). The interaction of RecQ with SSB is determined by the binding of the RecQ winged helix domain and the C-terminus of SSB. The

interaction of two proteins stimulates the function of RecQ helicase within duplex DNA bearing 3' ssDNA extension (Shereda 2007). These results taken together with our results suggest that the conserved interaction of helicase-SSB may extend to other cellular processes such as NER (nucleic excision repair). UvrD is involved in the NER process. UvrD and DNA polymerase I participate in the turnover of the UvrABC endonuclease (Caron 1985; Husain 1985; Kumura 1985; Orren D. K. 1992). Whereas biochemical studies have been done with respect to the function of UvrD in NER, the mechanism by which UvrD and DNA polymerase I turnover UvrB and UvrC to generate the ssDNA intermediates is not clear. The effect of SSB on UvrABC in NER remains unknown. It would be interasting to examine whether or not SSB interacts with UvrABC and stimulates the helicase activity in NER.

Possible Functional role of UvrD and SSB in overall mismatch repair system

The UvrD-SSB interaction detailed in this study suggests that the interaction between UvrD and SSB may play a critical role in coordinateing the overall repair process in living cells. The interaction of primase and χ subunit of the clamp loader with SSB promotes hand-off of the RNA primers from primase to the DNA polymerase III holoenzyme (Yuzhakov 1999). Previous studies have suggested that SSB also interacts with Exonuclease I (Genschel 2000). A plausible mechanism is that SSB initially interacts with UvrD and recruits UvrD onto DNA and that interaction strongly stimulates helicase activity of UvrD at nicked DNA fragments (Figure 2.3). SSB may then load ExoI and χ subunit of DNA polymerase III onto ssDNA sequences (Lahue 1989).

Crystal structure studies reveal that UvrD contains four domains: 1A (1-89, 215-280 aa) and 2A (281-377, 551-647 aa) domains are responsible for ATP binding and hydrolysis.

1B (90-214 aa) and 2B (378-550 aa) interact with the DNA duplex (Lee 2006). Although the crystal structure of *E. coli* SSB C-terminus has not yet been solved, the structure of *Thermus aquaticus* (*Taq*) SSB was determined (Fedorov 2006). While *E. coli* SSB forms a homotetramer (Chase 1986; Lohman 1994; Wold 1997), *Taq* SSB forms dimer (Dabrowski 2002; Eggington 2004; Witte 2005), however the acidic C-terminus is conserved. Based on the structure of the *Taq* SSB C-terminus, potential binding sites of SSB C-terminus to χ subunit of DNA polymerase III have been proposed (Fedorov 2006). The negatively charged and highly conserved residues E259, E260 and D261 from *Taq* SSB are proposed to interact with the highly conserved positively charged residues K124, R128, K132 and R135 of the χ protein (Fedorov 2006). Based on these putative interactions, we examined the crystal structures of UvrD. We found only a single region of UvrD that had an electrostatic charge density and surface structure that was similar to the proposed site on the χ subunit of pol III. This site (Arg 22, Lys 242; 1A domain) is near the region interacting with ssDNA (Figure 2.7). We plan to examine mutant of UvrD in this region in the future.

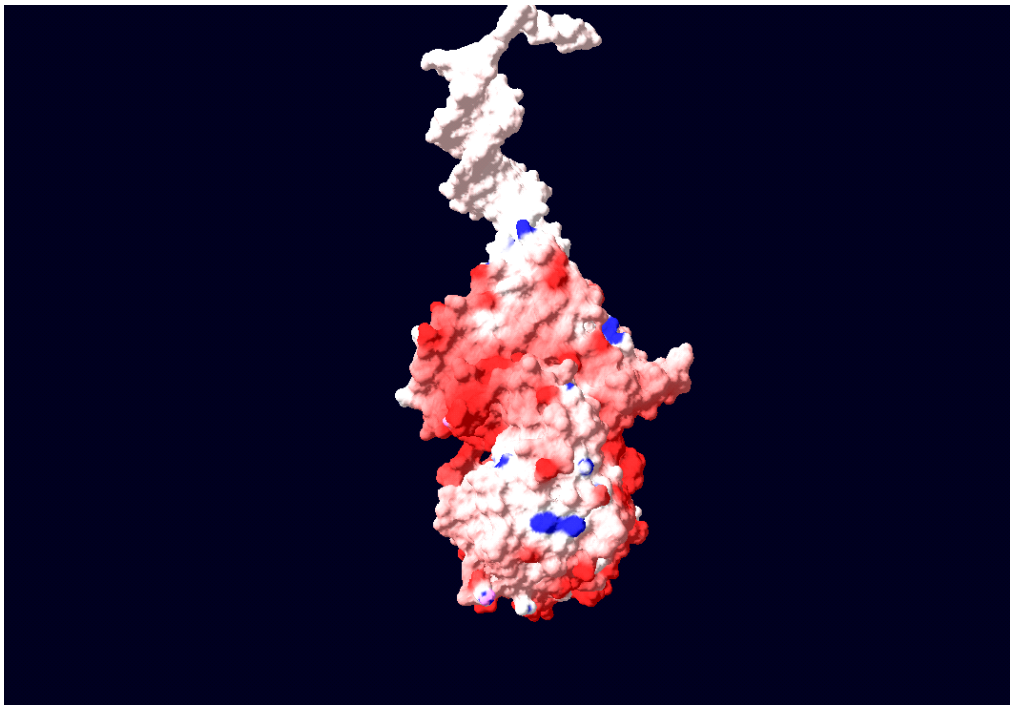

Figure 2.7 Structure of UvrD

Electrostatic structure of UvrD. Color on the surface corresponds to the atom charge. Red represents positive and blue represents negative.

Conclusions

The investigation of specific interaction of *E. coli* UvrD and SSB provides insight into the function of these proteins in MMR machinery. These proteins are not only involved in mismatch repair, but also interacting with other proteins involved in DNA metabolism such as replication and recombination. The observed results suggest that UvrD and SSB may be a bridge between activating proteins and downstream events. Results that UvrD interacts with SSB C-terminus, which is essential for interacting with other proteins involved in cellular processes.

Future work will study if these interactions are conserved in other processes. To test this idea, the effects of SSB on the function of UvrABC in NER process will be examined. In addition, single molecule fluorescence resonance energy transfer (FRET) can measure direct interaction of UvrD with SSB and binding affinity of protein-DNA. The interaction and stimulation of UvrD by SSB C-terminus further provides insight into the mechanism of the repair process. In chapter IV, we will uncover the binding activities of UvrD and SSB, and how SSB assists the loading of UvrD onto nicked DNA substrates.

Materials and Methods

DNA substrates

The various DNA substrates used in the helicase and anisotropy assays were prepared using synthetic DNA oligomers. The circular double nicked DNA, which has specific sites for nickase enzyme, was provided by Steve Matson (Biology Department in UNC-Chapel Hill). To make gapped DNA first, circular DNA was digested with *Nt.BbvCI* (NEB) and purified with a Qiagen PCR cleanup column. The complementary oligonucleotide 37 mer

(5'-TCA GCA ATC CTC AGC ^{5me}CAG GCC TCA GCT GGC CTC AGC G-3') were labeled on the 5'-end using [γ-^{32}P] ATP and T4 polynucleotide kinase (New England Biolabs). Free nucleotides were removed using a Qiagen Nucleotide Removal Kit. The labeled 37-mer was annealed to gapped DNA which was already made. The DNA fragments were separated on a 1 % agarose gel and purified using a QIAquick Gel Extraction Kit (Qiagen). The 24-basepair duplex with a 40-nt 3' overhang were made by annealing of labeled 24-mer to the 3' overhang 64-mer. The substrate DNAs were purified by 8 % non- denaturing gel electrophoresis.

Protein Purification

WtSSB and *E. coli* DNA Helicase II (UvrD) were provided by Steve Matson (UNC-Chapel Hill). Plasmids for overexpression of mutant SSB were a gift from Peter McGlynn. One liter of cells was grown until the O. D. $_{600}$ reached ~ 0.4 to 0.6, after which expression was induced by additing IPTG (0.1mM). After washing the cells with buffer (10mM Tris, 1mM Na_3EDTA, 0.1mM NaCl), cells were harvested and frozen at -80 $^{\circ}$C. Cells were thawed on ice and suspended in lysis buffer (50mM Tris, 0.2M NaCl, 15mM spermidine trichloride, 1mM Na_3EDTA, 10% (w/v) sucrose) with the addition of 1mM PMSF and 200ug/ml lysozyme. The lysate was incubated at 15°C for 30 min after the addition of 0.05% sodium deoxycholate and was sonicated a few seconds. The lysate was cleared at 21,000 rpm for 1hr in a SS 34 rotor, and 10 % polymin P pH 6.8 – 6.9 was added to the cleared lysate. After centrifuging for 20 min, the pellet was resuspended in TGE Buffer (50mM Tris, 1mM Na_3EDTA, and 20% (v/v) glycerol) + 400mM NaCl. The resuspension was centrifuged at 9,000 rpm in SS34 rotor for 20 min. Ammonium sulfate was added to the supernatant over 30min and centrifuged the ammonium sulfate precipitate was centrifuged at

21,000 rpm. The pellet was resuspended in TGE buffer + 300 mM NaCl and dialyzed overnight. The concentration of SSBΔC10 was determined by UV-vis spectroscopy.

Atomic Force Microscopy

Mixtures contained 20 mM Hepes [pH 7.8], 5 mM $MgCl_2$, 50 mM NaCl with UvrD and SSB and/or SSBΔC10 in a total volume of 20 μL. Each UvrD or SSB was equilibrated with buffer at 27°C and deposited onto freshly cleaved mica. For reaction of UvrD and SSB, the complex was incubated for 10minute at 25˚C and deposited onto mica and washed with deonized water.

Helicase activity assay

Reaction mixtures were in buffer (20 mM Tris [pH 7.5], 80 mM NaCl, 0.1 mg/ml BSA, 2.6 mM $MgCl_2$, 1 mM DTT) with 4 nM of double nicked DNA (^{32}P 5' -end labeled) and 40nM UvrD, 200 nM SSB or SSBΔC10. Reactions were initiated by adding 2 mM ATP to the final 10 μL reaction mixture and terminated by the adding 5 μL of stop solution (glycerol, EDTA, Bromophenol blue, SDS) at the indicated times. The reaction products were analyzed by electrophoresis on an 8% non-denaturing polyacrylamide gel visualized by phosphorimager (Molecular Dynamics, GE healthcare) using a Storm phosphorimager, and quantified using ImageQuant software.

References

Abbel-Monem, M., Channal, M. C. and Hoffmann-Berling, H. (1977). "DNA unwinding enzyme II of Escherichia coli. 2. Characterization of the DNA unwinding activity." Eur. J. Biochem. **79**: 39-45.

Abdel-Monem, M., Channal, M. C. and Hoffmann-Berling, H. (1977). "DNA unwinding enzyme II of Escherichia coli. 1. Purification and characterization of the ATPase activity." Eur. J. Biochem. **79**: 33-38.

Ali, J. A. M., N. K. and Lohman, T. M. (1999). "An oligomeric form of *E. coli* UvrD is required for optimal helicase activity " J. Mol. Biol. **293**: 815-834.

Amaratunga, M. a. L., T. M. (1993). "*E.coli* Rep Helicase Unwinds DNA by an Active Mechanism." Biochmistry **32**: 6815-20.

Bjornson, K. P., Amaratunga, M., Moore, K. J. M. and Lohman, T. M. (1994). "Single-turnover Kinetics of Helicase-catalyzed DNA Unwinding Monitored Continuously by Fluorescence Energy Transfer." Biochmistry **33**: 14306-16.

Brendza, K. M. e. a. (2005). "Auto-inhibition of *E. coli* Rep monomer helicase activity by its 2B sub-domain." Proc. Natl. Acad. Sci. **102**: 10081.

Cadman, C. J., and Mcglynn, P. (2004). "PriA helicase and SSB interact physically and functionally." Nucleic Acids Res. **32**: 6378-6397.

Caron, P. R., Kushner, S. and Grossman, L. (1985). "Involvement of helicase Ii (uvrD gene product) and DNA polymerase I in excision mediated by the UvrABC protein complex." Proc. Natl. Acad. Sci. U. S. A. **82**: 4925-4929.

Caruthers, J. M., and McKay, D. B. (2002). "Helicase structure and mechanism." Curr. Opin. Struct. Biol. **12**: 123-133.

Chao, K., Lohman, T. M. (1991). "DNA-induced dimerization of the *Escherichia coli* Rep helicase." J. Mol. Biol. **221**: 1165-81.

Chase, J. W. W., K. R. (1986). "Single-stranded DNA binding proteins required for DNA replication." Annu. Rev. Biochem. **55**: 103-136.

Cheng, W., Hsieh, J., Brendza, K. M. and Lohman, T. M. (2001). "*E.coli* Rep oligomers are required to initiate DNA unwinding *in vitro*." J. Mol. Biol. **310**: 327-350.

Curth, U., Genschel,J., Urbanke,C. and Greipel,J. (1996). "In vitro and in vivo function of the C-terminus of Escherichia coli single-strandedDNA binding protein. ." Nucleic Acids Res. **24**: 2706–2711.

Dabrowski, S., Olszewski, M., Piatek, R., Brillowska-Dabrowska, A., Konopa, G. and Kur, J. (2002). "Identification and characterization of single-stranded DNA binding proteins fro *Thermus thermophilus* and *Thermus aquaticus*-new arrangement of binding domains." Microbiology **148**: 3307-3315.

Dao, V. a. M., P. (1998). "Mismatch-, MutS-, MutL-, and Helicase II-dependent unwinding from the single-strand break of an incised heteroduplex." J. Biol. Chem. **273**: 9202-9207.

Delagoutte, E. a. v. H., Peter H. (2003). "Helicase mechanisms and the coupling of helicases within macromolecular machines. Part II." Q. Rev. Biophys. **36**: 1-69.

Eggington, J. M., Haruta, N., Wood, E. A. and Cox, M. M. (2004). "The single-stranded DNA binding protein of Deincoccus radiodurans." BMC Microbiol **4**: 2.

Fedorov, R., Witte, G., Urbanke, C., Manstein, D. J. and Curth, U. (2006). "3D structure of *Thermus aquaticus* single-stranded DNA-binding protein gives insight into the functioning of SSB proteins." Nucleic Acids Res. **34**: 6708-6717.

Genschel, J., Curth,U. and Urbanke,C. (2000). "Interaction of E. coli single-stranded DNA binding protein (SSB) with exonuclease I. The carboxy-terminus of SSB is the recognition site for the nuclease." Biol. Chem. **381**: 183–192.

Ha, T. e. a. (2002). "Initiation and reinitiation of DNA unwinding by the *Escherichia coli* Rep helicase." Nature **419**: 638-641.

Hall, M. C., Jordan, J. R. and Matson, S. W. (1998). "Evidence for a physical interaction between the *Escherichia coli* methyl-directed mismatch repair proteins MutL and UvrD." EMBO J. **17**: 1535-1541.

Handa, P., Acharya, N. and Varshney,U. (2001). "Chimeras between single-stranded DNA-binding proteins from Escherichia coli and Mycobacterium tuberculosis reveal that their C-terminal domains interact with uracil DNA glycosylases." J. Biol. Chem. **276**: 16992–16997.

Harmon, F. G. a. K., S. C. (2001). "Biochemical characterization of the DNA helicase activity of the *Escherichia coli* RecQ helicase." J. Biol. Chem. **276**(1): 232-243.

Husain, I., van Houten, B., Thomas, D. C., Abdel-monem, M. and Sangar, A. (1985). "Effect of DNA polymerase I and DNA helicase II on the turnover rate of UvrABC excision nuclease." Proc. Natl. Acad. Sci. U. S. A. **82**: 6774-6778.

Jones, J. M. a. N., H. (1999). "Duplex opening by primosome protein PriA for replisome assembly on a recombination intermediate." J. Mol. Biol. **289**: 503-516.

Jones, J. M. a. N., H. (2001). "*Escherichia coli* PriA Helicase:fork binding orients the helicase to unwind the lagging strand side of arrested replication forks." J. Mol. Biol. **312**: 935-947.

Kelman, Z., Yuzhakov,A., Andjelkovic,J. and O'Donnell,M. (1998). "Devoted to the lagging strand-the c subunit of DNA polymerase III holoenzyme contacts SSB to promote processive elongation and sliding clamp assembly." EMBO J. **17**: 2436–2449.

Kumura, K., Sekiguchi, M., Steinum, A. L. and Seeberg, E. (1985). "Stimulation of the UvrABC enzyme-catalyzed reactions by the UvrD protein (DNA helicase II)." Nucleic Acids Res. **13**: 1483-1492.

Lahue, R. S., Au, K. G., and Modrich, P. (1989). "DNA mismatch correction in a defined system." Science **245**: 160-164.

LeBowitz, J. H. a. M., R. (1986). "The *Escherichia coli* dnaB replication protein is a DNA helicase." J. Biol. Chem. **261**: 4738-4748.

Lee, J. Y., and Yang, W. (2006). "UvrD helicase unwinds DNA one base pair at a time by a two-part power stroke." Cell **127**: 1349-1360.

Lohman, T. M. (1992). "*E.coli* DNA Helicases: Mechanisms of DNA Unwinding." Mol. Microbial. **6**: 5-14.

Lohman, T. M. (1993). "Helicase-catalyzed DNA Unwinding." J. Biol. Chem. **268**: 2269-72.

Lohman, T. M. a. B., K. P. (1996). "Mechanisms of helicase-catalyzed DNA unwinding." Annu. Rev. Biochem. **65**: 169.

Lohman, T. M. F., M. E. (1994). "*Escherichia coli* single-stranded DNA-binding protein: Multiple DNA-binding modes and cooperativites." Annu. Rev. Biochem. **63**: 527-570.

Maluf, N. K., Fischer, C. J. and Lohman, T. M. (2003). "A dimer of Escherichia coli UvrD is the active form of the helicase in vitro." J. Mol. Biol. **325**: 913–935.

Maluf, N. K., Lohman, T.M. (2003). "Self-association equilibria of *Escherichia coli* UvrD helicase studied by analytical ultracentrifugation." J. Mol. Biol. **325**: 889-912.

Matson, S. W. (1986). "Escherichia coli helicase II (urvD gene product) translocates unidirectionally in a 3' to 5' direction." J. Biol. Chem. **261**: 10169-10175.

Matson, S. W., Bean, D. W. and George, J. W. (1994). "DNA helicases: Enzymes with essential roles in all aspects of DNA metabolism." BioEssays **16**(1): 13-22.

Mechanic, L. E., Hall, M. C. and Matson, S. W. (1999). "Escherichia coli DNA helicase II is active as a monomer." J. Biol. Chem. **274**: 12488–12498.

Meselson, M. (1998). "Methyl-directed repair of DNA mismatches." Academic Press, San Diego: 91-113.

Meyer, R. R. L., P.S. (1990). "The single-stranded DNA-binding protein of *Escherichia coli*." Microbiol. Rev. **54**: 342-380.

Modrich, P. (1989). "Methyl-directed DNA mismatch correction." J. Biol. Chem. **264**(12): 6597-600.

Modrich, P. (1991). "Mechanisms and biologicaleffects of mismatch repair." Annu. Rev. Genet. **25**: 229-253.

Modrich, P. a. L., R. (1996). "Mismatch repair in replication fidelity, genetic recombination, and cancer biology." Annu. Rev. Biochem. **65**: 101-133.

Moore, K. J. M. a. L., T. M. (1994). "Kinetic Mechanism of Adenine Nucleotide Binding to the *E. coli* Rep Monomer. II. Application of a Kinetic Competition Approach." Biochmistry **33**: 14565-78.

Moore, K. J. M. a. L., T. M. (1994). "Kinetic Mechanism of Adenine Nucleotide Binding to and Hydrolysis by the *E. coli* Rep Monomer. I. Use of Fluorescent Nucleotide Analogues." Biochmistry **33**: 14550-64.

Orren D. K., S., C. P., Hearst, J. E. and Sancar, A. (1992). "Post-incision steps of nucleotide excision repair in *Escherichia coli*. Disassembly of the UvrBC-DNA complex by helicase II and DNA polymerase I." J. Biol. Chem. **267**: 780-788.

Radman, M. (1989). "Mismatch repair and the fidelity of genetic recombination." Genome **31**: 68-73.

Ratcliff, G. C., and Erie, D. A. (2001). "A novel single-molecule study to determine protein-protein association constants." J.Am. Chem. Soc. **123**: 5632-5635.

Runyon, G. T., Wong, I. and Lohman, T. M. (1993). "Overexpression, purification, DNA binding , and dimerization of the *Escherichia coli* uvrD gene product (helicase II)." Biochmistry **32**: 602-612.

Sancar, A. (1994). "Mechanisms of DNA excision repair. ." Science **266**: 1954-1956.

Sandler, S. J. a. M., K. J. (2000). "Role of PriA in replication fork reactivation in Escherichia coli." J. Bacteriol. **182**: 9-13.

Shereda, R. D., Bernstein, D. A. and Keck, J. L. (2007). "A central role for SSB in E.coli RecQ DNA helicase function." J. Biol. Chem. **282**: 19247-19258.

Umezu, K. a. N., H. (1993). "RecQ DNA helicase of *Escherichia coli* characterization of the helix-unwinding activity with emphasis on the effect of single-stranded DNA-binding protein." J. Mol. Biol. **230**: 1145-1150.

Witte, G., Urbanke, C. & Curth, U. (2003). "DNA polymerase III chi subunit ties single-stranded DNA binding protein to the bacterial replication machinery." Nucleic Acids Res. **31**: 4434-4440.

Witte, G., Urbanke, C. and Curth, U. (2005). "Single-stranded DNA binding protein of Deinococcus radiodurans: a biophysical characterization." Nucleic Acids Res. **33**: 1662-1670.

Wold, M. S. (1997). "Replication protein A: a heterotrimeric, single-stranded DNA-binding protein required for eukaryotic DNA metabolism." Annu. Rev. Biochem. **66**: 61-92.

Wong, I., and Lohman TM. (1992). "Allosteric Effects of Nucleotide Cofactors on *E. coli* Rep Helicase-DNA Binding." Science **256**: 350-55.

Wong, I., Chao, K. L., Bujalowski, W. and Lohman, T. M. (1992). "DNA-induced Dimerization of the *E. coli* Rep Helicase: Allosteric Effects of Single Stranded and Duplex DNA." J. Biol. Chem. **267**: 7596-610.

Yamaguchi, M., Dao, V. and Modrich, P. (1998). "MutS and MutL activate DNA helicase II in a mismatch-dependent manner." J. Biol. Chem. **273**: 9197-9201.

Yang, Y., Sass, L. E., Du, C., Hsieh, P., Erie, D. (2005). "Determination of protein-DNA binding constants and specificities from statistical analyses of single molecules: MutS-DNA interactions." Nucleic Acids Res. **33**: 4322-4334.

Yang, Y., Wang, H., and Erie, D. A. (2003). "Quantitative characterization of biomolecular assemblies and interactions using atomic force microscopy." Methods **29**: 175-187.

Yuzhakov, A., Kelman, Z. and O' Donnell, M. (1999). "Trading places on DNA- a three-point switch underlies primer handoff from primase to the replicative DNA polymerase." Cell **96**: 153-163.

Chapter 3

SSB recruits UvrD onto nicked DNA

Introduction

The major functions of UvrD include catalyzing the unwinding of dsDNA sequences to separate complementary DNA duplexes and generating ssDNA intermediates coupled by other proteins to maintain genomic stability (Lohman 1996). Single-stranded DNA binding proteins (SSB proteins or SSBs) preferentially bind to ssDNA and are essential in the cellular processes such as replication, recombination and repair (Meyer 1990; Lohman 1994). Previous ensemble studies have determined that SSB interacts with some helicases and stimulates the function of unwinding with specificity in DNA substrates (Chapter 2) (Umezu 1993; Harmon 2001; Cadman 2004; Shereda 2007). However, the mechanism by which SSB stimulates UvrD catalyzed unwinding of dsDNA has not yet determined specifically. Previous chapter showed that SSB appears to increase the binding affinity of UvrD for the nicked DNA ($K_{½}$ of UvrD= 153 nM, $K_{½}$ of UvrD-SSB= 4.3 nM). We, therefore, examined the effects of SSB on UvrD helicase binding and unwinding activities at nicked duplex DNA using AFM.

UvrD belongs to the SF1 family of helicases and unwinds DNA in the 3' to 5' direction (Matson 1986). The unwinding of DNA catalyzed by UvrD uses the energy derived from ATP binding and hydrolysis. *E. coli* Rep helicase, which shares 40 % sequence homology with UvrD, forms heterodimers with SSB *in vitro* (Wong 1993). Although Rep

helicase exists as a stable monomer in the absence of DNA and translocates on ssDNA 3' → 5' direction, the monomers show no unwinding *in vitro* (Cheng 2001; Ha 2002; Brendza 2005).

The C-terminal acidic region of *E. coli* SSB is essential in DNA replication, recombination and repair. Single stranded binding protein, bacteriophage T4 gene 32 protein also has a highly acidic C-terminus and interacts with other phage T4 proteins involved in DNA metabolism (Chase 1894; Williams 1983; Chase 1984; Hurley 1993; Jiang 1993). Both PriA and RecQ helicase interact with the SSB C-terminus and this interaction stimulates their helicase activity (Umezu 1993; Harmon 2001; Cadman 2004; Shereda 2007).

To further examine the mechanism by which SSB stimulates unwinding of nicked DNA but not of owerhang or blunt DNA, we conducted a combination of AFM studies and DNA band shift assays to characterize the interaction of UvrD and SSB with DNA. Our AFM data show that both UvrD and SSB bind to nicks as well as DNA ends but that UvrD and SSB together show cooperative binding to the nick, showing an increased preference for the nick relative to the DNA ends. In addition, the band shift assays indicate that SSB inhibits binding to DNA ends or ss overhangs. Taken together, these results suggest that wtSSB recruits UvrD onto the nick to initiate helicase unwinding.

Results

WtSSB reduces UvrD binding to DNA ends and 3' overhangs

To examine the binding of UvrD to DNA in the presence and absence of SSB, different DNA substrates were used in a band shift assay. Although a circular nicked DNA is physiological relevant substrate for binding studies, we were not able to use this substrate

in band shift assays due to the large size of DNA. First, a 24 bp blunt duplex DNA was incubated with increasing concentrations of UvrD. UvrD bound the duplex DNA and slowed the mobility of DNA substrates. (Figure 3.1A lanes 1 and 2). When the concentration of UvrD is increased, supershifted complexes are observed (Figure 3.1A lanes 2-4). Given that UvrD alone dissociates from DNA during the course of an electrophoresis (Mechanic 2000), the smeared appearance seen in the gel is due to dissociation of the UvrD-DNA complex during the electrophoresis. At least two distinct UvrD-DNA complexes were formed, indicating that multiple UvrD proteins bind to the duplex DNA. Given that the effect of SSB saturates well below 200 nM (in tetramer) (Chapter 2), we chose this concentration for use in the binding reaction. Interestingly, the addition of wtSSB reduced the extent of UvrD binding to duplex DNA (Figure 3.1A compare lanes 2-4 with lanes 5-7). The binding of UvrD in the presence of SSB to blunt-ended DNA is ~ 3.5 fold less than UvrD alone (Figure 3.1B), indicating that wtSSB inhibits binding of UvrD to blunt-ended DNA. To examine if this inhibition depends on the interaction of SSB and UvrD, we also examined the effect of SSBΔC10 on UvrD binding. The addition of 200 nM SSBΔC10 does not reduce the amount of DNA bound by UvrD relative to that of the UvrD alone assay (compare lane 8 and 4). As shown Figure 3.1 A and B, both UvrD alone and UvrD- SSBΔC10 exhibit the same extent of DNA binding, indicating that SSBΔC10 has no effect on UvrD binding to the end of the duplex DNA. Taken together, these results suggest that wtSSB inhibits the loading of UvrD onto blunt-ended DNA.

To determine whether or not the inhibitory effect of SSB on UvrD-DNA complex depends upon the DNA substrates, experiments were conducted. A substrate that contained a 24-bp duplex with a 40-nt 3' overhang was used. SSBΔC10 (200 nM) and wtSSB (200 nM)

both bind to 3' overhang DNA (Figure 3.1C lanes 11 and 12). Similar to blunt-ended DNA, with the 3' overhang DNA supershifted bands seen with UvrD (Figure 3.1C lanes 2-5). At the lowest concentration of UvrD alone (25 nM), all of free DNA is bound by UvrD (Figure 3.1C). In contrast, in the presence of wtSSB (200 nM), a decrease in UvrD- DNA complexes and an appearance of SSB-DNA complexes is seen (compare lanes 2-5 with lanes 6-9). In addition, similar results are observed with SSBΔC10 (100 nM) UvrD (lane 10). SSBΔC10 inhibits UvrD binding to the end of a 3' ssDNA tail. The data presented with 3' overhang DNA shows the similar results to the 24 bp blunt DNA for wtSSB; however, SSBΔC10 inhibits binding to overhang DNA but not blunt DNA, suggesting that there is the competition for UvrD and SSB binding to overhang. SSB has high affinity for ssDNA but not blunt DNA so both wtSSB and SSBΔC10 inhibit binding to overhang but not blunt DNA. The band shift assays with blunt and overhang DNA suggest that wtSSB inhibits the loading of UvrD onto blunt-ended and 3' ssDNA extension DNA.

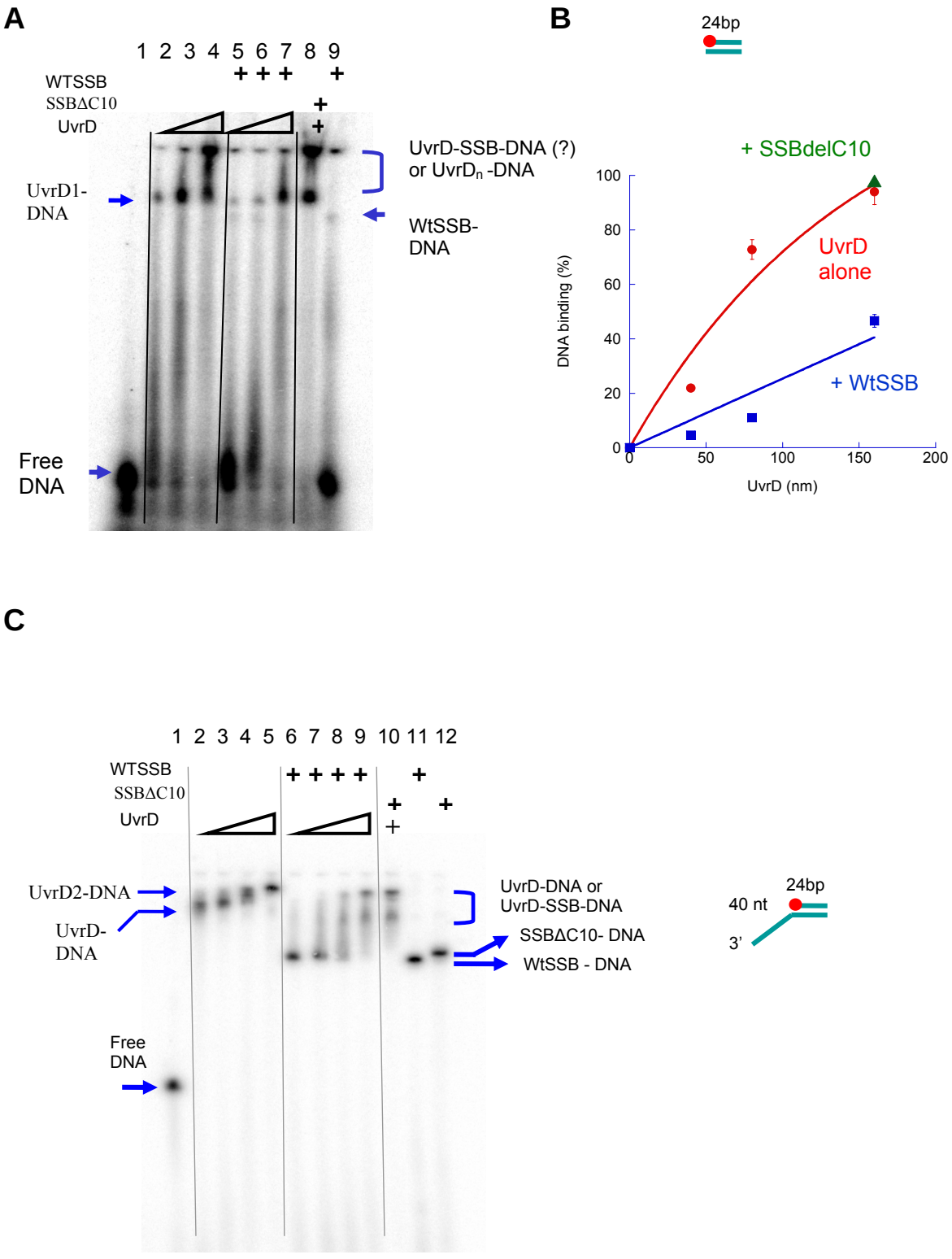
A
1 2 3 4 5 6 7 8 9
WTSSB
SSBΔC10
UvrD
UvrD1-DNA
Free DNA
UvrD-SSB-DNA (?) or UvrDn -DNA
WtSSB-DNA
B
24bp
+ SSBdelC10
+ WtSSB
UvrD alone
DNA binding (%)
UvrD (nm)
0
20
40
60
80
100
0
50
100
150
200
C
1 2 3 4 5 6 7 8 9 10 11 12
WTSSB
SSBΔC10
UvrD
UvrD2-DNA
UvrD-DNA
Free DNA
UvrD-DNA or UvrD-SSB-DNA
SSBΔC10- DNA
WtSSB - DNA
24bp
40 nt
3'

Figure 3.1

Figure 3.1 Band shift assays with UvrD, SSB, and UvrD-SSBs

(A) Gel mobility shift assays were performed with a ^{32}P 5' end labeled 24 bp blunt DNA as detailed under "Materials and Methods". The reactions contained 40, 80, or 160 nM UvrD and 100 nM SSB (or SSBΔC10 in tetramer). (B) Binding of UvrD to blunt DNA as measured by bandshift assays of (A). (C) The reactions were performed with 25, 50, 100, 200 nM UvrD and 200 nM SSB (or SSBΔC10).

SSB recruits UvrD onto nick within the DNA substrates

Previous studies suggested that UvrD is loaded onto a nick in the DNA and begins to unwind DNA for corrections of biosynthetic errors (Lahue 1989; Dao 1998). Although the nicked duplex DNA is the natural substrate for UvrD unwinding, there is no evidence of UvrD's binding preference to a nick or to ends. Because it is not possible to do band shift assays with circular nicked DNA, which has no ends, due to the large size of DNA, we used AFM to determine the binding preference of UvrD to nicked DNA versus DNA ends in the presence and absence of SSB.

First we visualized UvrD bound to DNA and SSB bound to DNA, and then compared those images to UvrD and SSB together bound to DNA to examine the effect of SSB on UvrD binding on the DNA substrates. We used a 400 bp fragment of containg a nick in the center. Based on these AFM scans, it became evident that protein binds to the DNA fragment in one of the following modes: nick, nick and one end, both ends, or one end (Figure 3.2 and 3.3B). Proteins bound to DNA molecules were counted and distribution of positions of the proteins along the DNA substrate was measured. Position distributions were then plotted in Figure 3.4 to determine where on the DNA the protein is bound. Representative images of protein-DNA complexes are shown in Figure 3.2 and 3.3B.

Figure 3.4A shows the position distribution of UvrD on the 400 bp substrate containing a nick in the center. Two peaks are seen in the distribution: one consistent with the position of the nick and the other at the end of the DNA. The breadths of the peak at the end result from the error in the measurement of the length of the fragments. UvrD by itself binds both the nick and the ends similarly on the substrates. WtSSB also binds to both the

nick and the ends but has about twice the affinity for the nicked site. Notably, there are two ends in this substrate but only one nick (Figure 3.4B).

To see whether wtSSB increases the binding of UvrD to the nick relative to the ends on the nicked DNA, the position distributions of UvrD bound to DNA and SSB bound to DNA alone were compared to those of UvrD and SSB together bound to DNA. In the presence of both SSB and UvrD the position of the protein on the DNA is predominantly at the nick (Figure 3.4C): hence the UvrD-wtSSB-DNA complex has apparently higher specificity to the nick than the ends (Figure 3.4C). The presence of wtSSB and UvrD shifts the protein complexes from the ends to the nick in the DNA substrates. These appear to be a cooperative interaction between UvrD and SSB at a nick because the preference at the nick is increased relative to both UvrD and SSB alone. In contrast, in the presence of SSBΔC10, the molecules were bound to both nick and ends and that there is no significant difference between the distribution of the proteins alone and together (Figure 3.4D).

Taken together with the AFM and band shift data, these data support the idea that SSB recruits helicase to the nick while inhibiting binding at the ends. These results reveal that wtSSB recruits UvrD, or vice versa, to the nick within DNA substrates. The data presented above are consistent with previous helicase assay data in which wtSSB appears to increase the binding activity of UvrD to nicked DNA ($K_{½}$ of UvrD = 153 nM, with SSB, $K_{½}$ = 4.3 nM in Chapter 2).

A **B**

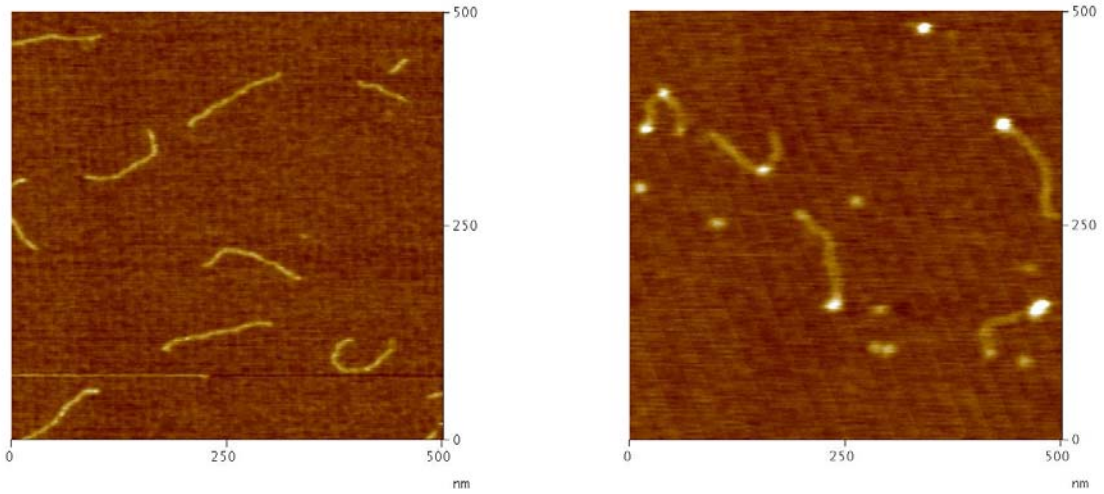

Figure 3.2 Representative AFM images

500 X 500 nm scans: (A) free DNA fragments (B) DNA deposited in the presence of UvrD

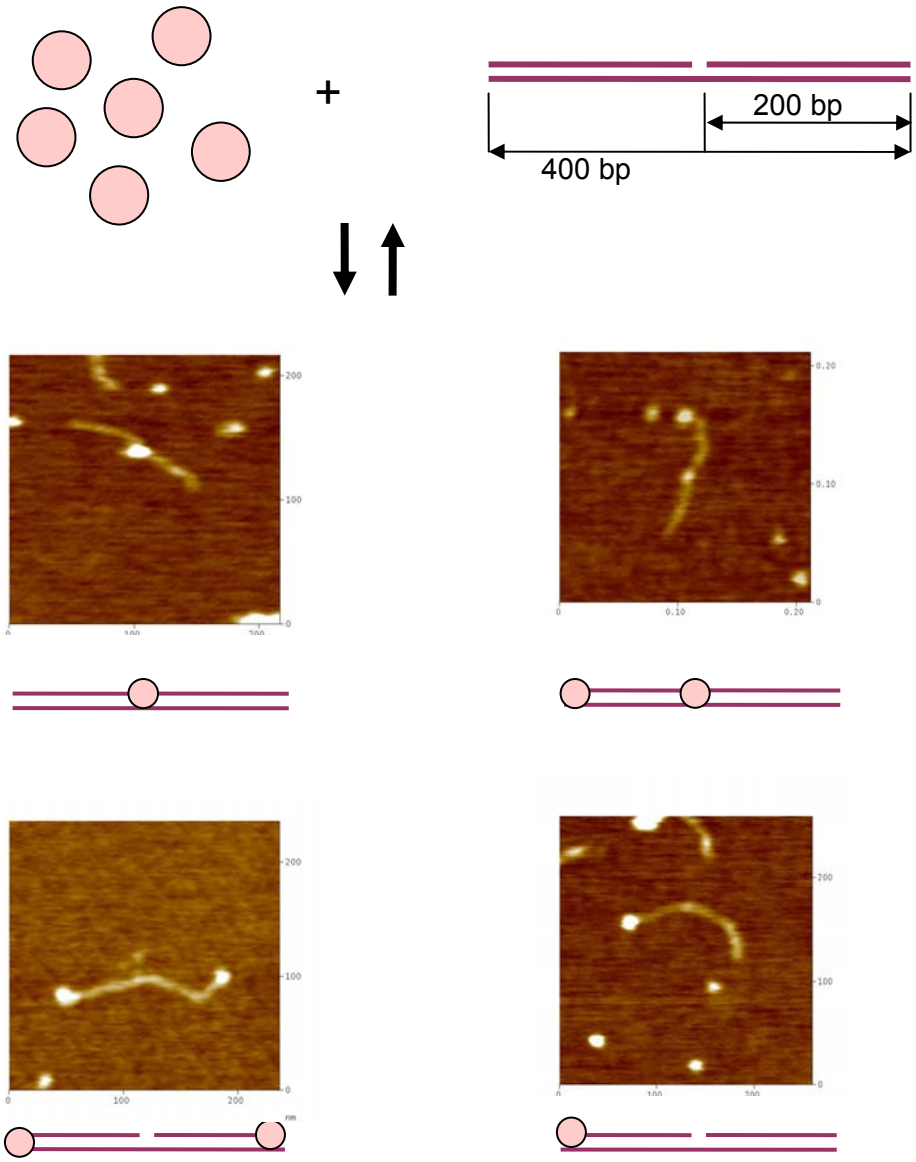

Figure 3.3

Figure 3.3 Illustration of protein-DNA binding and representative AFM images

Representative protein binding sites on the DNA are illustrated. Representative AFM images are shown with illustration. Measurement of positions of proteins on the DNA using Matlab software as detailed under "Materials and Methods".

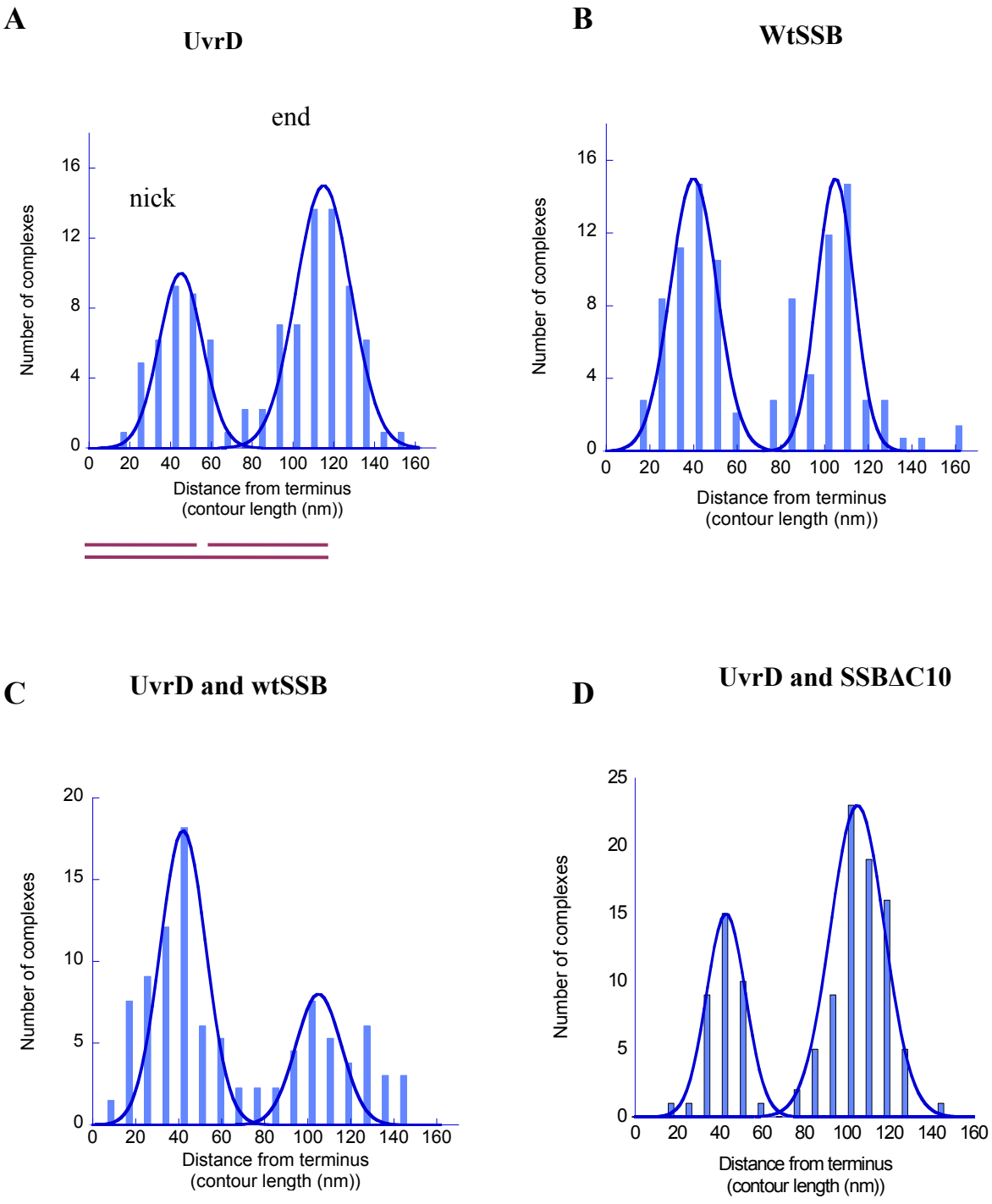
A
UvrD
end
nick
Number of complexes
Distance from terminus
(contour length (nm))
B
WtSSB
Number of complexes
Distance from terminus
(contour length (nm))
C
UvrD and wtSSB
Number of complexes
Distance from terminus
(contour length (nm))
D
UvrD and SSBΔC10
Number of complexes
Distance from terminus
(contour length (nm))

Figure 3.4

Figure 3.4 Histogram of position distributions of UvrD and/or SSB

(A) Distributions of positions for UvrD (40 nM) with Gaussian fits. Two peaks are seen. One peak shows the position of the nick, the other at the end of the DNA (B) Distributions of positions for wtSSB (50 nM) under a same condition (C) Distributions of positions for UvrD-wtSSB (D) Distributions of positions for UvrD-SSBΔC10 (50 nM)

Unwinding of UvrD alone and UvrD and SSB together

The helicase activity of UvrD uses the energy derived from hydrolysis of ATP (Matson 1987). To study the effects of adenine nucleotides on the unwinding of UvrD-SSB to DNA substrates, we used AFM to visualize UvrD-SSB-DNA complexes in the presence of ATP. Duplex DNA possessing a nick in center, 200 bp was used in this reaction. Figure 3.5A shows UvrD-wtSSB-DNA in the absence of nucleotides. In the absence of nucleotides, the complex of proteins binds to the nick which is in the center of the fragment and to the DNA ends. For those complexes at the nick, the two lengths of DNA from complex to the ends of the DNA (DNA arms) are similar (Figure 3.5A). However, in the presence of ATP, one length of the DNA arm from the protein complex is shorter than the other in AFM images, indicating that UvrD and SSB unwinds nicked DNA coupled by nucleotides (Figure 3.5B). To analyze these data, all DNA fragments on which proteins were bound counted and the length of the two arms from the nick deemed short and long were measured to generate histograms of the two lengths (Figure 3.6).

Figure 3.6A shows the length distributions of DNA with bound UvrD in the absence of ATP. The histogram in Figure 3.6B represents the distribution of DNA with bound UvrD and in the presence of ATP. Two peaks are seen in the distributions. One consists with the length of the shorter DNA, the other consists with that of the longer DNA. In the absence of ATP, the lengths of the two DNA arms are approximately equal; however, in the presence of ATP, one arm length remains approximately the same length while the other becomes shorter. These results indicate that UvrD is catalyzing the unwinding of the DNA. In addition, the complex of UvrD unwinds from the nick to end.

A

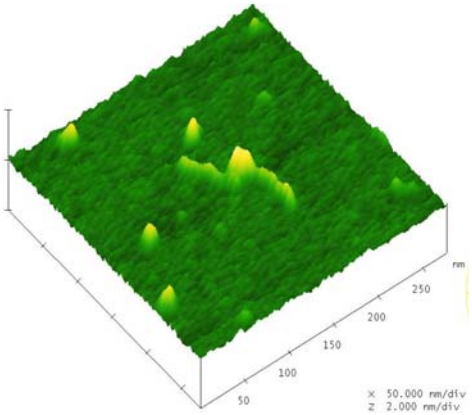

B

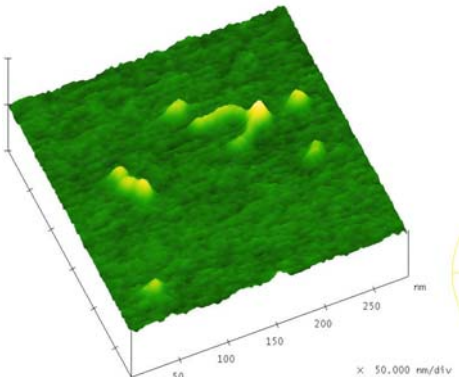

C

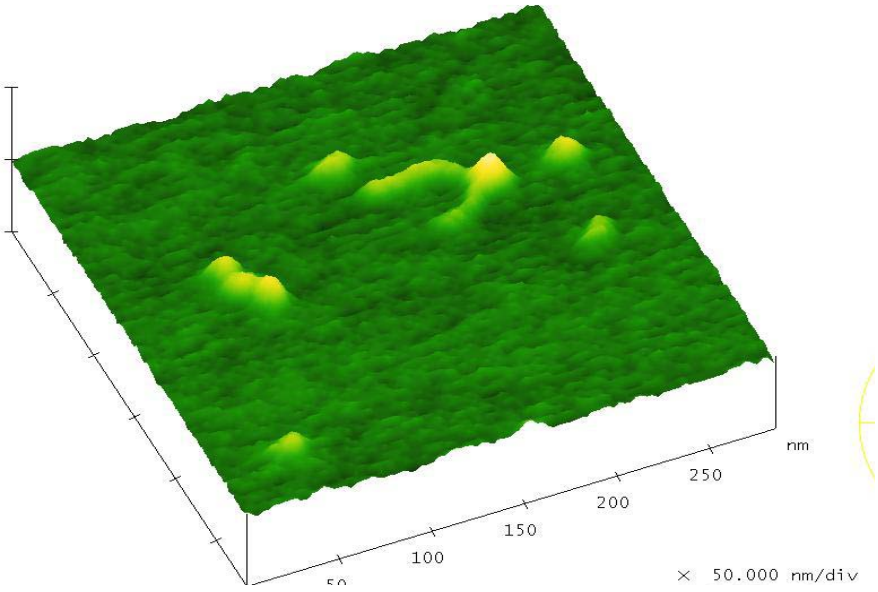

Figure 3.5

Figure 3.5 Representative of AFM images

(A) UvrD-SSB-DNA complex in the absence of nucleotides (B) UvrD-SSB-DNA complex in the presence of ATP (C) Measurement of short and long length of DNA using MatLab program.

As expected UvrD-catalyzed unwinding of duplex DNA is initiated by the energy derived from ATP hydrolysis and is consistent with data indicating that ATP and dATP are the favored NTPs in UvrD helicase reaction (Matson 1987). In addition, the observation that only one arm gets shorter in the presence of ATP suggest that helicase is only unwinding DNA in one direction, which is consistent with biochemical studies that indicate that UvrD unwinds DNA in a 3' → 5' direction (Matson 1986).

We also examined unwinding in the presence of SSB in Figure 3.6C and D. The lengths of the DNA two arms with just SSB are approximately equal as expected (data was not shown). As with UvrD in the absence of SSB and ATP, UvrD with SSB but without ATP also exhibits simlar arm lengths (Figure 3.6C) and the short arm gets shorter in the presence of ATP as expected (Figure 3.6D). Comparison of the length of the short arm in the presence and absence of SSB reveals that the short arm is shorter in the presence of SSB. These results suggest that SSB facilitates the unwinding of DNA. These results, taken together with those in the previous chapter, suggest that SSB both facilitates UvrD binding to nicked DNA and DNA unwinding.

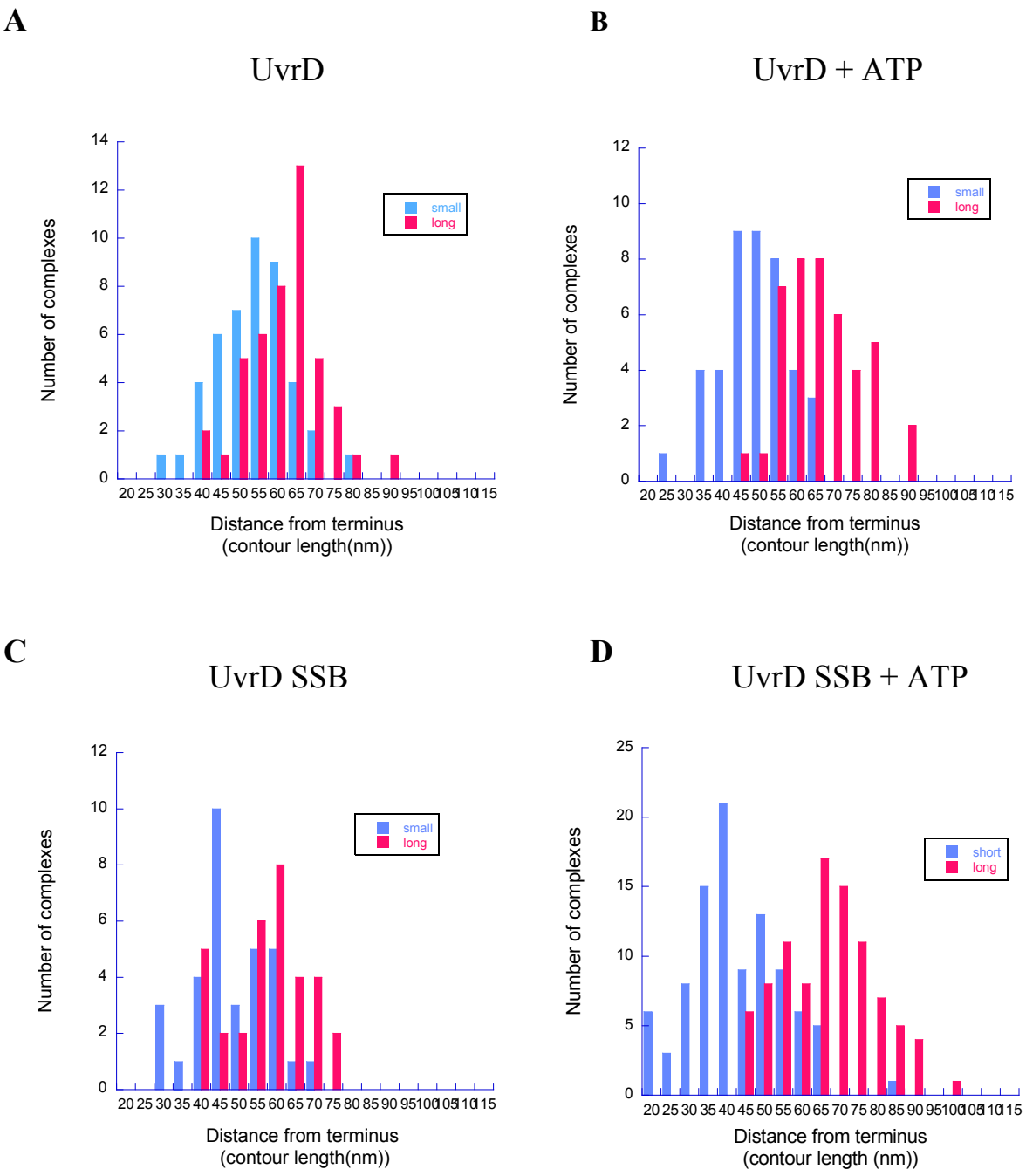
A
UvrD
Number of complexes
Distance from terminus
(contour length(nm))
small
long
B
UvrD + ATP
Number of complexes
Distance from terminus
(contour length(nm))
small
long
C
UvrD SSB
Number of complexes
Distance from terminus
(contour length(nm))
small
long
D
UvrD SSB + ATP
Number of complexes
Distance from terminus
(contour length (nm))
short
long

Figure 3.6

Figure 3.6 Length distribution of UvrD and/or wtSSB in the absence and presence of ATP

(A) The length distribution of the two arms of the DNA fragment of UvrD-DNA in the absence of nucleotides. The protein-DNA complexes are measured by Matlab software. We measured the lengths between edges of protein complexes and DNA ends. The blue bar represents the short length and the blue bar represents the long length (B) The length distribution of the DNA arms of UvrD-DNA in the presence of ATP (C) The length distribution of the DNA arms of UvrD-wtSSB- DNA in the absence of nucleotides (D) The length distribution of the DNA arms of UvrD-wtSSB –DNA in the presence of ATP

UvrD helicase* unwinding 3' → 5' *direction

Biochemical studies indicate that UvrD unwinds DNA in a 3'→5' direction (Matson 1986). Our data are consistent with this result; however, since the nick in the middle of the DNA we cannot tell which direction helicase is moving. To visualize the direction of helicase movement, we used a 600 bp DNA fragment where a nick is positioned 200 bp away from one end, with the 5' side of the nick, 200 bp (33%) away from the closest terminus (Figure 3.7A). Consequently, if UvrD unwinds in the 3'→5' direction, the long arm of the DNA should get shorter, and the short arm should remain approximately the same length. The images of UvrD-DNA and UvrD, wtSSB and DNA in the presence of ATP were collected (Figure 3.7B and D). To quantify the data, we measured the length of each of the DNA arms (see Methods). Figure 3.8 shows the position distributions of UvrD and DNA and UvrD, wtSSB and DNA in the presence of ATP. There are two peaks in the distributions; one peak consists with the length of the shorter DNA, the other consists with that of the longer DNA. The length of the short arm of UvrD is similar to the expected length in both in the absence and presence of SSB, although the breadth of the distribution is broader in the presence of SSB. In contrast, the length of the long arm gets shorter and has a significant broader distribution for both UvrD alone and UvrD and SSB. The shortening of the long arm however, is significantly greater in the presence of SSB, consistent with our results on the 400 bp fragment. These results demonstrate that UvrD preferentially unwinds in the 3'→5' direction, consistent with biochemical studies (Matson 1986).

A

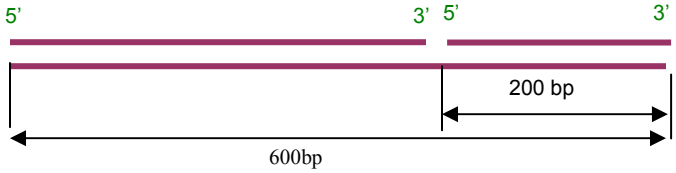

B

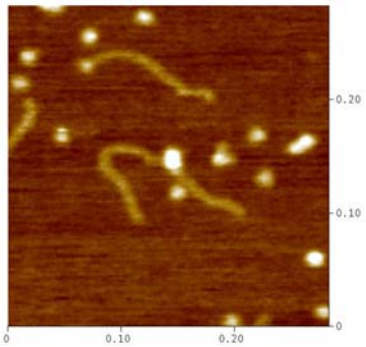

D

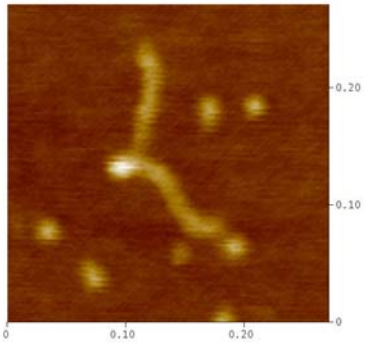

C

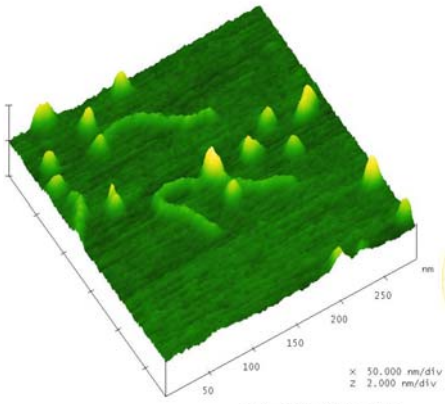

E

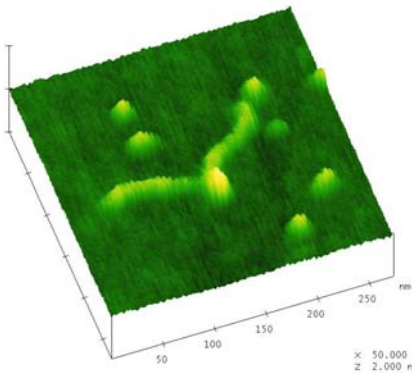

Figure 3.7

Figure 3.7 Representative AFM images

(A) The DNA substrates of a 600 bp possessing a nick which is 200 bp away from the closest terminus (B) Representative of AFM image of UvrD (40 nM) and DNA(10 nM) in the presence of ATP (1 nM) (C) Surface plot of (B). (D) Representative of AFM image of UvrD(40 nM) and wtSSB(50 nM) in the presence of ATP (1nM) (E) Surface plot of (D)

A

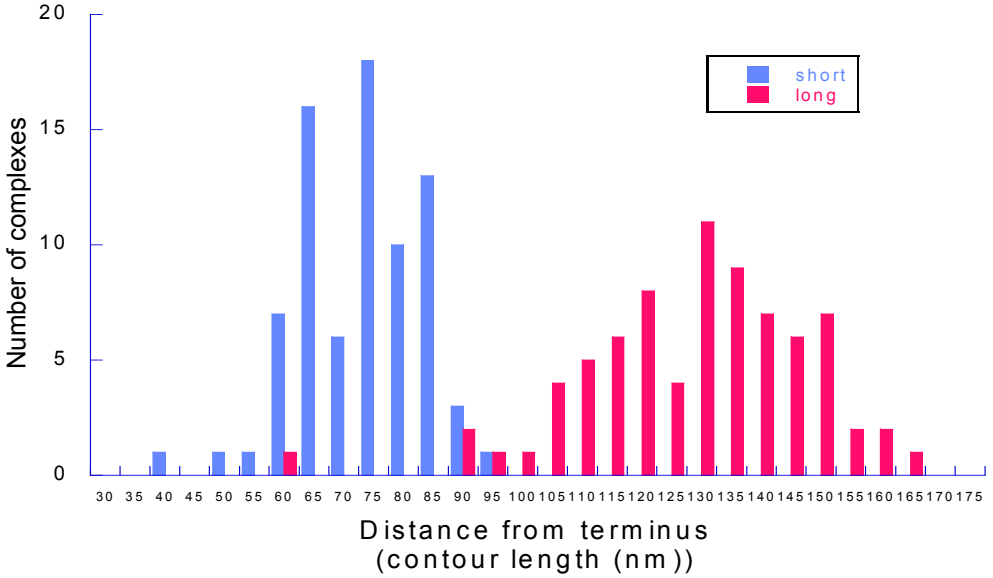
short
long
Number of complexes
0
5
10
15
20
30 35 40 45 50 55 60 65 70 75 80 85 90 95 100 105 110 115 120 125 130 135 140 145 150 155 160 165 170 175
Distance from terminus
(contour length (nm))

B

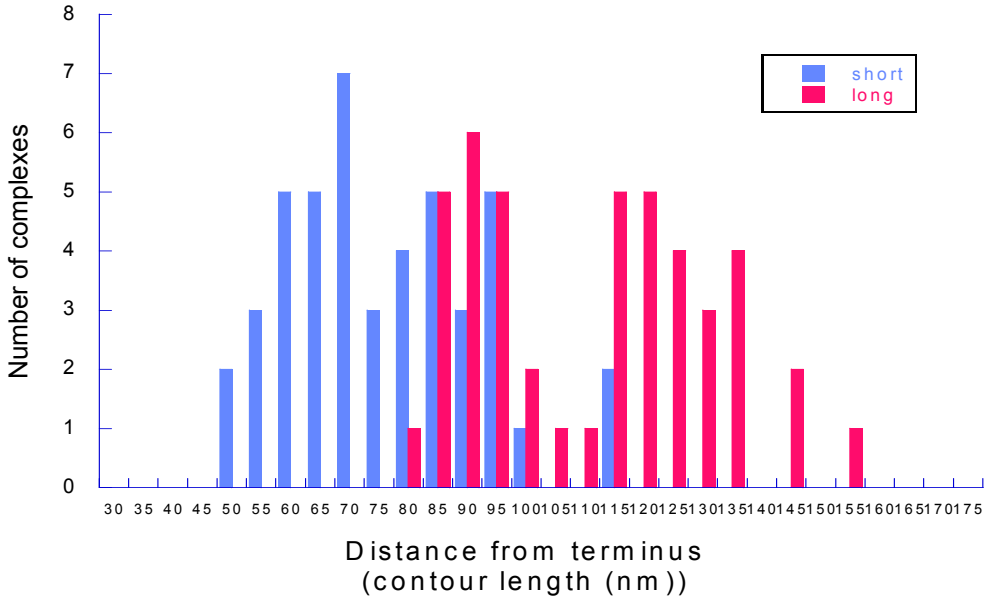
short
long
Number of complexes
0
1
2
3
4
5
6
7
8
30 35 40 45 50 55 60 65 70 75 80 85 90 95 100 105 110 115 120 125 130 135 140 145 150 155 160 165 170 175
Distance from terminus
(contour length (nm))

Figure 3.8

Figure 3.8 Distribution of the lengths of the DNA arms for UvrD and UvrD-wtSSB on nicked DNA

Distributions of the lengths of the DNA arms measured from the protein complex to the DNA ends. DNA (600 bp) for UvrD in the absence of ATP (A) and, UvrD and wtSSB in the presence of ATP (B).

Discussion

It has been demonstrated that both UvrD and SSB are essential components of the *E. coli* mismatch repair process (Lahue 1989; Meyer 1990; Cooper 1993; Grilley 1993; Lohman 1994). The physical interaction of these proteins has been discussed in this chapter 3. The interaction of SSB via its C-terminus with UvrD stimulates UvrD-catalyzed unwinding of double-nicked circular DNA, as evidenced by deletion mutant, SSBΔC10, which does not interact with UvrD. WtSSB strongly increases the affinity of UvrD to nicked DNA by 30-fold more relative to UvrD alone ($K_{½}$ of UvrD = 153 nM, $K_{½}$ of UvrD-SSB = 4.3 nM). In addition, in this chapter, we show that SSB increases the extent of unwinding on long DNA fragment suggesting that it may facilitate the unwinding activity of UvrD. Furthermore, the enhanced extent of unwinding also requires the C-terminus of SSB, suggesting that this effect is not simply due to the DNA binding activity of SSB. These results provide insight into the mechanism by which the interaction of UvrD and SSB catalyzes unwinding of DNA.

WtSSB loads UvrD onto nicked DNA

In this chapter, we characterized the effects of SSB on UvrD helicase unwinding activity. We used a physiologically relevant DNA substrate possessing a nick and blunt ends, since UvrD is recruited onto nick to activate the unwinding of DNA-containing errors in *vivo* (Dao 1998). In the presence of wtSSB, UvrD is favored to bind to the nick over the ends of the DNA substrates, while UvrD and SSB alone bind to both nick and ends (Figure 3.4). Thus, it can be concluded that wtSSB promotes the loading of UvrD, or vice versa, only to the nick, but not to the blunt-end.

The band shift assay experiments reported here show that UvrD alone is stable to bind to the end of blunt and 3' ssDNA tail in the absence of nucleotides. The addition of wtSSB reduced the binding of UvrD to blunt-ended DNA and 3' overhang DNA (Figure 3.1). These results indicate that wtSSB inhibits the binding of UvrD to the ends of blunt and overhang DNA substrates. These results fit well with AFM data, which show that complexes of UvrD and/or SSB are preferentially bound at the nick (Figure 3.1 and 3). Taken together, these results suggest that binding of UvrD to the DNA shifts from the ends to the nick and that wtSSB facilitates the loading of UvrD onto correct sites to initiate unwinding of DNA and activation of downstream events in mismatch repair. In addition, we show that the apparent recruitment of UvrD to nick requires the C-terminus of SSB (Figure 3.4), indicating that this recruitment is mediated by a direct interaction between UvrD and SSB.

SSB facilitates UvrD catalyzed DNA unwinding

It is well established that UvrD requires ATP to translocate along ssDNA (Abdel-Monem 1977; Oeda 1982; Matson 1987) and unwind dsDNA (Matson 1987). The AFM experiments, which were done in the presence of nucleotides, revealed that the energy derived by ATP hydrolysis is essential in unwinding of DNA sequences by UvrD as expected. Additionally in the presence of wtSSB, UvrD unwinds a greater portion of the DNA fragment, which suggests that SSB increases the unwinding activity of UvrD. Furthermore, this increase in extent of unwinding requires the C-terminus of SSB. Taken together with the DNA binding data, these results suggest that the interaction of SSB with UvrD stimulates both the loading of UvrD onto nicks and the unwinding of DNA.

Our AFM data show that UvrD preferentially unwinds DNA in a 3'→5' direction in the presence and absence of SSB. Because the mismatch repair pathway is bidirectional, UvrD must be able to unwind in either direction in MMR. Previous studies have revealed that MutL interacts with UvrD (Hall 1998) and that it stimulates the loading of UvrD onto the DNA (Mechanic 2000). Our results also suggest that the interaction of UvrD and SSB (Chapter 2) stimulates the loading of UvrD on the nicked DNA. Taken together, it is likely that the interaction of UvrD and other proteins, such as MutL, would affect UvrD binding and unwinding in both directions in MMR process.

The functional role of E. coli SSB

The binding of the C-terminus SSB of other proteins involved in replication and repair, such as the χ subunit of polymerase III (Kelman 1998; Witte 2003), Exonuclease I (Genschel 2000), RecQ (Shereda 2007), and PriA (Cadman 2004) might provide an insight into the determination of a specific binding mode of SSB with other proteins. FRET studies of dynamic structural changes in SSB binding mode have shown that deletion of C-terminus of SSB favors the equilibrium to the highly cooperative $(SSB)_{35}$ mode, suggesting that the binding of SSB C-terminus and other accessory proteins stabilize the $(SSB)_{35}$ mode (Roy 2007). It has been suggested that the interaction of SSB C-terminus and the χ subunit of polymerase III may stabilize the $(SSB)_{35}$ mode and lead to long protein clusters of SSB along the DNA (Roy 2007). From our AFM experiments, however, it has been shown that the binding of SSB and UvrD is compacted on nick or ends rather than long protein tracts forming along the DNA. Thus, the binding of SSB might favor the $(SSB)_{65}$ mode, suggesting that the interaction of SSB and UvrD may preclude formation of large UvrD-DNA

complexes that might inhibit UvrD helicase activity. Previous studies have shown that at higher SSB concentrations, binding of SSB to the ssDNA tail might prevent binding of PriA to the substrate and restrict its stimulation effect at branched DNA (Cadman 2004).

E. coli SSB interacts with other proteins involved in DNA metabolism (Chase 1986) and stimulates the plolymerase activity of both *E. coli* polymerase II and pol III holoenzyme (Molineux 1974; Fay 1982). Bacteriophage T4 gene 32 protein, which is a single stranded binding protein, does not stimulate these polymerases, although it does stimulate specifically the T4 DNA polymerase (Sigal 1972). Perhaps SSB is coordinator processes in MMR.

From the data presented in this chapter, we propose a mechanism by which UvrD-SSB catalyzed unwinding of duplex DNA is initiated from the nick. UvrD molecules load onto nicked and blunt-ended DNA. In the presence of SSB, the binding specificity of UvrD to the nick is highly enhanced. The interaction of SSB C-terminus and UvrD recruits the protein onto the nick by the $(SSB)_{65}$ mode and partially unwinding the duplex DNA at the nick. After the addition of ATP, the complex of UvrD-SSB significantly stimulates the unwinding of DNA in a 3'→ 5'. The produced unwound ssDNA is trapped by SSB.

SSB may link activating proteins to downstream events in mismatch repair machinery. The SSB C-terminus, which interacts with other proteins involved in replication and recombination, also plays a significant functional role in UvrD-catalyzed unwinding of DNA. The interaction of SSB with UvrD appears both to increase loading of UvrD onto nick and to stimulate DNA unwinding. The effect of SSB may further coordinate downstream events by interacting with Exo I (Genschel 2000) and the χ subunit of polymerase III (Kelman 1998; Witte 2003).

Conclusions

SSB may be a master coordinator in the mismatch repair reaction. SSB changes the binding affinity of UvrD to nicked DNA and regulates UvrD's function and it also interacts with ExoI and UvrD. In addition, UvrD interacts with MutL. Perhaps MutL corrdinates the initial events of repair and SSB coordinates the late stages of repair. It will be interesting to examine the effects of deleting the C-terminus of SSB on MMR in the future.

Materials and Methods

DNA substrates

Nicked 400 and 600 bp DNA-AFM

The nicked DNA substrate was prepared from PCR amplification reaction. 400 duplex DNA was performed with 5'-GCGCCATTCGCCATT-3' and 5'-TGCAGCTGGCACGACAG-3' primers and *E. coli* pUC18 (New England Biolabs). The plasmid was digested with *N.BstNB1* (NEB) nickase enzyme. The resulting 400 bp fragments containing a single strand nick at position 200 bp was separated by polyacrylamide gel electrophoretic mobility shift assay (EMSA) (Kuhn 2002) to analyze if they were nicked. Nicked and un-nicked DNA fragments were separated on an 8 % polyacrylamide gel. A DNA of 600 bp was performed with 5'-TGCAGCTGGCACGACAG-3' and 5'-CACATGCAGCTCCCG-3' primers and *E. coli* pUC18. The nick was 200 bp away from the closest terminus under the same conditions with 400 bp nicked DNA fragments.

Labled 24 bp DNA-bandshift assays

The 24 bp DNA was provided by Steve Matson (Biology department in UNC-

Chapel-Hill). The 24-mer was labeled on the 5'-end using [γ-^{32}P] ATP and T4 polynucleotide kinase. Free nucleotides were removed using a Qiagen Nucleotide Removal Kit. The labeled 24-mer were annealed to the complementary oligonucleotide 24-mer. The substrate DNAs were purified by 8 % non- denaturing gel electrophoresis.

Atomic force microscopy

Position distribution

Buffer conditions used included 20 mM HEPES (pH 7.8), 5 mM $MgCl_2$, and 50 mM NaCl. Basic procedures for UvrD-SSB and DNA binding imaging were (1) 4nM DNA, 40nM UvrD and/or 50 nM SSB (in tetramer) were made, (2) incubated for 10 min at room temperature and (3) deposited onto mica and scanned.

General methods

The buffer that I used in here was same with chapter 2 (20 mM HEPES (pH 7.8), 5 mM $MgCl_2$ and 50 mM NaCl). Mixtures of UvrD (40 nM), SSB (SSBΔC10) (50 nM in tetramer) and DNA (4-8 nM) were incubated for 10 minute at 25 °C in a total volume of 20 μL. If ATP was present, the reactions were incubated with ATP (1mM) and mixtures and incubated same time in the absence of nucleotides. After incubation, the sample was deposited onto mica and washed with deonized water.

Data analysis

DNA contour lengths were measured using either Nanoscope IIIa software or a custom program in Matlab software (The MathWorks, Inc.). In the Matlab program, two

protein-DNA junctions are picked and two DNA ends are input. The program was track the the DNA backbone from two ends and stopped at the closest protein-DNA junctions. The contours of the DNA were estimated by extrapolating tangent lines over the backbone of the DNA at the two protein-DNA junctions.

Identification of position distributions of protein-DNA complexes

The positions of the proteins binding sites on the DNA templates were determined by measuring the length of the DNA from the intersection of the two extrapolated DNA arms to each end. If the complex of proteins bound to the nick only, the binding position was then defined as the length of the shorter DNA tract. If the complex of proteins bound both the nick and end, the position was determined as the length of the shorter DNA tract and total contour length. Since a nick is positioned at the center, two DNA ends are identified as the same position, i.e. if the complexes bound to both ends, the position was defined as two contour length. Classification of position distributions of the complexes was based on the consideration of protein sizes measured from AFM images and uncertainty in the measurement of the DNA contour length.

Electrophoretic mobility shift assay

Reaction mixtures were in buffer (20 mM Tris [pH 7.5], 80 mM NaCl, 0.1 mg/ml BSA, 2.6 mM $MgCl_2$, 1 mM DTT) with ~ 1 nM (^{32}P 5-end labeled) of DNA and a titration of UvrD and/or 400 nM wtSSB (or SSBΔC10) concentrations. Reactions were incubated at 4˚C for 20 min and terminated by adding of 5 μL of solution (TBE, Bromophenol, Glycerol) to free DNA or 75% (v/v) Glycerol to all reaction tubes.

The products were resolved on an 8% non-denaturing polyacrylamide gel (48:1.5 acryl: bis) at 8V/cm at 4°C and analyzed by phosphor screen (Molecular Dynamics, GE healthcare).

Reference

Abdel-Monem, M., Channal, M. C. and Hoffmann-Berling, H. (1977). "DNA unwinding enzyme II of Escherichia coli. 1. Purification and characterization of the ATPase activity." Eur. J. Biochem. **79**: 33-38.

Ali, J. A. a. L., T. M. (1997). "Kinetic measurement of the step size of DNA unwinding by *Escherichia coli* UvrD helicase." Science **275**: 377-380.

Brendza, K. M. e. a. (2005). "Auto-inhibition of *E. coli* Rep monomer helicase activity by its 2B sub-domain." Proc. Natl. Acad. Sci. **102**: 10081.

Cadman, C. J., and Mcglynn, P. (2004). "PriA helicase and SSB interact physically and functionally." Nucleic Acids Res. **32**: 6378-6397.

Chase, J. W. W., K. R. (1986). "Single-stranded DNA binding proteins required for DNA replication." Annu. Rev. Biochem. **55**: 103-136.

Cheng, W., Hsieh, J., Brendza, K. M. and Lohman, T. M. (2001). "*E.coli* Rep oligomers are required to initiate DNA unwinding *in vitro*." J. Mol. Biol. **310**: 327-350.

Cooper, D. L., Lahue, R. S. , and Modrich, P. (1993). "Methyl-directed mismatch repair is bidirectional." J. Biol. Chem. **268** 11823-11829

Curth, U., Genschel,J., Urbanke,C. and Greipel,J. (1996). "In vitro and in vivo function of the C-terminus of Escherichia coli single-strandedDNA binding protein. ." Nucleic Acids Res. **24**: 2706–2711.

Dao, V. a. M., P. (1998). "Mismatch-, MutS-, MutL-, and Helicase II-dependent unwinding from the single-strand break of an incised heteroduplex." J. Biol. Chem. **273**: 9202-9207.

Fay, P. J., Johanson, K. O., MaHenry, C. S. and Bambara, R. A. (1982). "Size classes of products synthesized processively by two subassemblies of *Escherichia coli* DNA polymerase III holoenzyme." J. Biol. Chem. **257**: 5692-99.

Fedorov, R., Witte, G., Urbanke, C., Manstein, D. J. and Curth, U. (2006). "3D structure of *Thermus aquaticus* single-stranded DNA-binding protein gives insight into the functioning of SSB proteins." Nucleic Acids Res. **34**: 6708-6717.

Ferrari, M. E. B., W. and Lohman, T. M. (1994). "Co-operative binding of *Escherichia coli* SSB tetramers to single-stranded DNA in the (SSB)35 binding mode." J. Mol. Biol. **236**: 106-123.

Genschel, J., Curth,U. and Urbanke,C. (2000). "Interaction of E. coli single-stranded DNA binding protein (SSB) with exonuclease I. The carboxy-terminus of SSB is the recognition site for the nuclease." Biol. Chem. **381**: 183–192.

Grilley, M., Griffith, J., and Modrich, P. (1993). "Bidirectional excision in methyl-directed mismatch repair." J. Biol. Chem. **268**: 11830-11837

Gulbis, J. M., Kazmirski, S. L., Finkelstein, J., Kelman, Z., O'Donnell, M., and Kuriyan, J. (2004). "Crystal structure of the chi:psi subassembly of the *Escherichia coli* DNA polymerase clamp-loader complex." Eur. J. Biochem. **271**: 439-449.

Ha, T. (2001). "Single-mlecule fluorescence resonance energy transfer." Methods **25**: 78-86.

Ha, T. (2001). "Single-molecule fluorescence methods for the study of nucleic acids." Curr. Opin. Struct. Biol. **11**: 287-292.

Ha, T. e. a. (2002). "Initiation and reinitiation of DNA unwinding by the *Escherichia coli* Rep helicase." Nature **419**: 638-641.

Hall, M. C., Jordan, J. R. and Matson, S. W. (1998). "Evidence for a physical interaction between the *Escherichia coli* methyl-directed mismatch repair proteins MutL and UvrD." EMBO J. **17**: 1535-1541.

Harmon, F. G. a. K., S. C. (2001). "Biochemical characterization of the DNA helicase activity of the *Escherichia coli* RecQ helicase." J. Biol. Chem. **276**(1): 232-243.

Kelman, Z., Yuzhakov,A., Andjelkovic,J. and O'Donnell,M. (1998). "Devoted to the lagging strand-the c subunit of DNA polymerase III holoenzyme contacts SSB to promote processive elongation and sliding clamp assembly." EMBO J. **17**: 2436–2449.

Kuhn, B. M., Abdel-Monem, M., and Hoffmann-Berling, H (1978). "DNA helicases." Cold Spring Harbor Symp. Quant. Biol. **43**: 63-67.

Kuhn, B. M., Abdel-Monem, M., Krell, H., and Hoffmann-Berling, H (1979). "Evidence for two mechanisms for DNA unwinding catalyzed by DNA helicases " J. Biol. Chem. **254**: 11343-11350.

Kuhn, H., Protozanova, E., and Demidov, V. (2002). "Monitoring of single nicks in duplex DNA by gel electrophoretic mobility-shift assay." Electrohporesis **23**: 2384-2387.

Lahue, R. S., Au, K. G., and Modrich, P. (1989). "DNA mismatch correction in a defined system." Science **245**: 160-164.

Lee, J. Y., and Yang, W. (2006). "UvrD helicase unwinds DNA one base pair at a time by a two-part power stroke." Cell **127**: 1349-1360.

Lohman, T. M. a. B., K. P. (1996). "Mechanisms of helicase-catalyzed DNA unwinding." Annu. Rev. Biochem. **65**: 169.

Lohman, T. M. F., M. E. (1994). "*Escherichia coli* single-stranded DNA-binding protein: Multiple DNA-binding modes and cooperativites." Annu. Rev. Biochem. **63**: 527-570.

Matson, S. W. (1986). "Escherichia coli helicase II (urvD gene product) translocates unidirectionally in a 3' to 5' direction." J. Biol. Chem. **261**: 10169-10175.

Matson, S. W. a. G., J. W. (1987). "DNA helicase II of *Escherichia coli*. Characterization of the single-stranded DNA-dependent NTPase and helicase activities." J. Biol. Chem. **262**: 2066-2076.

Mechanic, L. E., Frankel, B. A. and Matson, S. W. (2000). "*Excherichia coli* MutL loads DNA helicase II onto DNA." J. Biol. Chem. **275**: 38337-38346.

Meyer, R. R. L., P.S. (1990). "The single-stranded DNA-binding protein of *Escherichia coli*." Microbiol. Rev. **54**: 342-380.

Molineux, I. J. a. G., M. L. (1974). "Properties of the Escherichia coli DNA Binding (Unwinding) Protein: Interaction with DNA Polymerase and DNA" Proc. Natl. Acad. Sci. U. S. A. **71**: 3858-62.

Oeda, K., Horiuchi, T. and Sekiguchi, M. (1982). "The UvrD gene of E. coli encodes a DNA-dependent ATPase." Nature **298**: 98-100.

Raghunathan, S., Kozlov, A. G., Lohman, T. M. and Waksman, G. (2000). "Structure of the DNA binding domain of *E. coli* SSB bound to ssDNA." Nature Struct. Biol. **7**: 648-652.

Roy, R., Kozlow, A. G., Lohman, T. M., and Ha, T. J. (2007). "Dynamic structural rearrangements between DNA binding modes of *E. coli* SSB protein." J. Mol. Biol. **269**: 1244-1257.

Shereda, R. D., Bernstein, D. A. and Keck, J. L. (2007). "A central role for SSB in E.coli RecQ DNA helicase function." J. Biol. Chem. **282**: 19247-19258.

Sigal, N., Delius, H., Kornberg, T., Gefter, M. L. and Alberts, B. M. (1972). "A DNA-Unwinding Protein Isolated from Escherichia coli: Its Interaction with DNA and with DNA Polymerases" Proc. Natl. Acad. Sci. U. S. A. **69**: 3537-41.

Umezu, K. a. N., H. (1993). "RecQ DNA helicase of *Escherichia coli* characterization of the helix-unwinding activity with emphasis on the effect of single-stranded DNA-binding protein." J. Mol. Biol. **230**: 1145-1150.

Williams, K. R., LoPresti, M. B, Setoguchi, M. and Konigsberg, W. H. (1980). "Amino acid sequence of the T4 DNA helix-destabilizing protein." Proc. Natl. Acad. Sci. U. S. A. **77**: 4614-4617.

Witte, G., Urbanke, C. & Curth, U. (2003). "DNA polymerase III chi subunit ties single-stranded DNA binding protein to the bacterial replication machinery." Nucleic Acids Res. **31**: 4434-4440.

Wold, M. S. (1997). "Replication protein A: a heterotrimeric, single-stranded DNA-binding protein required for eukaryotic DNA metabolism." Annu. Rev. Biochem. **66**: 61-92.

Wong, I., Amaratunga, M. and Lohman, T. M. (1993). "Heterodimer formation between *Escherichia coli* Rep and UvrD proteins." J. Biol. Chem. **268**: 20386-20391.

Chapter 4

MutL loads UvrD onto the DNA

Introduction

MutL homologs are conserved from bacteria to humans, suggesting that the initial steps of MMR have been conserved throughout the evolution of eukaryotes. Because of this conservation, the *E. coli* MMR pathway is an attractive model system to study, since it is better characterized than MMR pathways in eukaryotes. *E. coli* MutL plays a critical role in MMR by interacting with other activating proteins, such as MutS, MutH and UvrD (Grilley 1989; Allen 1997; Ban 1998; Drotschmann 1998; Hall 1998; Yamaguchi 1998). MutL interacts with MutS and MutH to initiate MMR, and MutL also interacts with UvrD and stimulates its helicase activity (Yamaguchi 1998). As such, MutL appears to coordinate the initiation of MMR with the downstream events that lead to repair.

Previous studies have shown that MutL contains an N-terminal ATPase region (residues 1-349) and a C-terminal dimerization region (residues 432-615) (Ban 1998; Ban 1999). MutL is a dimer and an ATPase, and mutations in MutL that impair either ATP binding or ATP hydrolysis by MutL abolish mismatch repair (Ban 1998; Ban 1999; Spampinato 2000). MutL homologs have been identified in yeast, human and all other organisms other than viruses (Kolodner 1996; Modrich 1996). Prokaryotic MutL is homodimeric, while eukaryotic MutL homologs form heterodimers e.g. the MLH1-PMS1 complex in yeast and the MLH1-PMS2 in human (Prolla 1994). The ATPase region of MutL

and MutL homologs is conserved and belongs to the GHL ATPase family (Ban 1998; Ban 1999; Dutta 2000; Guarne 2001; Hu 2003). The GHL family consists of the ATPase domains of gyrase, Hsp90 and MutL. It has been shown that GHL family ATPases undergo conformational changes induced by ATP binding and/or hydrolysis (Ban 1999; Dutta 2000; Corbett 2003; Immormino 2004; Dollins 2005; Ali 2006; Chu 2006; Shiau 2006; Sacho 2008).

Interaction of MutL and UvrD is thought to be required for activating the methyl-directed excision system. Previous studies have shown that MutL stimulates UvrD helicase activity (Yamaguchi 1998; Spampinato 2000)). In the presence of a mismatch, MutS and MutL activate UvrD helicase activity at a nick (Dao 1998; Yamaguchi 1998); however, the mechanism by which the UvrD-catalyzed unwinding reaction is enhanced by MutL remains to be determined.

In this chapter, the conformational changes of MutL in the absence and presence of ATP (or ADP) were examined using AFM. AFM images showed two different shapes of MutL, which are dependent on nucleotide binding. These conformational changes provide further support for a role of MutL in interaction and coordination of downstream events in MMR. In this work, the interaction between MutL and UvrD was visualized by AFM. This interaction between MutL and UvrD eventually appears to promote the loading of UvrD onto DNA and translocates the MutL-UvrD complex along the DNA duplex. In the presence of MutL, UvrD appear to translocate further along DNA than in the absence of MutL.

Results

Conformational change of MutL is nucleotide dependent

To determine how binding of ATP affects the conformation of *E. coli* MutL, we imaged MutL in the presence and absence of nucleotide cofactors. In the absence of nucleotides, the MutL dimer (20 nM in monomer) predominantly has a V-shape, whereas in the presence of ATP (or ADP), it has a ball shape (Figure 4.1). The V-shape is consistent with models of MutL based on the crystal structure of the N and C terminus (Kosinskia 2005) (Figure 4.1A). To examine shape changes, each protein peak was fit to an ellipse and the major and minor axes were determined (Figure 4.2). In this analysis, only dimers of proteins were analyzed. In the absence of nucleotide there is a significant difference between the lengths of the major and minor axes, indicating that the protein is elongated (Figure 4.2A). In the presence of ADP or ATP, the the lengths of the major and minor axes are similar to one another, indicating that the binding of ATP (or ADP) induces a condensed state (globular) of MutL (Figure 4.2B and C). Given that the N-terminal ATPase fragment is monomeric in the absence of nucleotide and that is dimeric in the presence of the nonhydrolyzable ATP analog, AMPPNP (Ban 1998), these results suggest that the binding of ATP or ADP induces conformational changes within the N-terminal domain, which is connected to the C-terminal domain of MutL. These findings are consistent with a conformational change of MutL, including association and dissociation of the N-terminal ATPase region during the ATP hydrolysis cycle (Ban 1999) and also with the conformational changes seen within MutLα (Sacho 2008).

A

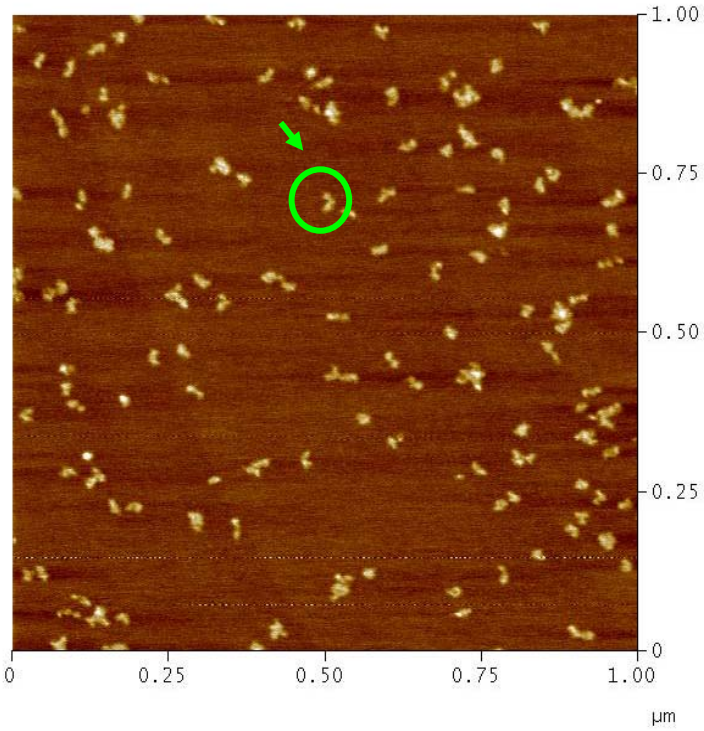

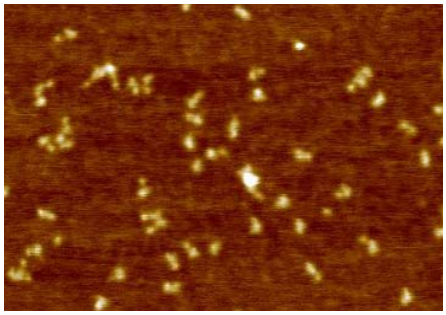

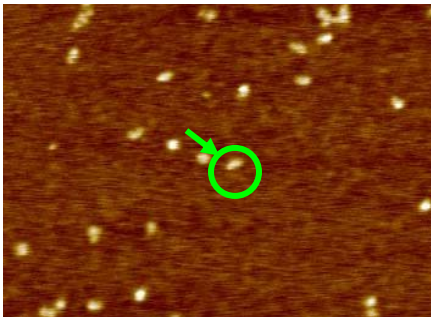

B **C**

Figure 4.1

Figure 4.1 Representative AFM images of MutL

(A) In the absence of nucleotides in 1 x 1 μm (B) In the presence of ATP (1mM) and (C) ADP (1mM): under the same scan size. The circle and arrow point to MutL molecule either 'v-shape' (A) and 'ball-shape' (C)

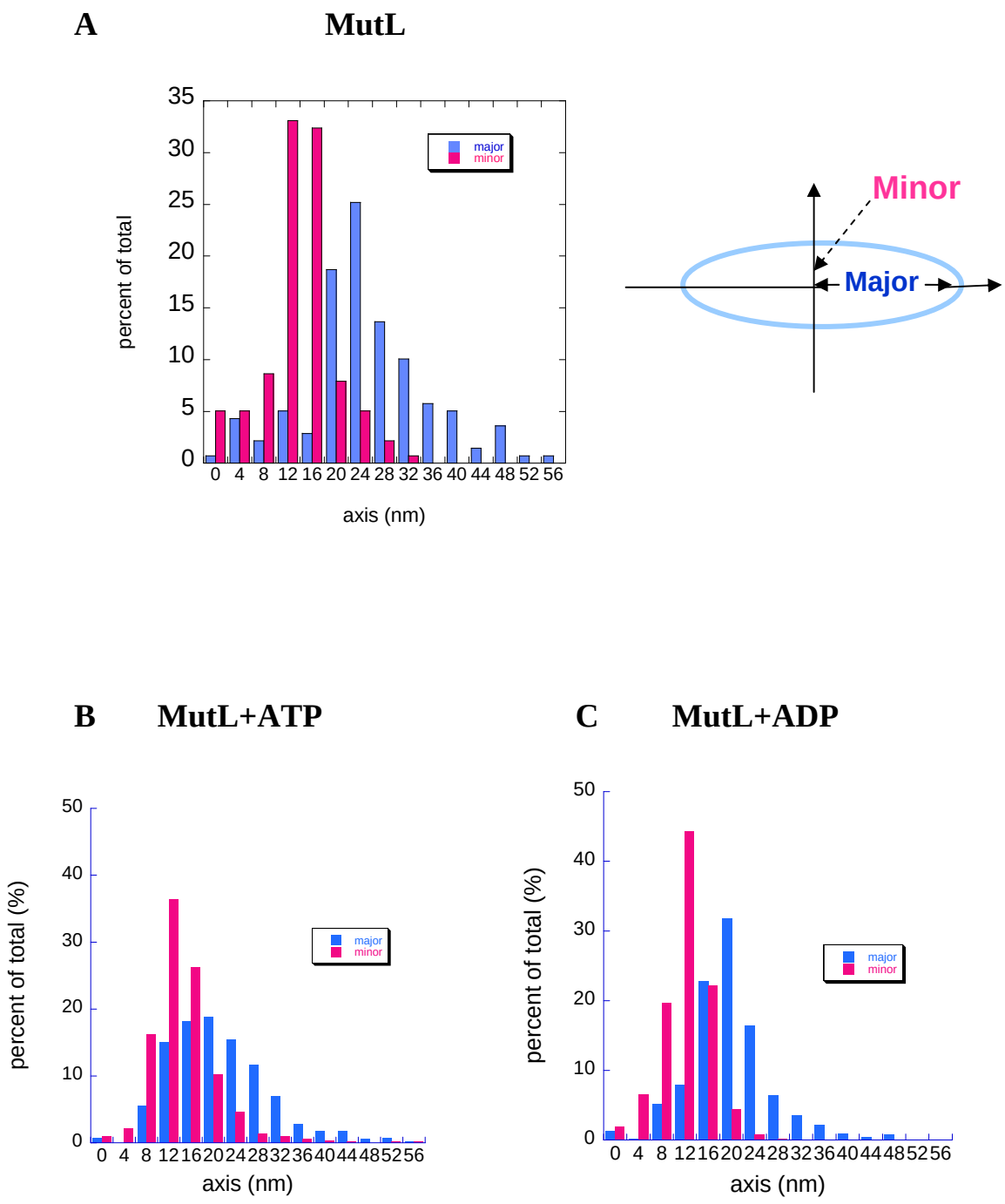
A
MutL
35
30
25
20
15
10
5
0
percent of total
major
minor
0 4 8 12 16 20 24 28 32 36 40 44 48 52 56
axis (nm)
Minor
Major
B
MutL+ATP
50
40
30
20
10
0
percent of total (%)
major
minor
0 4 8 12 16 20 24 28 32 36 40 44 48 52 56
axis (nm)
C
MutL+ADP
50
40
30
20
10
0
percent of total (%)
major
minor
0 4 8 12 16 20 24 28 32 36 40 44 48 52 56
axis (nm)

Figure 4.2

Figure 4.2 Histogram of conformational change of MutL

(A) MutL in the absence of nucleotide cofactors. (B) MutL in the presence of ATP (C) MutL in the presence of ADP. The MutL molecules shown in Figure 4.1 were analyzed by modeling the X-Y dimensions as an ellipse. The major axis is colored in blue and the minor axis in red.

Visualization of the interaction of MutL and UvrD

Yeast two-hybrid experiments suggest that there is an interaction between MutL and UvrD (Hall 1999); however, thus far, there is no direct evidence of a physical interaction between these two proteins. To visualize the physical interaction of MutL with UvrD, we used AFM to characterize the interaction between MutL with UvrD. First, MutL and UvrD were imaged alone by AFM, and the volumes of the proteins were analyzed. Volumes, as measured by AFM, can be related to a protein's molecular weight by the equation V = (1.2 MW) – 14.7, where V is the volume measured by AFM and MW is the molecular mass (Ratcliff 2001). The predicted volumes of MutL and UvrD are shown in Table 4.1

The distribution of MutL volumes seen in Figure 4.3A shows that the majority of proteins exist at 80 to 155 nm^3, which is consistent with the predicted volumes of monomer and dimer. Based on AFM images, UvrD is present as both monomer and dimer, with peaks centered around 78 and 160 nm^3 (Figure 4.3B) (Table 4.1). These numbers are consistent with previous AFM studies of UvrD volume (Ratcliff 2001) and solution studies (Runyon 1993). MutL and UvrD were then combined in solution before deposition for AFM imaging. Protein molecules were analyzed for oligomerization of MutL and of UvrD (Figure 4.3C). The predicted volume for a MutL-UvrD complex is 250 nm^3 and 345 nm^3 for a MutL-$UvrD_2$ complex (Table 4.1). The volume analysis shows higher volume species that would be consistent with dimer of MutL interacting with monomer and dimer of UvrD (Figure 4.3C). The first peak seen in this distribution is around 80 nm^3, where monomer UvrD or monomer MutL were populated. The second peak represents dimer UvrD or dimer MutL. Two minor peaks depict the interaction of MutL-UvrD, and their volumes are around 250 and 350 nm^3, which represent the binding of MutL to a monomer or dimer of UvrD. From the volume

analysis, approximately ~10% of the population represents complexes of MutL and UvrD. This result suggest that the affinity for MutL and UvrD is in the low micromolar range (Ratcliff 2001).

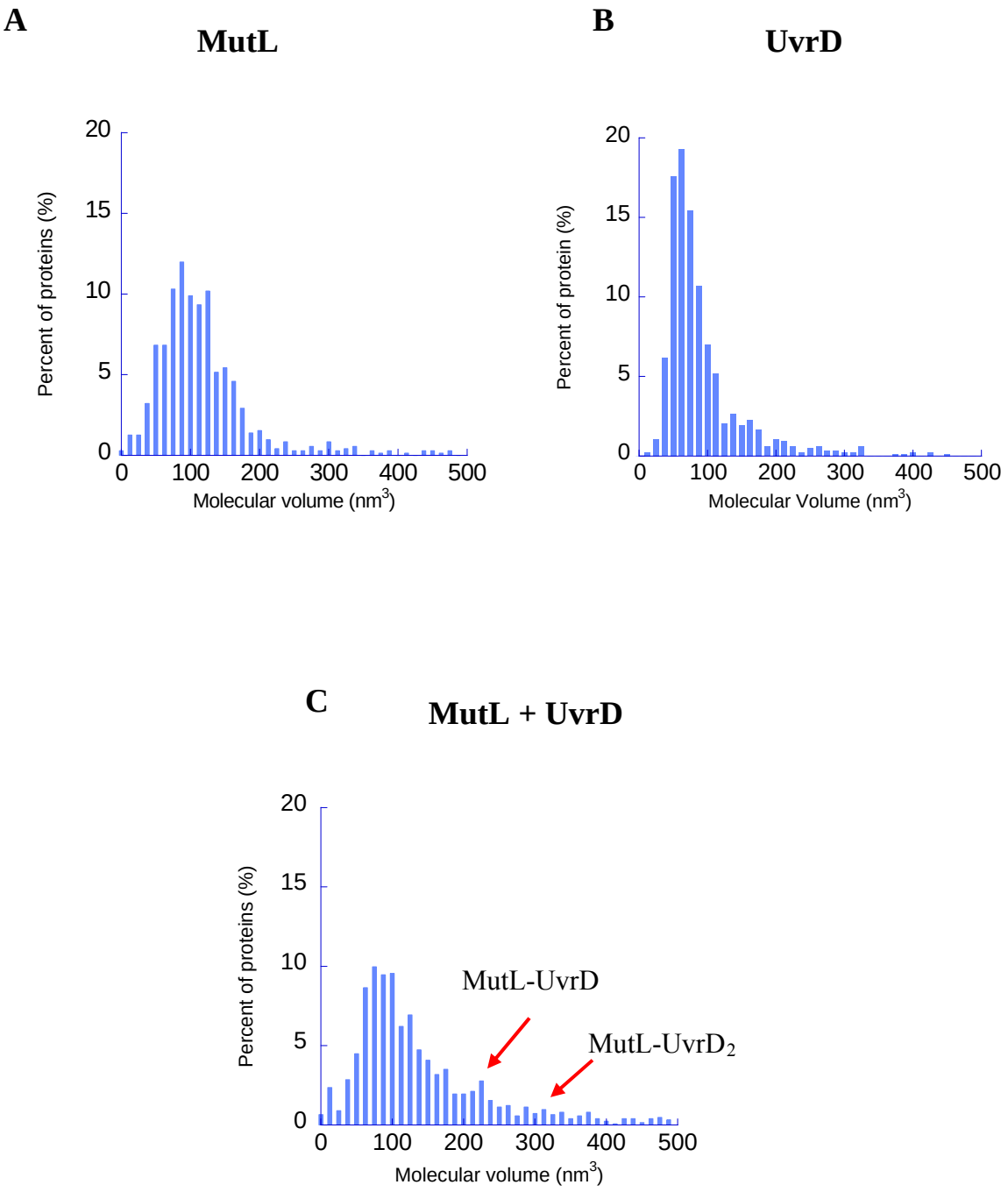
A
MutL
Percent of proteins (%)
Molecular volume (nm3)
B
UvrD
Percent of protein (%)
Molecular Volume (nm3)
C
MutL + UvrD
Percent of proteins (%)
MutL-UvrD
MutL-UvrD2
Molecular volume (nm3)

Figure 4.3

Figure 4.3 The volume histogram of MutL and UvrD alone vs MutL and UvrD together

(A) The volume histogram of MutL in the absence of nucleotides. 20nM monomer of MutL deposited (B) The volume histogram of UvrD (20nM in monomer) (C)Tthe volume histogram of MutL (25 nM) and UvrD (25 nM).

complex	molecular mass (kDa)	predicted AFM volume (nm^3)
Monomer MutL	70	69.3
dimer MutL	140	153
monomer UvrD	82	83.7
dimer UvrD	162	182
dimer MutL- monomer UvrD	220	250
dimer MutL – dimer UvrD	300	345

Table 4.1 Predicted AFM volumes for MutL and UvrD

Predicted volumes were calculated by the equation V = (1.2 MW) – 14.7, where V is the volume measured by AFM and MW is the molecular mass.

Binding activity of UvrD alone and MutL and UvrD together

UvrD utilizes the energy from ATP hydrolysis to unwind DNA (Matson 1987). To determine whether the binding occupancies of UvrD on DNA are nucleotide-dependent, we analyzed the effects of adenine nucleotides on UvrD-DNA binding. Duplex DNA with a 3-nt 3' overhang was used in this reaction. In the absence of adenine nucleotides, UvrD distributed along the DNA randomly (Figure 4.4), binding to the 3' ssDNA end and internal sites (Table 4.2). However, in the presence of ATP, UvrD favors binding to internal sites along the DNA rather than to 3' ssDNA ended-DNA (Table 4.2). This shift might be due to either the translocation of UvrD along the DNA or a new preference to bind directly to internal sites. In the presence of AMPPNP, a nonhydrolyzable ATP analog, UvrD still favors the binding to internal sites on the DNA.

These results suggest that UvrD prefers to bind to internal sites on the DNA rather than to the end of DNA in the presence of ATP (or AMPPNP), suggesting that ATP binding promotes UvrD binding to internal sites of the DNA or moving of UvrD from ends to internal DNA sites. Since UvrD prefers bind to DNA internally in the presence of AMPPNP, it is likely that UvrD binds to internal sites on the DNA directly, rather by translocation along the DNA.

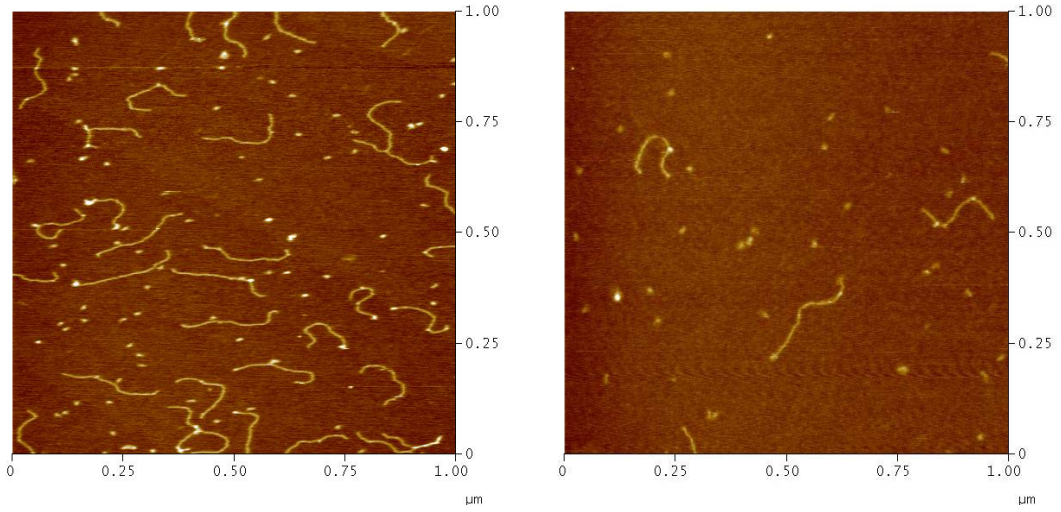

Figure 4.4 Representative AFM images

1 X 1 µm scans: (A) UvrD-DNA deposited in the absence of nucleotides (B) UvrD-DNA deposited in the presence of ATP

	UvrD, DNA w/ ATP	UvrD, DNA w/AMPPNP	UvrD, DNA w/o nucleotides
Total DNA fragments	85	100	144
Bound to ends	18%	16%	**27%**
Bound internally	**40%**	**36%**	20%
Bound to both	4%	12%	**20%**
Free DNA	38%	36%	33%

Table 4.2 UvrD binding occupancies on the DNA in the absence and presence of nucleotides

In the absence of nucleotides, UvrD bound to DNA without any preference. However, in the presence of ATP (or AMPPNP), UvrD preferred to bind to internal sites on DNA. There is higher percent of unbound DNA in this reaction.

Large complexes of UvrD and MutL

It has been demonstrated that MutL loads UvrD onto the DNA (Mechanic 2000). While there have been a variety of studies regarding the interaction of MutL with UvrD, little is known about how MutL functionally stimulates the activity of UvrD. To examine the structure of UvrD-MutL-DNA complexes, we incubated UvrD, MutL, 3-nt overhang DNA, and ATP for 5 min, and deposited the complexes and imaged. We compared AFM images of UvrD alone and of UvrD and MutL with DNA in the presence of ATP (Figure 4.5). Monomers and dimers of UvrD bound to DNA in the presence of ATP are shown in Figures 4.5 A and B. In contrast, in the presence of MutL, large protein complexes were observed on the DNA in the presence of ATP, indicating that large complexes are due to the interaction of MutL and UvrD (Figures 4.5 C and D). No large complexes were seen with just UvrD, ATP, and DNA (Figure 4.6A). The histogram of the AFM volumes of UvrD alone on the DNA shows volumes consistent with monomers or dimers of UvrD. Incubation of MutL with UvrD results in a shift of the protein sizes to larger volumes on DNA (Figure 4.6B).

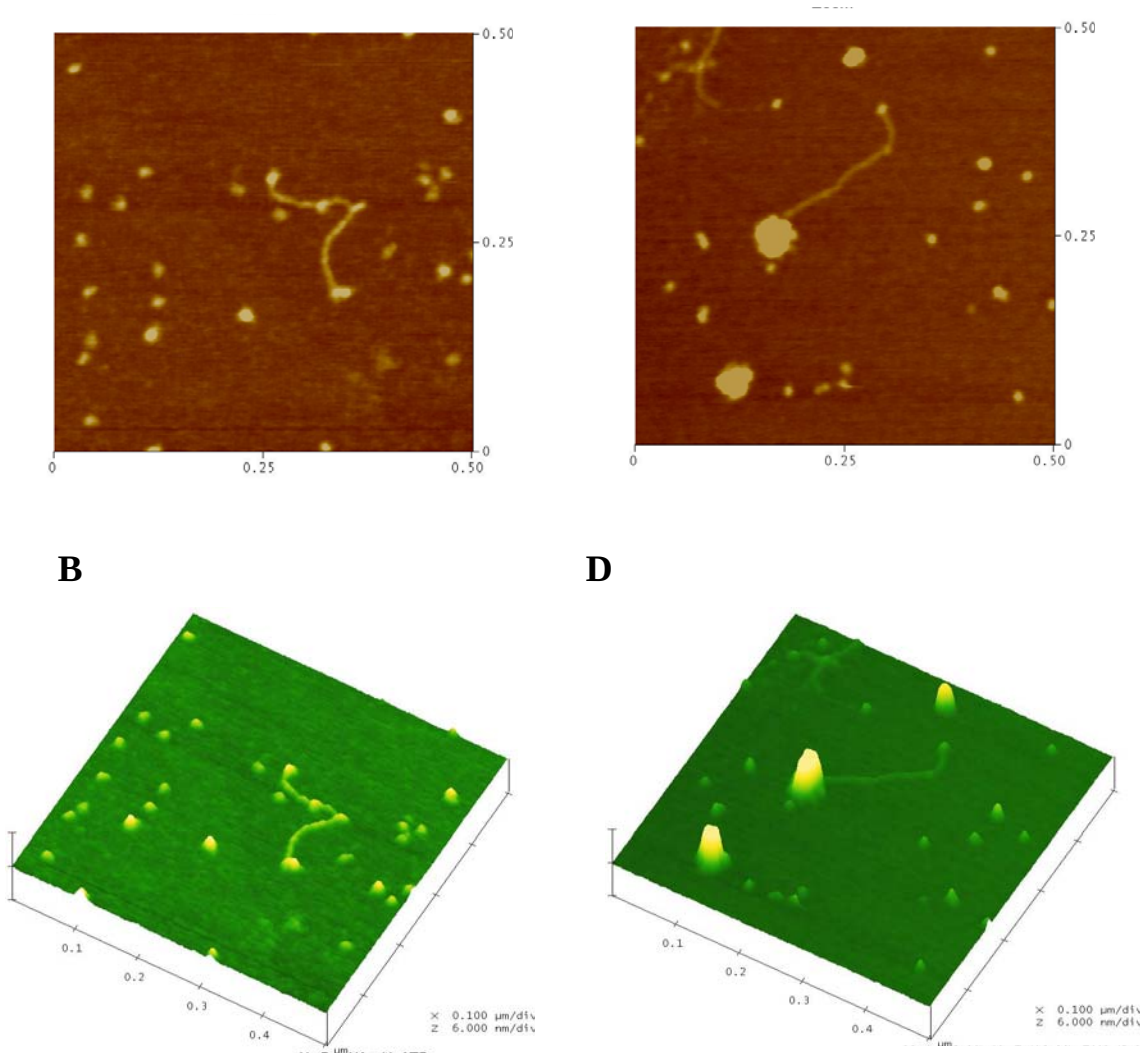
A UvrD
C UvrD-MutL
B
D
0.50
0.25
0
0.25
0.50
0.1
0.2
0.3
0.4
× 0.100 µm/div
Z 6.000 nm/div

Figure 4.5

Figure 4.5 Binding of UvrD and/or MutL to the 817 bp DNA containing a 3' ssDNA tail

500 X 500 nm scans: **(A)** Representative AFM image of UvrD on the DNA (817 bp) in the presence of ATP (1mM). The protein and DNA concentrations are 25 nM (monomer) and 10 nM, respectively. **(B)** Surface plot of A. **(C)** Representative AFM image of MutL (25 nM) and UvrD (25 nM) on the DNA in the presence of ATP (1mM) (**D)** surface plot of C.

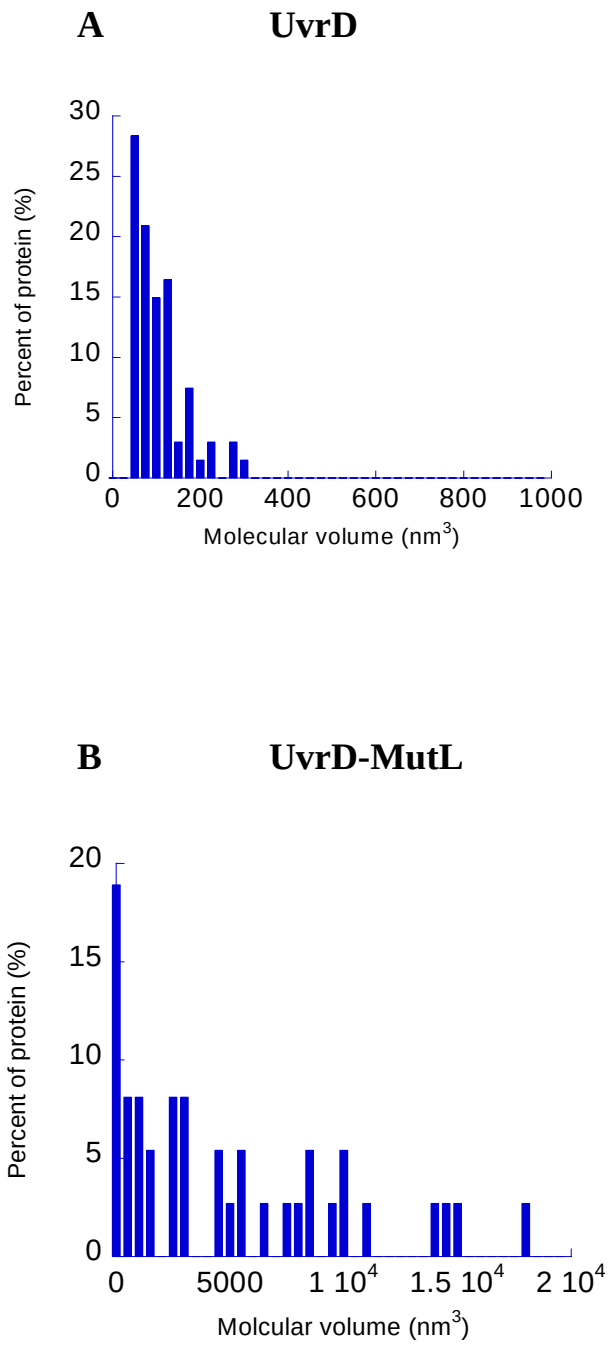

Figure 4.6 Histogram of volume of UvrD and/or MutL on the DNA

(A) UvrD on the DNA (B) UvrD-MutL on the DNA under the same conditions with Figure 4.5. It is note that the x-axis is different between A and B.

Binding of UvrD-MutL along DNA

Figures 4.5C, 4.6B, and 4.7 show that UvrD and MutL form large protein complexes on the DNA in the presence of ATP. To characterize the length of the DNA covered by proteins, and the positions of these UvrD and MutL complexes on the DNA, all DNA molecules with bound protein complexes were counted, and the length of the protein complex and distance of the protein complex from the DNA ends were measured (Figure 4.7 and 4.8). Position distributions were then plotted in Figure 4.8 to determine where on the DNA the proteins were bound. In these reactions, duplex DNA with a 3-nt 3'-overhang was used. The mean distance of the proteins on the DNA is roughly 20% from one end (36 data points). Most of the complexes were significantly larger than UvrD, and ATP alone (Table 4.3) and the mean length of the DNA covered by the protein complex is approximately 40 nm (Figure 4.8).

To examine the effect of nucleotides on MutL and UvrD binding on the DNA, a nonhydrolyzable ATP analog, AMPPNP, was used instead of ATP. The complexes on the DNA are significantly small than those seen in the presence of ATP (Table 4.3). It is likely that MutL and UvrD can not form larger complexes until UvrD initiates unwinding of DNA using energy of ATP hydrolysis.

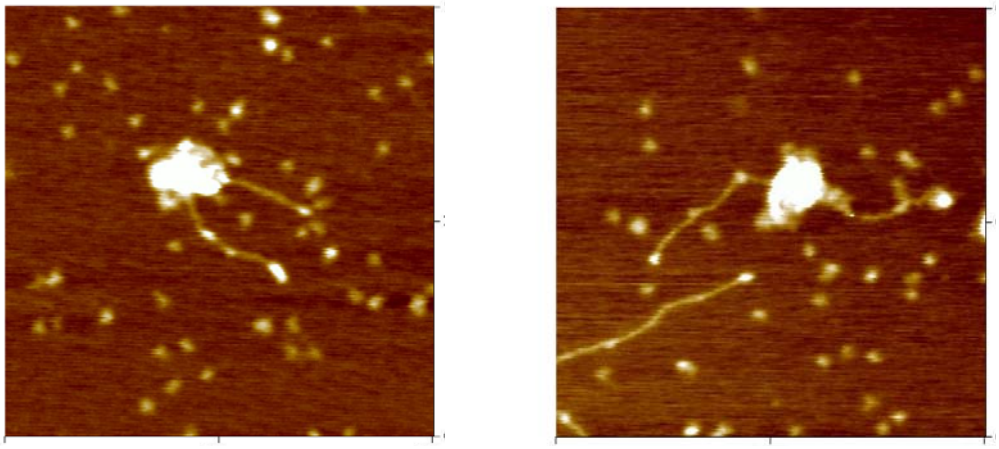

Figure 4.7 Representative AFM images of MutL-UvrD bound to internal site on the DNA in the presence of ATP

500 X 500 nm scans: Representative AFM images of MutL (25 nM) and UvrD (25 nM) on the DNA (817 bp containing a 3' ssDNA tail) in the presence of ATP (1mM). The same images with 4.5 C. Large size volumes of proteins are shown along DNA.

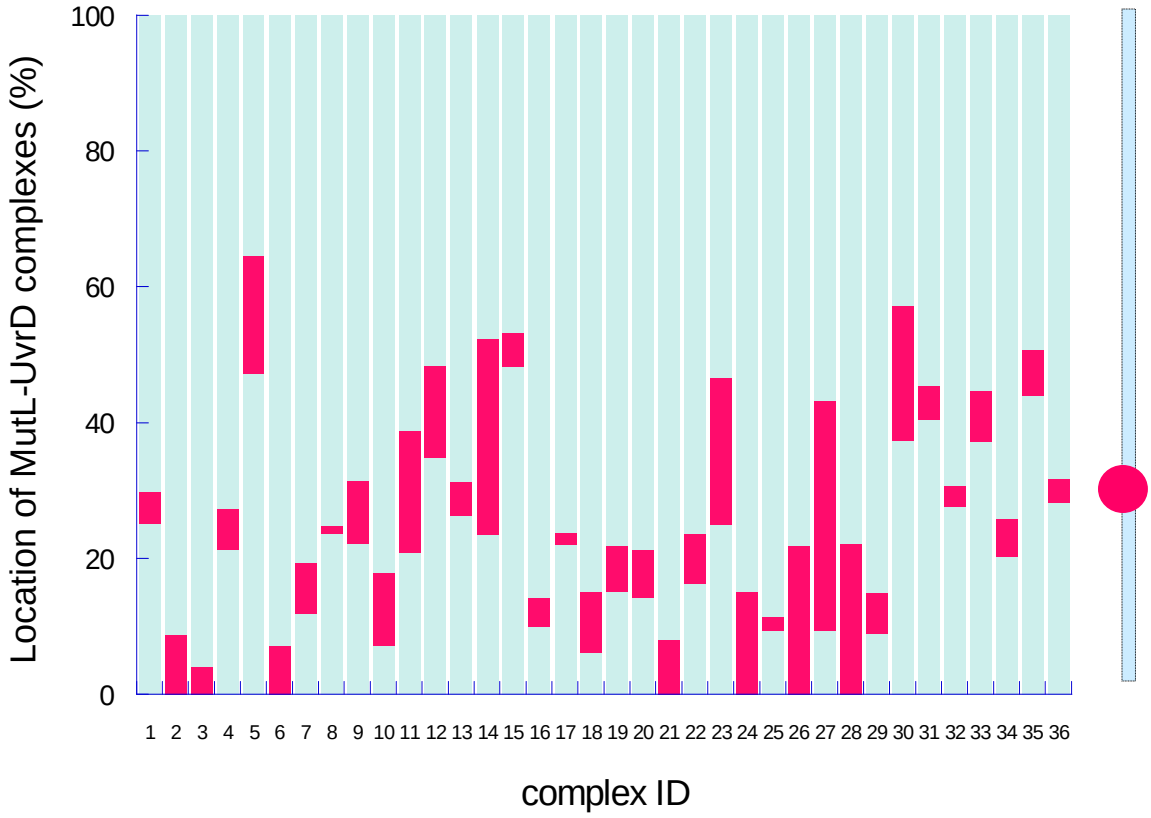
Location of MutL-UvrD complexes (%)
100
80
60
40
20
0
1 2 3 4 5 6 7 8 9 10 11 12 13 14 15 16 17 18 19 20 21 22 23 24 25 26 27 28 29 30 31 32 33 34 35 36
complex ID

Figure 4.8

Figure 4.8 Positions of MutL-UvrD assemblies on 817 bp possessing 3' ssDNA tail

MutL and UvrD bound to 817 bp duplex DNA in the presence of ATP were analyzed from chosen images that were similar to Figure 4.4C and 4.6. The solid red bar represents the length spanned by the MutL and UvrD complexes in the presence of ATP (1mM). The light blue bar represents the full length of the DNA. The location of MutL and UvrD complexes was then defined as the ratio of the length of the shorter DNA tract divided by the total contour length.

	MutL and UvrD w/ ATP	MutL and UvrD w/ AMPPNP
Large complexes bound to ends	17.5%	15%
Large complexes bound internally	**72.5%**	15%
Small complexes bound to ends	2.5%	23%
Small complexes bound internally	7.5%	**47%**

Table 4.3 MutL and UvrD binding occupancies on the DNA in the presence of nucleotides.

Discussion

ATP induces conformational changes in E. coli MutL

Using AFM, we observed conformational changes of MutL involved in the process of ATP binding and hydrolysis (Figure 4.1). The binding of ATP induces conformational changes within the MutL homodimer, likely within in the N-termini, leading to a more compact protein conformation. These results are in agreement with earlier crystallographic studies that suggests that MutL undergoes conformational change by association of N-terminus domain during ATP hydrolysis cycle (Ban 1999).

Recently, Sacho et. al. (2008) observed large conformational changes in two eukaryotic homologs of MutL (MutLα). MutLα exists in four different conformational states, as observed by AFM. In the presence of ATP (or ADP), the N-terminal domains of MutLα and folded onto the dimerized C-terminal domain, while in the absence of adenine nucleotides, the N-terminal domains were elongated from the dimerized C-termini. These data are consistent with our observation of adenine nucleotide induced conformational changes in *E. coli* MutL, except that MutL exists in two dominant states, while MutLα exists in four different states.

The binding of ADP to MutL showed more closed state than that of ATP (Figure 4.2B and C). This "more closed" state seen with ADP is consistent with crystallographic structure studies of the *E. coli* Hsp90 homology HtpG, which show that the binding of ADP induces large conformational changes, moving the N-terminal domains closer to each other (Shiau 2006).

Oligomerization of MutL and UvrD on DNA may facilitate DNA unwinding

The AFM experiments, which have examined the binding occupancies of UvrD in the absence and presence of nucleotides, indicated that the binding preference for UvrD on the DNA shifts from the end, to internal sites in the presence of ATP (or AMPPNP) (Table 4.2). If UvrD binding to DNA internally was solely due to the translocation of UvrD along duplex DNA, we weould not expect the position distribution of UvrD on the DNA to shift from ends to internal sites in the presence of AMPPNP, since UvrD is an ATP-dependent helicase unwinding DNA (Matson 1987). Results from the addition of AMPPNP suggested that this was not the case. The observation of UvrD bound internally on the DNA in the presence of AMPPNP suggests that UvrD is bound to DNA directly (Table 4.2). It suggests that helicase may be able to initiate unwinding at internal site.

Previous studies suggested the interaction of MutL and UvrD by the two-hybrid reaction in which deletion analysis of MutL and UvrD showed the possible binding region of MutL to UvrD (Hall 1998). We directly visualized MutL and UvrD interactions in the absence and presence of adenine nucleotides. AFM images were analyzed to compare each individual protein alone to the volumes measured for the combined MutL-UvrD complex. The AFM volume analysis shows that new peaks are seen in the histogram of MutL and UvrD volumes, indicating that MutL interacts with UvrD independent of the presence of adenine nucleotides (Figure 4.3).

In the absence of MutL, UvrD monomers and dimers are seen bound both internally and at the ends of the DNA in the presence of ATP (Figure 4.5A). MutL and UvrD form large complexes along the DNA, while there are no large complexes shown in for UvrD and DNA in the absence of MutL (Figure 4.5 and 4.6). Because these large complexes are only

seen in the presence of MutL, UvrD, DNA, and ATP, it is likely that these complexes result from UvrD catalyzed unwinding of DNA. MutL has been shown to bind to ssDNA (Mechanic 2000) and we show evidence for a direct interaction between UvrD and MutL. Perhaps, as UvrD initiates unwinding, MutL interacts with the ssDNA, stabilizing the single stranded state. MutL may also help to recruit additional UvrD molecules to facilitate unwinding. Because dimers or higher order oligomers of UvrD appear to be required for optimal helicase activity (Runyon 1993; Ali 1999). The interaction of MutL with UvrD might promote the oligomerization of UvrD and thereby promote optimal helicase activity.

Previous helicase and binding assay studies of MutL and UvrD have shown that MutL stimulates the loading of UvrD onto DNA (Mechanic 2000). Incubation of MutL and UvrD resulted in increased unwound products of 20 bp partial duplex and, in the presence of MutL, UvrD unwinding of 851 bp partial duplex are increased (Mechanic 2000). Although it could not be determined from our AFM studies if MutL is a processivity factor, AFM visualized the interaction of MutL and UvrD and the large complexes of these proteins positioned along the DNA from one end, suggesting that MutL increases UvrD binding to DNA and subsequently translocates UvrD along the DNA. Perhaps MutL increases the helicase activity of UvrD both by recruiting UvrD to the DNA and by stabilizing the ssDNA. Further studies will be required to test these ideas.

Conclusions and future directions

We were able to visualize the interaction of activating proteins in mismatch repair system using AFM. It has been demonstrated that MutL is essential to coordinate the functions of mismatch repair. Our results suggest that MutL exists in at least two states upon

ATP binding and hydrolysis. While we compared these MutL and UvrD complexes with UvrD alone on the DNA, future work will test these complexes in the presence of SSB. In addition, the effect of MutL on UvrD helicase activity will be visualized with AFM. Meanwhile, additional binding studies of UvrD on the DNA will be done. Different substrates, such as nicked DNA, are needed to study, due to its physiological relevant in MMR system. Nicked DNA is the nature substrate for helicase, since UvrD loads onto a nick in the mismatch repair pathway.

Materials and Methods

DNA substrates

Duplex DNA was prepared from *E. coli* pUC18 (NEB). The DNA fragments were digested with DrdI restriction enzyme (NEB), where 817 and 1869 were the length of the resulting linear fragments. Two fragments were separated on a 1 % agarose gel and purified using Micropure-EZ enzyme filters (Microcon).

Protein Purification

DNA Helicase II (UvrD) was provided by Matson (UNC-Chapel Hill). MutL was purified as described previously (Robertson 2006).

Atomic force microscopy

Combined mixtures of MutL (25 nM) and UvrD (25 nM) were incubated with the buffer (20 mM Hepes（pH 7.8), 5 mM $MgCl_2$ and 50 mM NaCl) for 5 minutes at room temperature. For MutL alone, 20 nM of MutL was equilibrated with buffer and deposited

onto freshly cleaved mica and washed with deionized water. If ATP or ADP (1 mM) were present in the reaction, ATP was added into the mixture (MutL and/or UvrD) and then incubated for 5 minutes at room temperature. For protein-DNA complex, MutL (25 nM) and/or UvrD (25 nM) and DNA (4-10 nM) were incubated for 10 minutes at room temperature.

The images were captured in air with a Nanoscope IIIa (Digital Instruments) microscope in tapping mode. Volume analysis was done using Nanoscope III v5. 12r3 software (Veeco, Santa Barbara, CA), NIH ImageJ (Rasband 1997-2006) and Image SXM v1.69 software (Barrett 2006).

Reference

Abbel-Monem, M., Channal, M. C. and Hoffmann-Berling, H. (1977). "DNA unwinding enzyme II of Escherichia coli. 2. Characterization of the DNA unwinding activity." Eur. J. Biochem. **79**: 39-45.

Abdel-Monem, M., Channal, M. C. and Hoffmann-Berling, H. (1977). "DNA unwinding enzyme II of Escherichia coli. 1. Purification and characterization of the ATPase activity." Eur. J. Biochem. **79**: 33-38.

Ali, J. A. M., N. K. and Lohman, T. M. (1999). "An oligomeric form of *E. coli* UvrD is required for optimal helicase activity " J. Mol. Biol. **293**: 815-834.

Ali, M. M., Roe, S. M., Vaughan, C. K., Meyer, P., Panaretou, B., Piper, P. W., Prodromou, C., and Pearl, L. H. (2006). "Crystal structure of an Hsp90-nucleotide-p23/Sba1 closed chaperone complex." Nature **440**: 1013-1017.

Allen, D. J., Markhow, A., Grilley, M., Taylor, J., Thresher. R., Modrich, P. and Griffith, J. D. (1997). "MutS mediates heteroduplex loop formation by a translocation mechanism." EMBO J. **16**: 4467-4476.

Au, K. G., Welsh, K. et al. (1992). "Initiation of methyl-directed mismatch repair." J. Biol. Chem. **267**(17): 12142-8.

Ban, C., Junop, M. and Yang, W. (1999). "Transformation of MutL by ATP binding and hydrolysis: a switch in DNA mismatch repair." Cell **97**: 85-97.

Ban, C. a. Y., W. (1998). "Crystal structure and ATPase activity of MutL: implications for DNA repair and mutagenesis." Cell **95**: 541-552.

Caron, P. R., Kushner, S. and Grossman, L. (1985). "Involvement of helicase Ii (uvrD gene product) and DNA polymerase I in excision mediated by the UvrABC protein complex." Proc. Natl. Acad. Sci. U. S. A. **82**: 4925-4929.

Caruthers, J. M., and McKay, D. B. (2002). "Helicase structure and mechanism." Curr. Opin. Struct. Biol. **12**: 123-133.

Chu, F., Maynard, J. C., Chiosis, G., Nicchitta, C. V., and Burlingame, A. L. (2006). "Identification of novel quaternary domain interactions in the Hsp90 chaperone, GRP94." Protein Sci. **15**: 1260-1269.

Cooper, D. L., Lahue, R. S. , and Modrich, P. (1993). "Methyl-directed mismatch repair is bidirectional." J. Biol. Chem. **268** 11823-11829

Corbett, K. D., and Berger, J. M. (2003). "Structure of the topoisomerase VI-B subunit: implications for type II topoisomerase mechanism and evolution." EMBO J. **22**: 151-163.

Dao, V. a. M., P. (1998). "Mismatch-, MutS-, MutL-, and Helicase II-dependent unwinding from the single-strand break of an incised heteroduplex." J. Biol. Chem. **273**: 9202-9207.

Dollins, D. E., Immormino, R. M., and Gewirth, D. T. (2005). "Structure of unliganded GRP94, the endoplasmic reticulum Hsp90. Basis for nucleotide-induced conformational change." J. Biol. Chem. **280**: 30438-30447.

Drotschmann, K., Aronshtam, A., Fritz, H. J. and Marins, M. G. (1998). "*The Escherichia coli* MutL protein stimulates binding of Vsr and MutS to heteroduplex DNA." Nucleic Acids Res. **26**: 948-953.

Dutta, R., and Inouye, M. (2000). "GHKL, an emergent ATPase/kinase superfamily" Trends Biochem. Sci. **25**: 24-28.

Gilchrist, C. A. a. D., D. T. (1987). "*Escherichia coli* rep gene: sequence of the gene, the encoded helicase, and its homology with uvrD." Nucleic Acids Res. **15**: 465-475.

Grilley, M., Griffith, J., and Modrich, P. (1993). "Bidirectional excision in methyl-directed mismatch repair." J. Biol. Chem. **268**: 11830-11837

Grilley, M., Welsh, K. M., Su, S.-S., and Modrich, P. (1989). "Isolation and Characterization of the Escherichia coli mutL Gene Product." J. Biol. Chem. **264**: 1000-1004

Guarne, A., Junop, M. S., and Yang, W. (2001). "Structure and function of the N-terminal 40 Da fragment of human PMS2: a monomeric GHL ATPase." EMBO J. **20**: 5521-5531.

Hall, M. C., Jordan, J. R. and Matson, S. W. (1998). "Evidence for a physical interaction between the *Escherichia coli* methyl-directed mismatch repair proteins MutL and UvrD." EMBO J. **17**: 1535-1541.

Hall, M. C., Matson, S. W. (1999). "The Escherichia coli MutL protein physically interacts with MutH and stimulates the MutH-associated endonuclease activity." J. Biol. Chem. **274**: 1306-1312.

Hu, X., Machius, M., and Yang, W. (2003). "Monovalent cation dependence and preference of GHKL ATPases and kinases." FEBS lett. **544**: 268-273.

Immormino, R. M., Dollins, D. E., Shaffer, P. L., Soldano, K. L., Walker, M. A. and Gewirth, D. T. (2004). "Ligand-induced conformational shift in the N-terminal domain of GRP94, an Hsp90 chaperone." J. Biol. Chem. **279**: 46162-46171.

Junop, M. S., Obmolova, G., Rausch, K., Hsieh, P. and Yang, W. (2001). "Composite active site of an ABC ATPase MutS uses ATP to verify mismatch recognition and authorize DNA repair." Mol. Cell **7**(1): 1-12.

Kolodner, R. (1996). "Biochemistry and genetics of eukaryotic mismatch repair." Genes Dev. **10**: 1433-1442.

Lahue, R. S., Au, K. G., and Modrich, P. (1989). "DNA mismatch correction in a defined system." Science **245**: 160-164.

Matson, S. W. (1986). "Escherichia coli helicase II (urvD gene product) translocates unidirectionally in a 3' to 5' direction." J. Biol. Chem. **261**: 10169-10175.

Matson, S. W. a. G., J. W. (1987). "DNA helicase II of *Escherichia coli*. Characterization of the single-stranded DNA-dependent NTPase and helicase activities." J. Biol. Chem. **262**: 2066-2076.

Mechanic, L. E., Frankel, B. A. and Matson, S. W. (2000). "*Excherichia coli* MutL loads DNA helicase II onto DNA." J. Biol. Chem. **275**: 38337-38346.

Modrich, P. (1987). "DNA Mismatch Correction." Annu. Rev. Biochem. **56**: 435-466

Modrich, P. a. L., R. (1996). "Mismatch repair in replication fidelity, genetic recombination, and cancer biology." Annu. Rev. Biochem. **65**: 101-133.

Nakura, J., YE, L., Morishima, A., Kohara, K. and Miki, T. (2000). "Helicases and aging." Cell. molec. Life Sci. **57**: 716-730.

Prolla, T. A., Pang, Q., Alani, E., Kolodner, R. D. and Liskay, R. M. (1994). "Interactions between the MSH2, MLH1 and PMS1 proteins during the initiation of DNA mismatch repair." Science **265**: 1091-1093.

Robertson, A., Pattishall, S. R., and Matson, S. W. (2006). "The DNA binding activity of MutL is required for Methyl-directed mismatch repair in *Escherichia coli*." J. Biol. Chem. **281**(13): 8399-8408.

Ratcliff, G. C., and Erie, D. A. (2001). "A novel single-molecule study to determine protein-protein association constants." J.Am. Chem. Soc. **123**: 5632-5635.

Runyon, G. T., Wong, I. and Lohman, T. M. (1993). "Overexpression, purification, DNA binding , and dimerization of the *Escherichia coli* uvrD gene product (helicase II)." Biochmistry **32**: 602-612.

Sacho, E. J., Kadyrov, F., Modrich, P., Kuncel, T. A. and Erie, D. A. (2008). "Direct visualization of asymmetric adenine nucleotide-induced conformational changes in MutL(αλπηα)." Mol. Cell **29**: 112-121.

Schofield, M. J., Nayak, S., Scott, T. H., Du, C. and Hsieh, P. (2001). "Interaction of *Escherchia coli* MutS and MutL at a DNA mismatch." J. Biol. Chem. **276**: 28291-28299.

Shiau, A. K., Harris, S. F., Southworth, D. R., and Agard, D. A. (2006). "Structural analysis of *E. coli* hsp90 reveals dramatic nucleotide-dependent conformational rearrangements." Cell **127**: 329-340.

Spampinato, C. a. M., P. (2000). "The MutL ATPase Is Required for Mismatch Repair." J. Biol. Chem. **275**: 9863-9869.

Su, S.-S., Lahue, R. S., Au, K. G., and Modrich, P. (1988). "Mispair Specificity of Methyl-directed DNA Mismatch Correction in Vitro." J. Biol. Chem. **263**(14): 6829-6835.

Su, S.-S. a. M., P. (1986). "Escherichia coli mutS-encoded protein binds to mismatched DNA base pairs." Proc. Natl. Acad. Sci. U. S. A. **83**(14): 5057-5061.

Welsh, K. M., Lu, A. L., Clark, S., and Modrich, P. (1987). "Isolation and characterization of the Escherichia coli mutH gene product " J. Biol. Chem. **262**: 15624-15629

Spampinato, C. a. M., P. (2000). "The MutL ATPase Is Required for Mismatch Repair." J. Biol. Chem. **275**: 9863-9869.

Yamaguchi, M., Dao, V. and Modrich, P. (1998). "MutS and MutL activate DNA helicase II in a mismatch-dependent manner." J. Biol. Chem. **273**: 9197-9201.